N71-36443

THE EFFECTS OF RADIATION ON LITHIUM DOPED SOLAR CELLS

20 July 1971 ER-11150

Final Report for Contract JPL 952586

LOCKHEED

LOCKHEED-GEORGIA COMPANY

A DIVISION OF LOCKHEED AIRCRAFT CORPORATION

THE EFFECTS OF RADIATION ON LITHIUM DOPED SOLAR CELLS

20 July 1971 ER-11150

Final Report for Contract JPL 952586

LOCKHEED-GEORGIA COMPANY
A DIVISION OF LOCKHEED AIRCRAFT CORPORATION
Marietta, Georgia

ER 11150

THE EFFECTS OF RADIATION ON LITHIUM DOPED SOLAR CELLS

Final Report for Contract
JPL 952586
Performed for Jet Propulsion
Laboratory, California
Institute of Technology, as
Sponsored by the National
Aeronautics and Space Administration
Under Contract NAS 7-100

20 July 1971

M. C. Whiffen

E. B. Trent

LOCKHEED-GEORGIA COMPANY
A DIVISION OF LOCKHEED AIRCRAFT CORPORATION
Marietta, Georgia

ABSTRACT

This report describes irradiation of lithium doped p/n solar cells at temperatures of 223°, 303°, and 353°K. Irradiation was conducted in vacuum and the source was ^{90}Sr beta particles at a rate of 10^{12} e/cm^2/day. The cells were irradiated to a fluence of 2×10^{14} e/cm^2. Conventional n/p cells were included for comparison. Results of the test show that crucible grown lithium cells are superior at 353°K while float zone grown lithium diffused cells are slightly superior at 303°, and at 223°K, where lithium mobility is very low, conventional n/p cells are superior.

Acknowledgement:

The participation of Mr. R. R. Dayton and Mr. W. R. Krull has contributed to the fulfillment of this work.

SUMMARY

The work described in this report was directed toward an effort to fill the need for a more efficient electrical power system for orbiting vehicles. It describes an engineering test of the effect of electrons on the performance of lithium diffused p/n silicon solar cells. The electrons were provided by a ^{90}Sr - ^{90}Y source approximating the electron spectrum encountered in earth orbit space flights. The exposure was accomplished in vacuum with cells loaded and illuminated with solar quality light. The effect of temperature on cell performance was evaluated by maintaining four distinct temperatures in the system: 223°, 303°, 333°, and 353°K. Groups of conventional n/p silicon cells were included for comparison purposes.

The objective of the test was to compare the electrical power output of various lithium p/n cell designs or production processes including such parameters as silicon growth method, lithium diffusion schedule and redistribution cycle with the power output of conventional n/p cells for a simulated synchronous orbit mission. The higher conversion efficiency of p/n solar cells over n/p cells cannot be realized during long exposure to space radiation due to their higher susceptibility to radiation damage. The high energy electron radiation produces defects within the semiconductor lattice creating trapping centers which impede the flow of minority carriers and thereby reduce the power output of the cell. It is felt by some investigators, however, that the highly mobile lithium atom, diffused into the base region of the p/n cell will anniliate or compensate radiation induced traps and virtually anneal the damage as it is produced, thus yielding a significant improvement in the power available from p/n solar cells during long exposure to orbital electron environment.

Time dependent drift of the lithium atoms in and around the junction region could conceivably affect their availability to anneal the damage. Hence, it was necessary to perform a test close to the same time scale as the orbital vehicle is expected to survive. The irradiation began with unexposed cells and ended with a fluence of 2.0×10^{14} electrons per square centimeter resulting from essentially 200 days of continuous exposure at a flux of 10^{12} e/cm^2 per day. This total exposure has been estimated by at least one source (reference 1) to be equivalent to 2-4 years in synchronous orbit dependent on solar activity.

The results of the test show that the conventional n/p cells are superior to the lithium diffused cells at the low temperature where the lithium mobility is low. At the intermediate temperature of 303°K the float zone grown lithium diffused cells were slightly superior to the remaining types while at the highest temperature evaluated (353°K) the crucible grown lithium cells were found to be superior. At 333°K no selection was possible. Extrapolation of the results to longer exposure times indicate that further testing would not alter the conclusion that n/p cells are most desirable for long flights at temperatures up to 300°K and that crucible grown lithium p/n cells are most efficient at temperatures above this.

It is recommended that a test of duration equivalent to the flight time should be made with cells at 303° and 333°K.

TABLE OF CONTENTS

1.0 INTRODUCTION

The p/n solar cells are more desirable for space power sources than n/p cells because their efficiencies are higher. However, conventional p/n cells have been found to be more readily degraded by the radiation encountered in space flights than the n/p cells. This has led to the use of the less efficient n/p cells for satellite power sources.

The introduction of lithium into the p/n cells has been found to improve the radiation resistance of this type of cell, the improvement presumably arising from an annealing process which occurs by the diffusion of lithium ions to the damage sites produced by the radiation. This damaging and annealing process is a function of the type, energy, and flux of radiation, of the concentration and gradient of available lithium ions in the cell and of the cell temperature, since the ion mobility in silicon varies sharply with the temperature.

The maximum power output of earlier production batchs of lithium diffused solar cells was much lower than the maximum power output of the conventional n/p cell. However, improved production techniques have yielded lithium cells with power characteristics superior to the n/p cell. Thus with higher initial power plus improved radiation resistance the lithium diffused p/n cells should be candidates for mission use. Prior to such use it is reasonable to experimentally assure that improved performance will accrue over the expected life-time of a mission. Such a test would ideally be be conducted in the space environment in which the cells would be used but this would be both too expensive and too lengthy (since the test would necessarily be the mission length). This report describes laboratory test, and its results, which reduces both the expense and the test time.

The experiment consisted of exposing groups of solar cells to a simulated space environment. The cells include both conventional n/p cells and state-of-the-art lithium diffused p/n cells. The space environmental parameters simulated include pressure, temperature, illumination and radiation. Pressure was maintained below 10^{-6} Torr which was low enough to simulate space so far as known or expected effects on the cells were concerned. Illumination was by xenon lamp with close spectral filtering which reasonably approximates solar illumination with air mass zero. Groups of cells were maintained at 223, 303, 333 and 353°K, thus spanning the range of temperatures to which the cells might be subjected on missions. The radiation was restricted to the ^{90}Sr - ^{90}Y electrons spectrum and the attendant x-rays. The significant environmental parameter omitted was the proton flux.

The following sections describe, in order, the experimental arrangement, the data reduction, the test results and the derived conclusions.

2.0 TECHNICAL DISCUSSION

2.1 EXPERIMENTAL DESIGN

Photographs of the experimental area and data acquisition equipment are in figures 61 and 62. A view of the test cells taken through the light access window is in figure 63.

2.1.1 Environmental Chamber

The environmental chamber was specially designed and fabricated for this irradiation test. The chamber is stainless steel with facilities for a ^{90}Sr source, four heat sinks on which the test cells were mounted, a hermetically sealed electrical feed through for each test cell, and a fused silica window to provide entrance for the illumination. The primary criteria in the design of the chamber were minimization of hydrocarbon contamination and the ability to maintain the pressure below 10^{-6} Torr.

The top assembly drawing of the chamber is shown in Figure 1. The chamber consists of three major sections. The center section is the main body of the chamber which contains the test specimens and the fused silica window. This section is approximately 0.356 meters in outside diameter and 0.564 meters in length. To the right of the main body is the source storage section consisting of two tubes 0.102 meters in diameter and 0.87 meters long. The cross-hatched section is a cast lead shield into which the source may be retracted to reduce the radiation level when access to the system is required. The shield is cast in sections for easy removal. Push rods extend through the lead shield and are magnetically coupled to the source plaques which are mounted on guides inside the chamber.

To the left of the main body is the vacuum pumping system which consists of two ion pumps, one titanium sublimation pump, and three Vacsorb pumps. The ion pumps have maximum pumping speeds of 25 literc/second and 125 liters/second. The 550 liter/second sublimation pump is an integral part of the smaller ion pump. The three vacsorb roughing pumps are connected to the main body through the large straight-through, ion pump and are individually valved into a section which may be isolated from the main system when the roughdown is accomplished.

During the test only the smaller ion pump was normally in operation. The power supply current for this small ion pump drove an L&N recorder equipped with cam-operated microswitches to turn the large ion pump on and off. The set points for the large pump were 5×10^{-7} Torr and 9×10^{-7} Torr. After initial pumpdown the chamber pressure remained between 1 and 3×10^{-7} Torr except during such times as source movement. These were the only instances that the large pump cycled on. The sublimation pump was found to be unnecessary and was not operated.

Chamber cleanliness was obtained by carefully designed and executed cleaning procedures carried out during fabrication of individual assemblies and assembly of the complete chamber. All surfaces were glass-shot-peened and then solvent-cleaned. Weldments were acid-cleaned prior to the solvent wash. The various parts of the chamber were bolted together using OFHC copper seals except that one viton O-ring was required to seal the fused silica window to the chamber. The completely assembled chamber was pumped down and baked at 373°K to obtain the final cleanup. The duration of the bake-out was 40 hours, and a base pressure less than 1×10^{-7} Torr at temperature was obtained. (Test cells were not in the chamber during bake-out.)

The test cells were mounted on the test item flange as depicted in Figure 2. This flange is 0.00635 meters thick stainless steel and forms the closure for one end of the main chamber. The cells were fastened to minor heat sinks as described in paragraph D of this section. The minor sinks were bolted to the major heat sinks of the flange. The major sinks are four massive copper bars vacuum oven-brazed into the flange such that one side of the bars was inside the chamber and the other side was exposed to the atmosphere. The temperature of these bars were maintained at 353, 333, 303, and 223°K. The temperatures of the 353°, 333° and 303° bars were individually controlled by the on-off action of five watt power resistors mounted on the air side of the bars. There were six uniformly spaced resistors on the 353° bar, eleven on the 333° bar and nine on the 303°bar. For each bar the resistors were connected in parallel, with one side connected to a Variac through a pair of microswitches mounted on an expanded range L&N recorder. The L&N recorders were driven by thermocouples mounted on the air side of each sink.. Cam action within the recorders turned the power on or off as required. The voltage setting of the Variacs determined the period of operation of the microswitches.

The 223°K sink was the evaporator of a two stage mechanical refrigeration system. The initial stage consisted of a package refrigeration system which reduced the temperature of the final stage condenser to 264°K. The final stage was an unthrottled Freon 502 system.

No difficulties arose in either the refrigeration, heating or control systems during the entire course of the experiment. The temperature of the 223°K bar was maintained within $\pm$ 2°K with normal operation between 222 and 223°K. The higher temperature bars were maintained at nominal

$\pm 0.5^{o}K$ with one exception. The single exception occurred when the power to the heater-controller system was inadvertently disconnected for a period of 66 hours. During this time the temperature of the 303° bar decreased to 250°K, the 333° bar to 303°K and the 353° bar to 323°K.

2.1.2 Illumination

The illumination of the test solar cells was accomplished with a dual system: a Spectrolab solar simulator X-25 was used exlusively for data collection and a Xenotech XE-20 Floodlight was used for illumination during the time period between data collections. The dual system precluded the effects of long operating time degradation of the calibrated source (X-25) for data collection. The spectral distribution of the X-25 source shown in Figure 4 is filtered to match the solar spectra as closely as possible. The Xenotech source was an unfiltered xenon lamp providing about one solar constant at the test plane. It was used only for steady-state illumination.

The X-25 used for data collection was calibrated prior to the irradiation with NASA balloon flight standard cell #177. The calibration provided an illumination of 140 watts/meter^2 through the chamber window at the plane of the solar cells with the lens system of the X-25 2.44 meters from the plane of the cells. A second measurement was made in front of the window for later reference. The angle of incidence of the light was perpendicular to the plane of all cells. During the course of the experiment the illumination used during data collection was monitored in two ways. Firstly, the balloon flight standard cell (#177) was positioned at the front window with its temperature fixed at 301°K. The output of this cell was used to adjust the settings of the X-25, as determined by the initial calibration.

There was no change required in those settings until the eighteenth data collection cycle (a fluence of 1.5 x 10^{14} e/cm^2). From this time on there was a gradual change which required altering the settings a total of less than 1% to maintain the fixed illumination.

The red-blue ratio using Corning filters Red 7-69 and Blue 1-57 was also measured during routine data collection for this cell at the front window. The ratio was 0.81 and no measurable change occurred during the test, thus the X-25 performance was excellent. The total time the X-25 was in operation during the experiment was less than 250 hours.

The second monitoring measurements were made on a cell from Centralab Lot C12 located behind the small observation window of the test item flange which is depected in Figure 1. This cell observed the X-25 illumination through both the large fused silica window and the observation window. The red-blue ratio was also measured for this cell with the same filters used for balloon flight standard cell. The output of this cell appeared to degrade with exposure time while the red-blue ratio increased from 0.82 to 1.25 during the irradiation. This behavior could be attributed to degradation of the cell itself or the resistor across it, or to degradation of either or both of the windows. At a fluence of 1.6 x 10^{14} e/cm^2 measurements were made to resolve the cause of this behavior. The balloon flight standard cell demonstrated a red-blue ratio for illumination through the two windows similar to that obtained with the monitor cell. The small observation window was removed and found to have browned due to irradiation. Red-blue ratios with the observation window removed were equivalent to those obtained in front of the large fused silica window. The observation window was replaced and the test continued. The data from this cell has subsequently been ignored.

Although the X-25 contained the 9613L optical system to provide a uniform illumination, the cells on the upper row of the 353° bar and on the 223° bar were partially shadowed by the source rod guides. To correct for this shadowing and to provide the best data from the experiment the intensity at each cell was determined prior to and following all irradiation as described below. The light level across the plane of the cells was mapped using each cell as a calibrated reference. First the short circuit current of each cell was measured individually at the same point in the X-25 light beam after being soldered to its heat sink. This point was set to 140 watts/meter^2 by reference to the balloon flight standard and the cell temperature was maintained by a copper heat sink. Then the cells were attached to their respective positions in the test chamber and short circuit current measured in the experimental arrangement with precautions taken to assure that the cell temperature was within $\pm$ 1°K of the original calibration temperature (301°K). The measured currents were normalized with the cells calibrated current at 140 watts/meter^2. The post calibration was performed two days following the termination of the irradiation. Some concern was felt for the effects of annealing during the time of the post calibration so a series of measurements were made over a three day period. These measurements showed the annealing to be negligible for the 303°, 333°, and 353° cells and to be less than 1% per day for the 223°K cells. Post calibration was accomplished in less than eight hours. Results of the pre and post illumination uniformity calibration are presented in table 1.

The Xenotech Xe-20 illumination source used between data collections failed at a fluence of 1 x 10^{14} e/cm^2 and subsequent illumination was by tungsten floodlights at a much reduced light level.

2.1.3 Irradiation Sources

The irradiation source is composed of two sections, each containing five stainless steel tubes of ^{90}Sr-^{90}U oriented so as to deliver a uniform electron flux distribution of 10^{12} electrons per square centimeter per day over the plane of the solar cells. Each stainless steel tube had a diameter of 3.18×10^{-3} meters, an active length of 0.508 meters, a wall thickness of 2.54×10^{-4} meters and contains 10 curies of ^{90}Sr.

An empirical procedure was used to develop the source-solar cell geometry. Ten source tubes were used that were identical to those used in the radiation test except each contained only 13 microcuries of ^{90}Sr. An anthracene detector and multichannel analyzer (MCA) were used to make flux and spectral measurements on these diluted source tubes. System calibration was performed using a weak ^{60}Co source.

The primary method of energy disposition in the scintillation detector under consideration is by single Compton scatter. The Compton process is the dominant method of interaction between gamma rays and organic scintillators in the energy range of 20 eV to 30 MeV. The total energy of the incoming photon may be deposited in the scintillator only after multiple Compton scatters terminating in photoelectric absorption. Since the dimensions of the anthracene detector (1.5-inch diameter x 1-inch thick) are too small to allow for the multiple scatter process, the response of the detector to the ^{60}Co source is quite similar to the response to the ^{90}Sr source.

An expression for the degradedphoton arising from a Compton collision is:

$$E_2 = \frac{E_1}{1 + \frac{E_1}{mc^2}(1 - \cos \emptyset)}$$

where E_1 and E_2 represent the energy of the incident and scattered photons, respectively. Setting ϕ equal to 180^o and subtracting E_2 from E_1 yields the familiar expression for the kinetic energy of the Compton electron:

$$E_o = \frac{E_1}{1 + \frac{.51}{2E_1}}$$

In the case of ^{60}Co, where there are two primary photons, the value for E_o is based on the average photon energy (1.25 MeV). Setting E_1 equal to 1.25 MeV, we find E_2 equals 0.21 MeV, and E_o equals 1.04 MeV. The peak of the Compton distribution collected by the 512-channel MCA will be at 1.04 MeV. This spectrum is shown in Figure 5. The peak of the ^{60}Co Compton distribution was located in channel 170 of the MCA corresponding to an energy disposition in the detector of 1.04 MeV. By simple division then we determine that each channel of the analyzer is 3.85 KeV in width. With the detector system calibrated in this manner we can now look at a source having unknown energy distribution and determine its characteristic decay spectrum.

Spectral and flux measurements of the ^{90}Sr-^{90}Y sources were made after the calibration procedure was completed. Determination of the correct source geometry and source to detector or source to solar cells spacing was accomplished by a trial and error method based on an assumed workable geometry. Factors considered in making a first assumption of a workable geometry were:

1) The physical dimensions of the source rods
2) The cross-sectional area of the solar cell plane
3) Flux uniformity requirements
4) Light uniformity requirements

5) Dimensions of the light beam

6) Prior knowledge of the shape of an iso-response curve for a source in the form of a long right circular cylinder

7) Desired vacuum system design

8) Within relatively broad limits the spectral distribution of the source is dependent of the source to detector (or solar cell) separation.

Considering the above factors, a good first approximation of the source geometry could be obtained. For instance, minimum and maximum displacement of sources in the horizontal and vertical planes within the desired vacuum system was determined. The isoresponse curve of the source would be elipsoidal therefore a central attenuator would be required. The resulting source geometry which gave a relatively flat flux distribution at the solar cell plane is shown in Figure 6. The arrangement in effect reduces the electron source from 100 curies to 32 curies.

The flux was determined by storing counts or data in the MCA for a known period of time. These counts were then dumped from the MCA to a flexowriter giving a tabulation of counts accumulated in each analyzer channel. Totaling the counts, dividing by the time of the count and cross-sectional area of the detector entrance surface gave the flux in electrons/cm^2/sec. The process of changing source geometry, source strength, source to detector spacing and center attenuator was repeated until an equivalent flux of 10^{12} e/cm^2/day was attained. After attaining a center line flux of 10^{12} the detector was moved in a fixed plane (the plane to be occupied by the solar cells in the vacuum chamber) to the four clock positions 3, 6, 9, and 12 and the flux measured. The flux distribution was determined to be 1×10^{12} e/cm^2/day plus or minus 5%.

Reference is made above to an equivalent flux of 10^{12} e/cm^2/day. The actual measured flux was much lower, of course, since diluted or low activity source rods were used in the experimental procedure and linear extrapolations performed. The validity of the extrapolation technique had been verified in the performance of other unrelated contracts (Reference 2) using the same ^{90}Sr-^{90}Y sources diluted and full strength. In the referenced report a procedure is described wherein the anthracene crystal is used to measure the flux from the diluted source rods. The measured values were used to predict the flux from the full strength source tubes. To verify the resulting data a Faraday Cup was placed in a large vacuum chamber with the full strength source tubes and the actual electron current measured. For the geometry used the measured current was 4.35×10^{-10} amperes which compared favorably to a computed current of 4.40×10^{-10} amperes. The diluted source tubes contain 0.6 microcuries ^{90} Sr per inch and the full strength tubes contain 0.5 curies ^{90}Sr per inch. Spectral measurements were then made with the source and detector in a minimum scatter geometry and with the source and detector inside a heavy walled aluminum tube to simulate the scatter geometry of the actual chamber. No significant spectral shift was observed. The measured spectrum is shown in Figure 7.

2.1.4 Solar Cells

The test chamber contained 144 solar cells, each $(1X2)x\ 10^{-2}$ meters in size. The performance of each cell was observable external to the chamber through hermetically sealed feed-throughs attached to Ti-Ag contacts on the cell. The cells were soldered to minor heat sinks depicted on the left in Figure 2. These heat sinks were copper T sections 3.18×10^{-3} meters thick with the top of the T sized to accommodate two cells. Both the cells and the sinks had been pre-tinned, thus the mounting process consisted only of alignment of the cells and application of heat in an inert atmosphere. The minor heat sinks with cells attached were then bolted to the major heat sinks described in paragraph B of this section.

The arrangement of the cells on the test item flange is shown on the right in Figure 2. The cells were divided among four temperatures: the bottom 18 cells of Figure 2 were at 223°K, the next higher 44 cells were at 303°K, the next 54 cells were at 333°K and the top 28 cells were at 353°K. At each temperature there are a number of groups, each containing cells of the same type, as shown in matrix form in Figure 3. The number in the matrix indicates the number of cells in the group. The cell selection was based on obtaining a maximum of information about the performance of a cell type coupled with a measurement of its performance relative to other cell types. The range of comparisons available is evident from Figure 3 and is further evidenced in later sections.

During the irradiation each cell was loaded by an eleven ohm resistor. The load was removed when performance measurements were made. No cover glass was used. Three groups of cells were covered with thin aluminum foil during the irradiation to evaluate the effect of illumination on the cell degradation. This foil was swing out of the way by a magnetic coupling during the measurements.

2.1.5 Data Collection

The semi-automatic data acquisition system that was used to measure the I-V characteristics of the test cells is shown in block diagram form in Figure 8. The system operated as follows: A precision resistor was manually connected across the load leads. The automatic system switched the first cell into the load leads and the voltage developed across the load resistance was determined by the digital voltmeter. The sample number and voltmeter reading were automatically recorded on punched paper tape and in typewritten format by a Flexowriter. The system then indexed to the next solar cell and the measurement process was repeated. This automatic process continued until the system had indexed each of the 144 test cells. The indexing was then interrupted and the next load resistor was manually connected into the measurement system and the sequence repeated through the array of cells. This process continued until the voltage across each of 16 loads spanning the solar cell characteristic curve had been measured for each test cell. The 230 individual measurements required about 150 minutes. The typewritten format was retained for record purposes. The paper tape data was transferred to cards for computer processing.

The voltage measurements were made directly across the solar cell thus each load included the leads from the cell to the load resistor decade box. Each of these total loads was calibrated to obtain an accurate current value.

The data acquisition system operated satisfactorily during the experiment. During the measurement of one complete data set of 2304 voltage values there were commonly 6 to 10 bad pieces of data. These bad data points were easily recognized and smoothed. On a few occasions the entire set of data from a cell was found to be inconsistent, but overall the system proved sufficient.

2.2 DATA COLLECTION AND ANALYSIS

Data was collected a total of 22 times during the experiment which terminated at an electron fluence of 2.0×10^{14} e/cm^2. Each collection cycle covered every cell of the test matrix at each of 16 load resistance points, thus providing 16 data points on the I-V characteristic curve for each cell at each collection.

The computer program used to reduce the data is presented in the Appendix and a flow chart is in Figure 9. The major objective of the program was to determine the maximum power point for a set of data and to output the current, voltage, and power at this point. In addition the program evaluated the parameters Ig, Io, Rs and n of the solar cell equation

$$I = Ig - Io (\exp (B (V-IRs)/n) - 1) \quad (1)$$

where I, V are the experimentally determined current and voltage and B is an input constant dependent on the cell temperature. Because the major goal was the determination of the maximum power, the program used an altered form of equation (1). Substituting P/I for V the equation becomes

$$P = I \left(\frac{n}{B} \log \frac{(1 + Ig - I)}{Io} - IRs \right). \quad (2)$$

This is the basic equation which the program solved.

The program first related the data to cell nomenclature, then calculated the current for each measured voltage using the known, input resistance. From the resultant I-V pairs, the power was calculated thus providing P-I pairs for use in equation (2). An iterative procedure based on the Newton-Ralphson method was then used to find parameters for equation (2) such that the standard error of estimate of the power was minimized. The maximum power point was then determined by iterative approach to the condition $dP/dI = 0$. This sequence was done for the data from each of the 144 individual cells in the test. The composites were then assembled, each consisting of one of the groups shown in the matrix of Figure 3. In this case the points for all the cells in the composite were used in the curve fitting procedure. In other respects the procedure was essentially the same as for individual cells. The output consists of the equation parameters the standard error of estimate of power, and the current, voltage and power at the maximum power point for each cell and each composite plus the I-V pairs for the individual cells. The power and current parameters of each composite were corrected for light level by dividing each quantity by the average light level factor for the group as noted in table 1. These corrected values appear in the plotted data. The data presented in Appendix II have not been corrected for light level.

The sources of possible error in the measurement system include the digital voltmeter, the stepping-switch and make-up connector contacts, and the light source. The voltmeter was calibrated to the manufacturers specification of 0.01% prior to the test and this calibration was rechecked at the end of the test. No detectable change had occurred during the test period. All switches had gold plated contacts thus the contact potential was reduced less than 10 microvolts which was considered negligible. A manual connection was made at the point where the loads during exposure were disconnected and the measuring system connected for data acquisition. This connection would normally produce either a negligible effect or would be very large and hence easily recognized (such an effect apparently occurred on two occasions during the test). These types of connections are normally repeatible within at least 0.1 ohms.

The light source presents the most probable source of error in the system. It was aligned at the start of the test, the red-blue ratio was measured and the light intensity at the plane of the solar cells was mapped. The possible occurrences during the test include misalignment of the source, change in the spectral quality due to aging, change in the intensity due to aging, and inherent flicker in the arc.

The possibility of misalignment occurring during the test was ruled out by a remeasurement of the light intensity at the cells at the conclusion of the test. There was no observed change in the spectral quality as measured by the red-blue ratio. Such a measurement was made at each data collection and no detectable change was found except for that described in III.B. The intensity of the source is adjustable. At the start of each data collection the source intensity was set to a standard value by use of a balloon flight standard cell held manually at the front window of the system. This adjustment was found to depend slightly on the location of the cell and significantly on the location of hands, etc. from which light could be reflected to the cell. Such errors were reduced by careful manipulation.

A test was conducted at the conclusion of one of the data collections to evaluate the system performance. A set of 10 voltage measruements was made on each of 10 of the cells in the matrix. The measurements were made by stepping through the cells repeatedly, thus including the effect of the stepping switch contact. The standard deviations for the cell voltages varied from a low of 0.05 mV to a high of 0.28 mV. The lowest measured voltages during data collection were about 12 mV, hence the maximum measured standard deviation represents about 2.5% of this value, thereby the expected uniformity of the data for the first point on the characteristic curve is very poor. The second point is less sensitive by a factor of six due to the increased voltage, thus the statistics of the data should be very good after the first point, since the maximum expected standard deviation is less than one-half of one percent of the measured voltage value for most of the data.

A minimal effort has been expended to analyze the data statistically. The standard error of estimate calculated during the curve fitting is a quantitative measure of goodness of fit and was not intended to provide a basis for statistical analysis. As a first attempt to analyze the validity of the results the standard deviation of the individual values within the composites was calculated. It was found that these deviations varied drastically from one composite to another because of intial cell variation. The range of values for intial power in a composite was as low as ± 1.5% of the mean and as high as ± 8% of the mean. These have been plotted on the last point of each of the maximum power curves. Subsequently an attempt was made to normalize the cells within a composite to the same initial power but this was found inappropriate because the cells in the composites behave differently with exposure. Further effort should obviously be made to evaluate the results statistically.

2.3 RESULTS

The performance of the cells has been evaluated on the basis of maximum power, the current and voltage at the maximum power point, the short circuit current, and the open circuit voltage. The results for these parameters are presented in graph form in Figures 10 through 58 and in tabular form in Appendix II. The maximum power, maximum power current and voltage, open circuit voltage, and short circuit current are presented for each test group.

Figure 59 shows the relative maximum power degradation at $2 \times 10^{14} e/cm^2$ of each cell type as a function of temperature. Relative maximum power degradation at a particular temperature is determined by taking the ratio of post irradiation maximum power to pre-irradiation maximum power at that temperature. The effect of presenting data in this fashion is to normalize with respect to absolute maximum power differences between the various cell types and also with respect to the absolute maximum power temperature dependence of each cell type. Figure 59 shows that:

1) For n/p cells, relative maximum power degradation is essentially independent of temperature over the range 223 to 353°K.
2) For float zone p/n lithium cells, relative maximum power degradation decreases with temperatures over the range 303 to 353°K.
3) For crucible grown p/n lithium cells, relative maximum power degradation increases with temperature over the range 223 to 353°K.

Figure 60 is a plot of power at the end of the test versus temperature for the different cell types.

Table 2 contains the initial power for each composite along with the smooth curve values at 10^{14}e/cm^2 and at the end of the test, 2 x 10^{14} e/cm^2, plus an extrapolated value at 5 x 10^{14}e/cm^2. Figures 10 and 12 compare composites that were covered with aluminum foil, and hence not illuminated, during the exposure with equivalent composites that were illuminated.

3.0 CONCLUSIONS

1. At low temperature (223°K) the conventional n/p cells are superior in performance to the crucible grown lithium cells to which they were compared. This superiority increases with increasing fluence.

2. Centralab Lot C12 cells outperformed the Heliotek Lot H8A which had the same lithium diffusion schedule. This was true for all temperatures and fluences tested.

3. The float zone grown lithium cells were slightly superior to the conventional n/p cells at 303°K. Both these types outperformed all the crucible grown lithium cells at this temperature to the fluence tested.

4. There is no definitely superior group at 333°K. Further testing is necessary at this temperature.

5. Centralab Lot C12 stands out in performance at 353°K while the remaining groups are similar.

6. The test to determine the effect of illuminating or not illuminating the cells during exposure was inconclusive but implies there is no difference.

4.0 RECOMMENDATIONS

The test results and conclusions lead to the following recommendations:

1. That further effort be expended to thoroughly analyze the data obtained during this test, particularly the statistics, to evaluate significant differences. The lack of such a full analysis has limited the conclusions which can be drawn from the test results and essentially invalidates any extrapolations made.

2. That the test be continued to the exposure expected from a full term flight. The continuation test should include cells exposed in this test in addition to more advanced lithium diffused cells. This is particularly important at or near the intermediate temperatures used in this test. The following items should be given consideration in any new test:

   a) Cell groups should be selected so that the initial power of each cell in a group is as near the same as possible.
   b) Cells from the same production, but of significantly different initial power, should be included to evaluate initial power as a selection criteria.
   c) The test be long enough to reach the anticipated fluence of an expected flight.
   d) A new source geometry be devised to increase the electron flux at the cells, thus reducing exposure time and expense. It is reasonable that an entire flight could be experienced in a one year test thus making such terrestial testing even more attractive.

REFERENCES

1. Velte, J. I. et al, Models of the Trapped Radiation Environment, Vol 3 "Electrons at Synchronous Altitudes NASA SP 3024, 1967.

2. Radiation Effects on Composit Structures, Lockheed ER 8582, 1967.

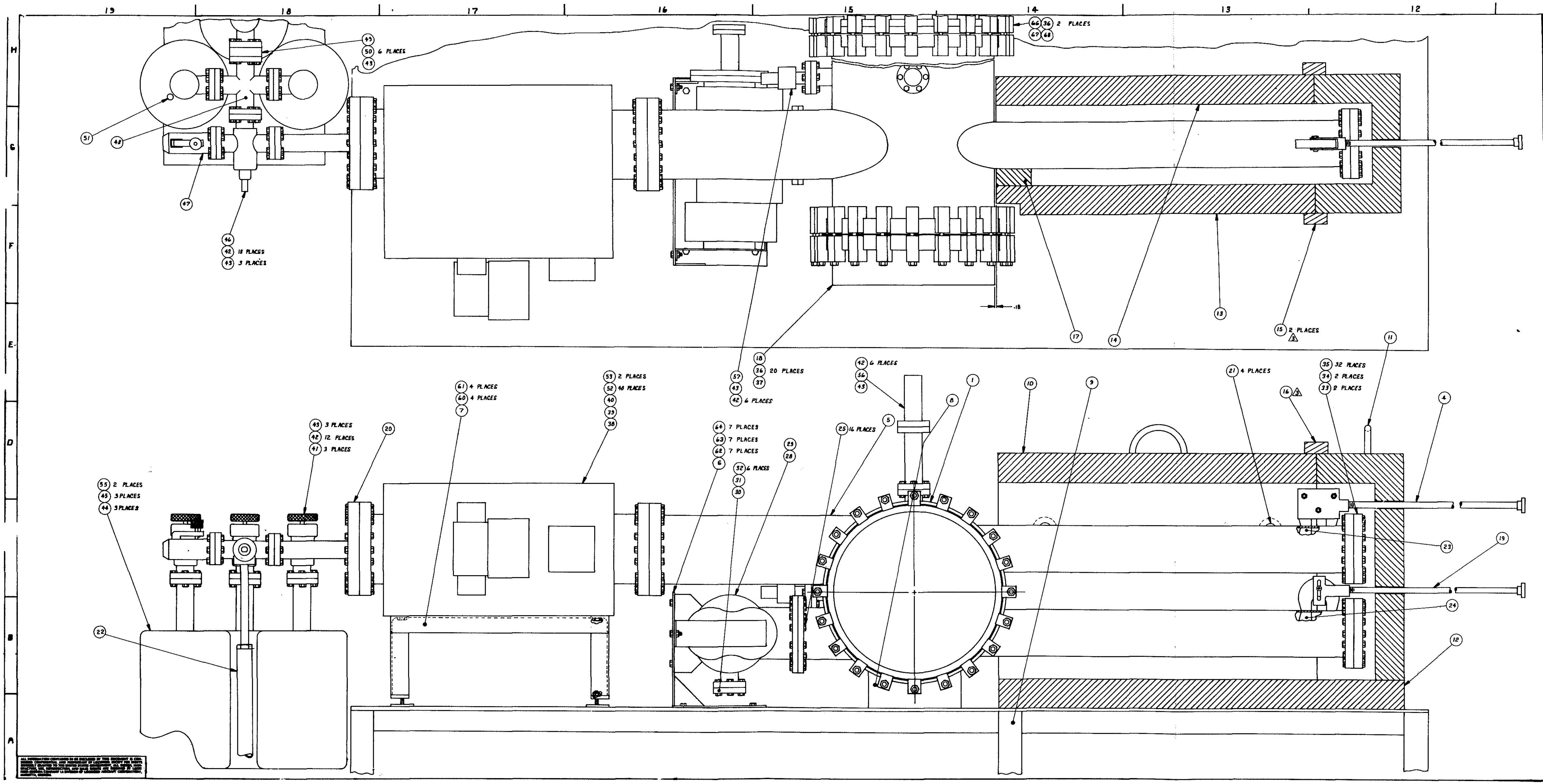

FIGURE 1 - VACUUM CHAMBER

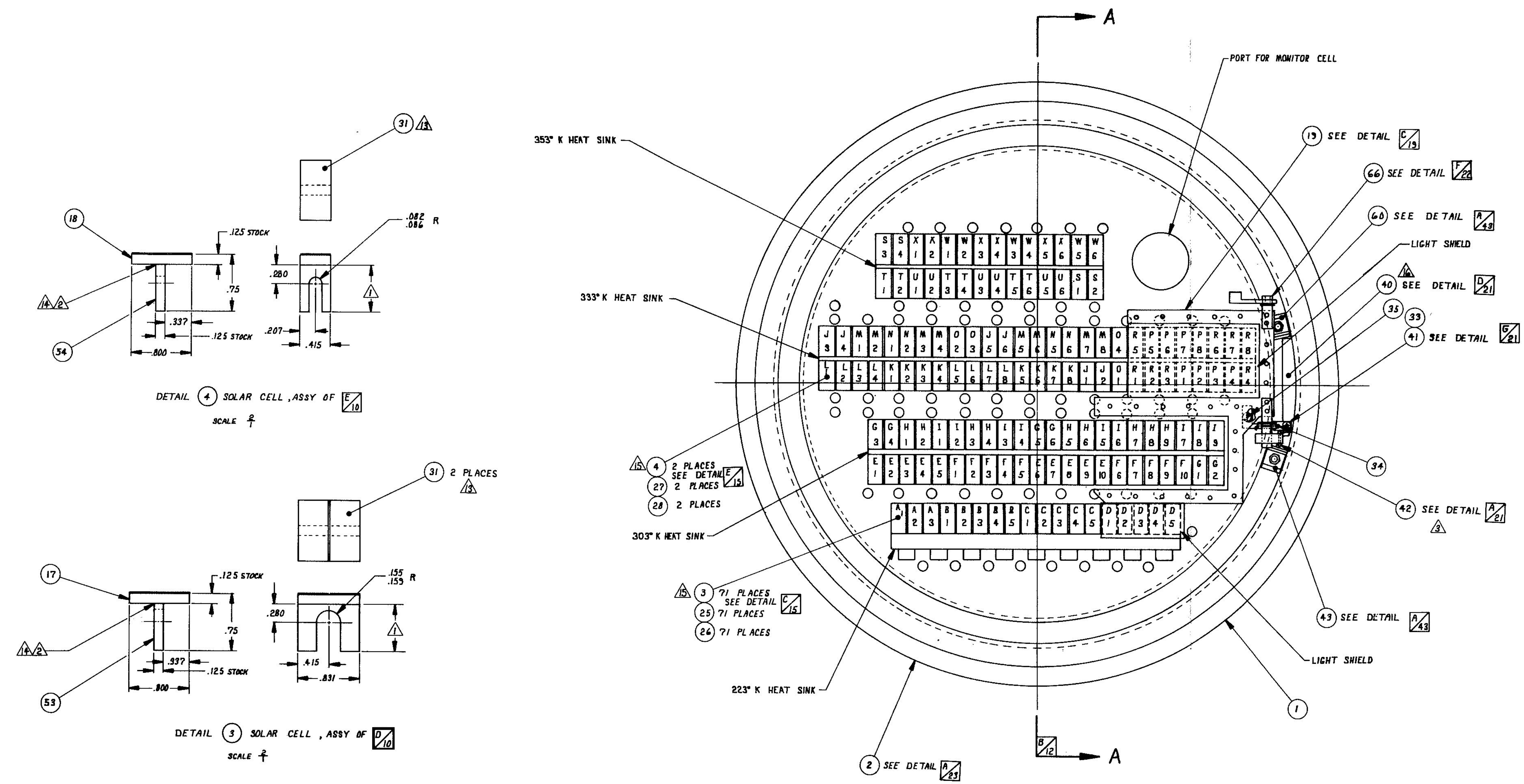

FOR GENERAL NOTES, SEE SHEET ONE.

FIGURE 2 - TEST ITEM FLANGE

NL010154

SOLAR CELL TYPE	223°C		303°K	333°K		353°K
CONVENTIONAL N/P 10 OHM-CM	A3		G6	J6		S4
CRUCIBLE GROWN CENTRALAB C-12 598°K- 8 HOUR DIFFUSION	B5	DARK D5	E10	K8	DARK P8	T6
CRUCIBLE GROWN HELIOTEK H8A 598°K - 8 HOUR DIFFUSION	C5		F10	L8	DARK R8	U6
CRUCIBLE GROWN CENTRALAB 698°K- 90 MIN + 120 MIN DIFFUSION			H9	M8		W6
FLOAT ZONE CENTRALAB 698°K - 90 MIN + 120 MIN DIFFUSION			I9	N4		X6
FLOAT ZONE CENTRALAB 698°K - 90 MIN DIFFUSION				04		

FIGURE 3 TEST MATRIX

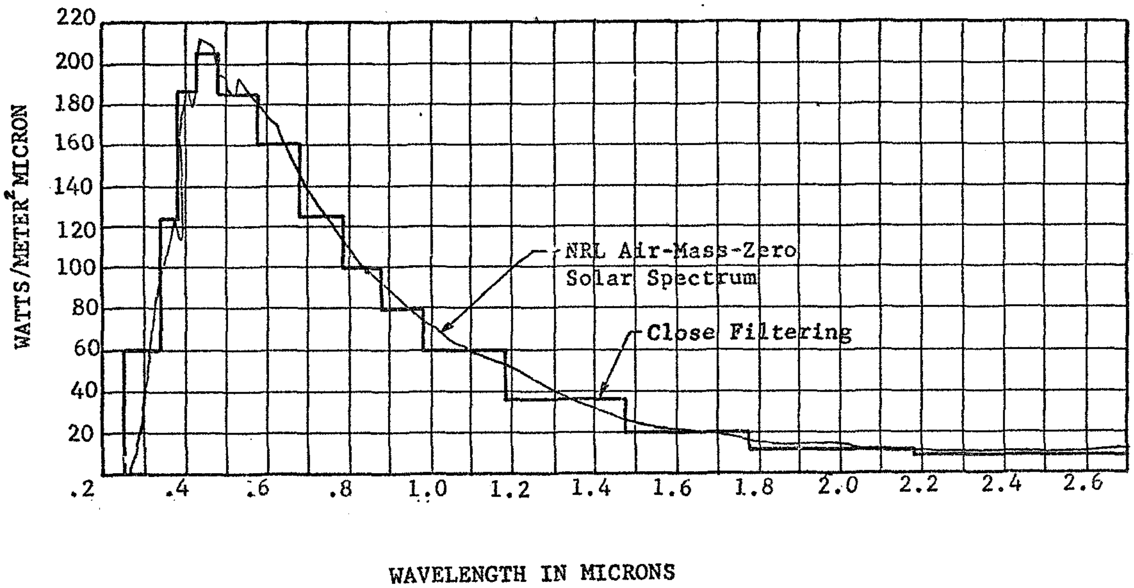

FIGURE 4 - SPECTRAL DISTRIBUTION OF X - 25

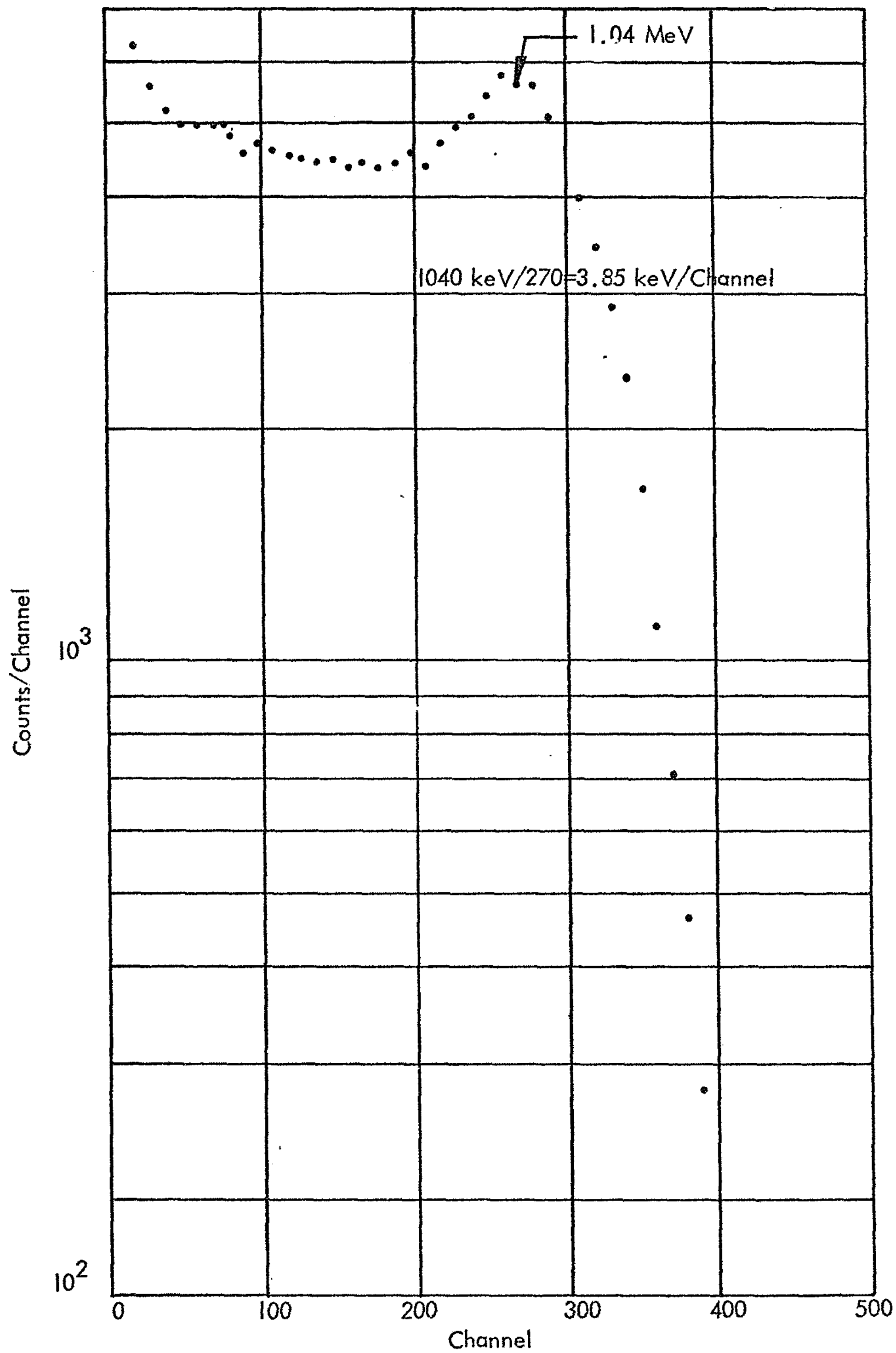

Figure 5 - COMPTON SPECTRUM OF ^{60}CO

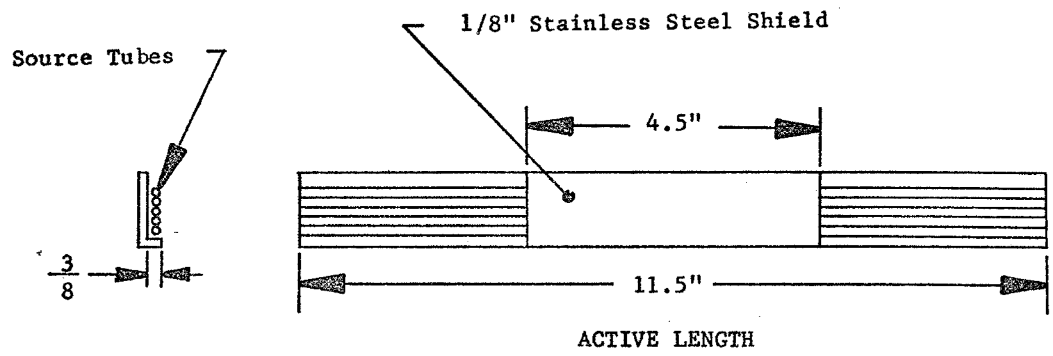

SOURCE PLAQUE (TYPICAL OF TWO)

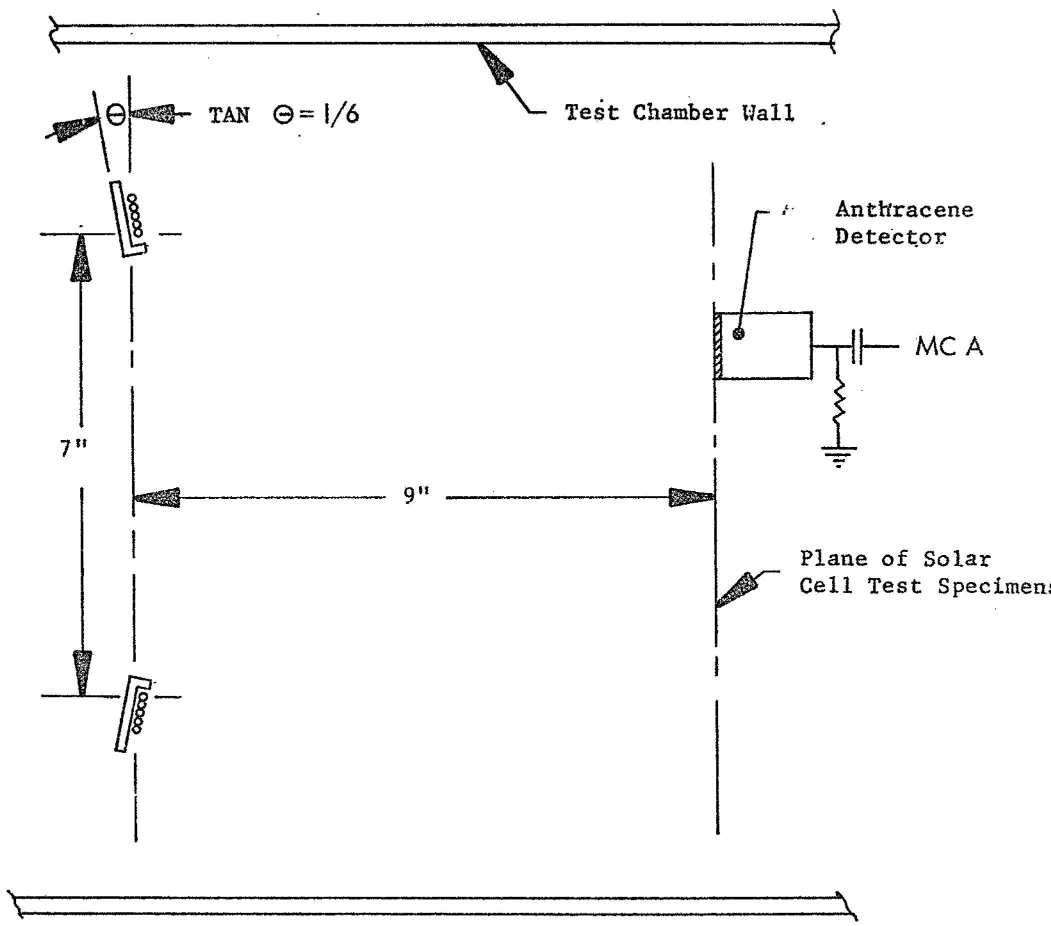

FIGURE 6 - SOURCE TEST AND MAPPING CONFIGURATION

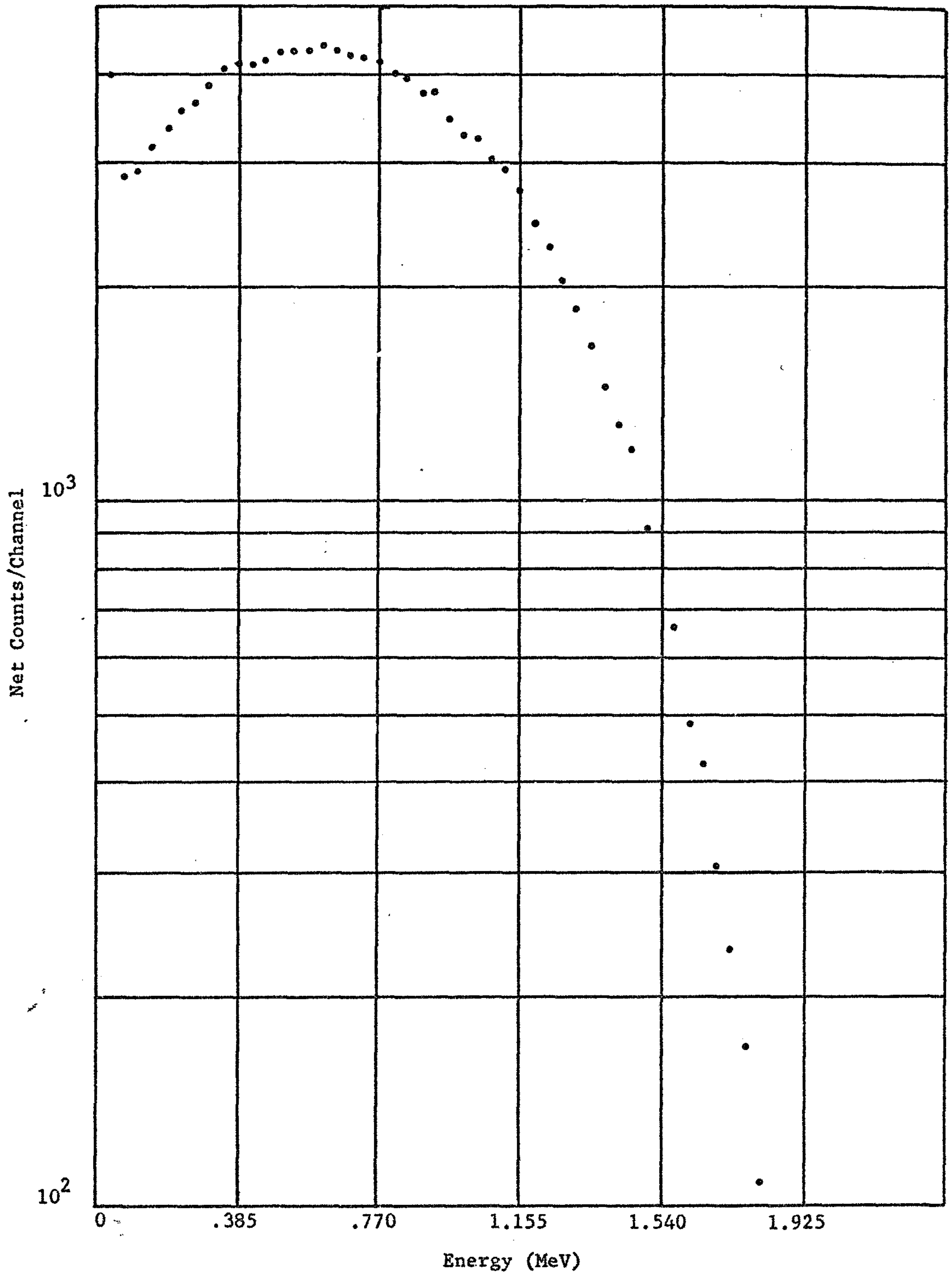

FIGURE 7 - ^{90}Sr - ^{90}Y SPECTRUM

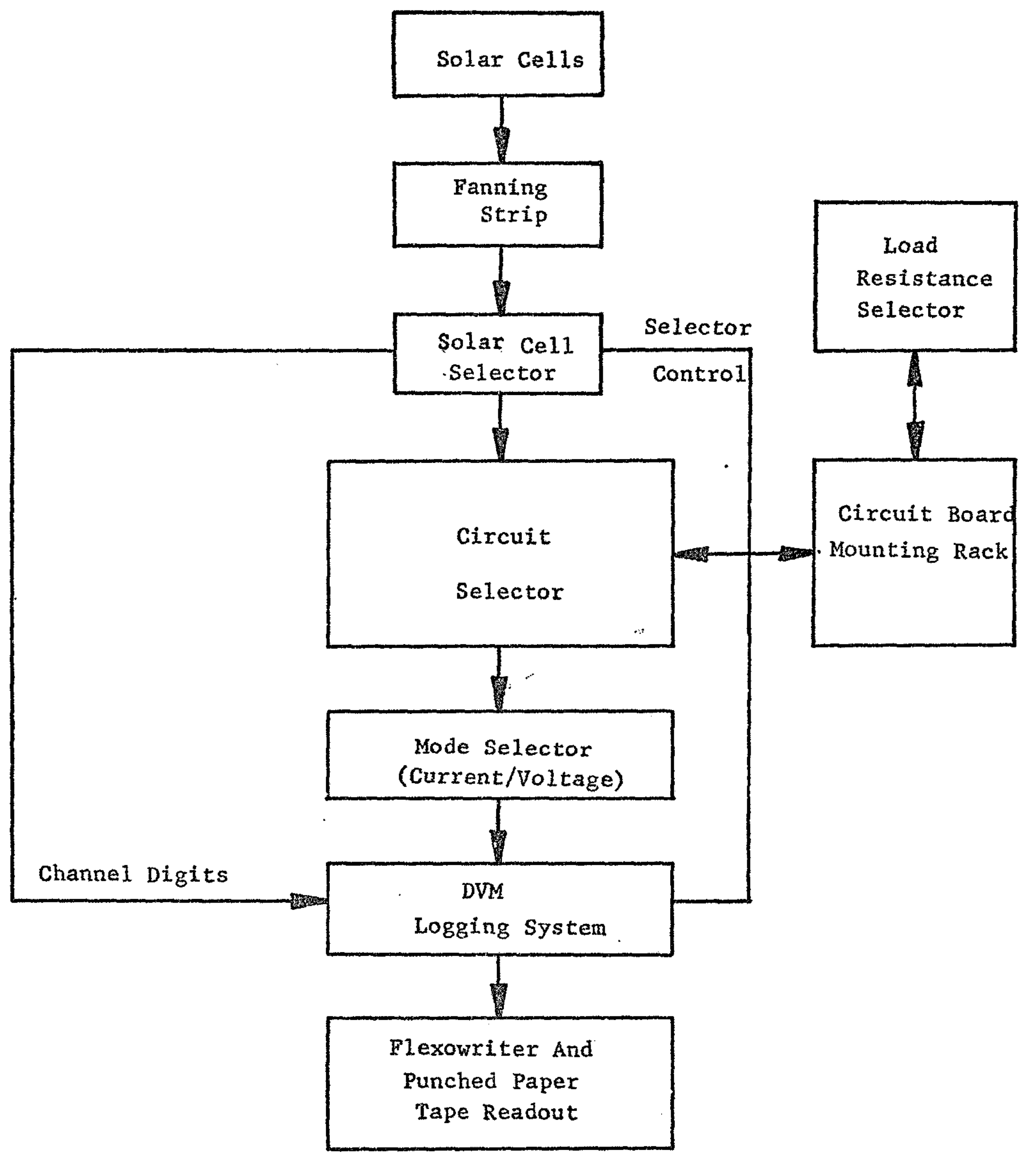

FIGURE 8 INSTRUMENTATION DATA COLLECTION SYSTEM

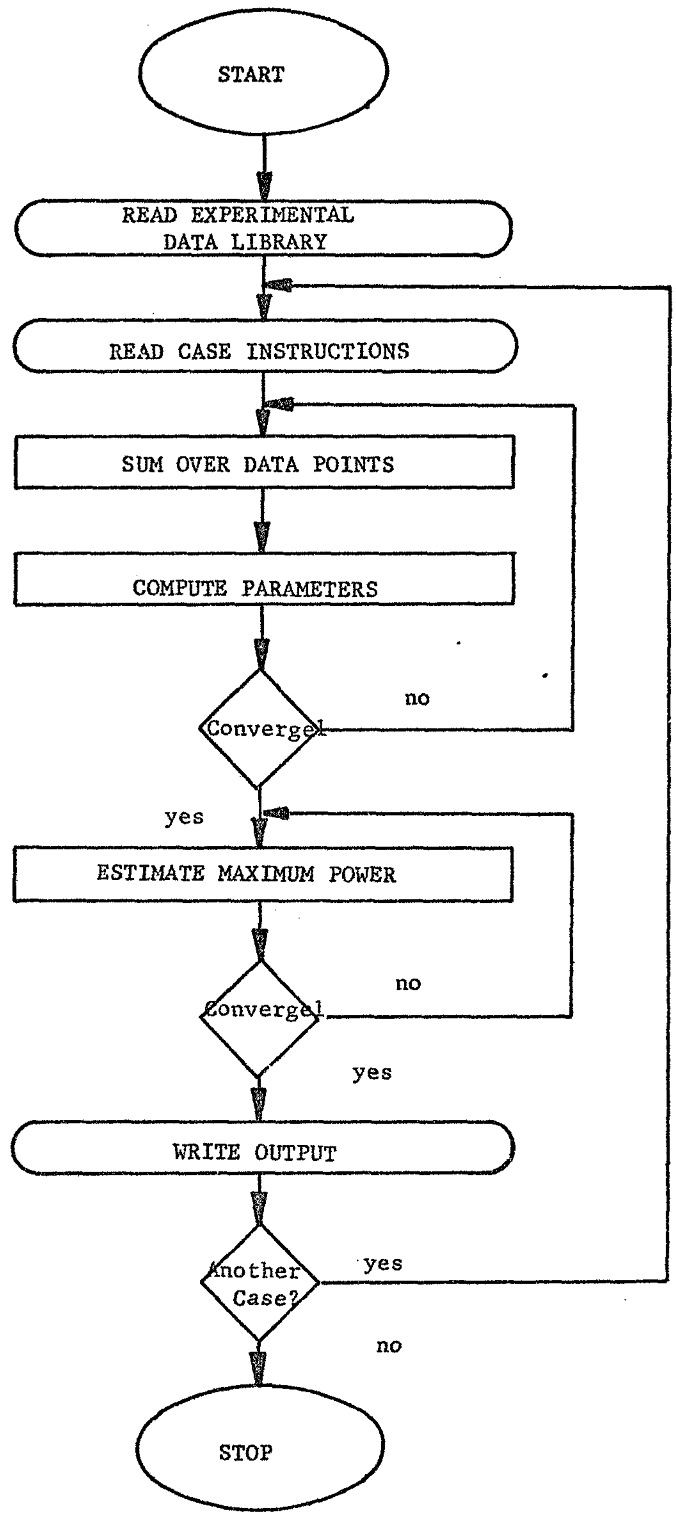

FIGURE 9
COMPUTER PROGRAM FLOW CHART

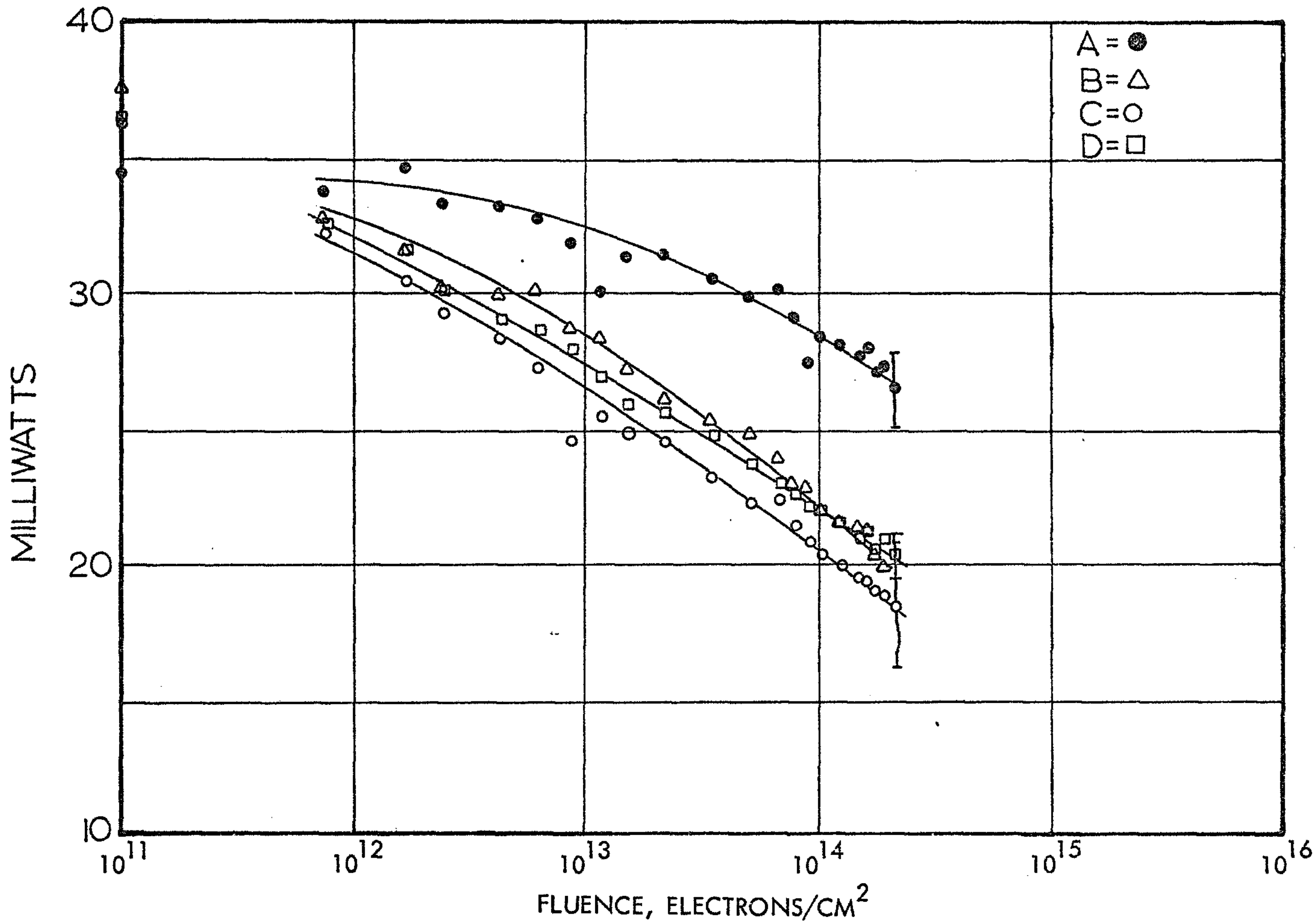

FIGURE 10
MAXIMUM POWER AT 223° K

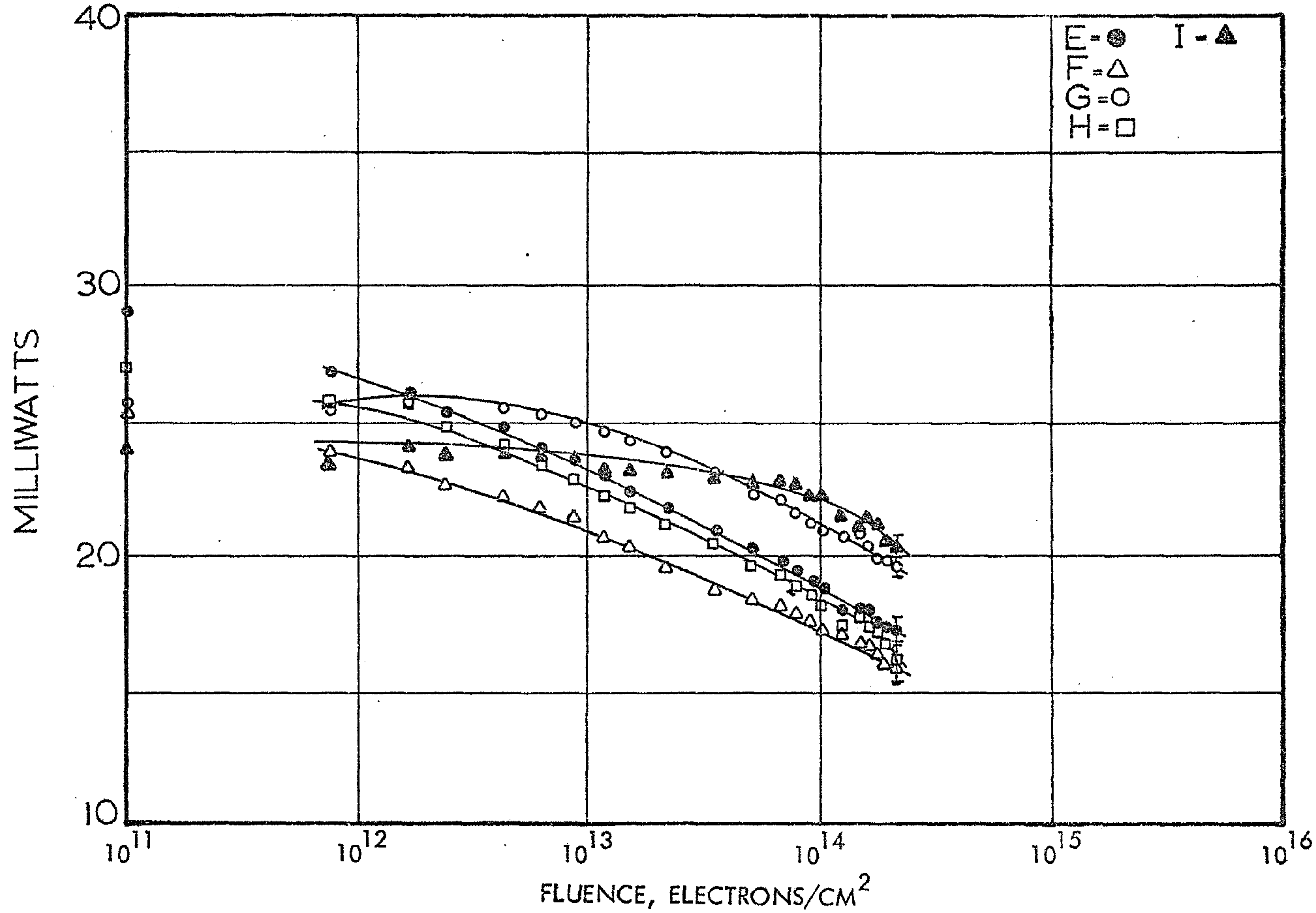

FIGURE 11

MAXIMUM POWER AT 303° K

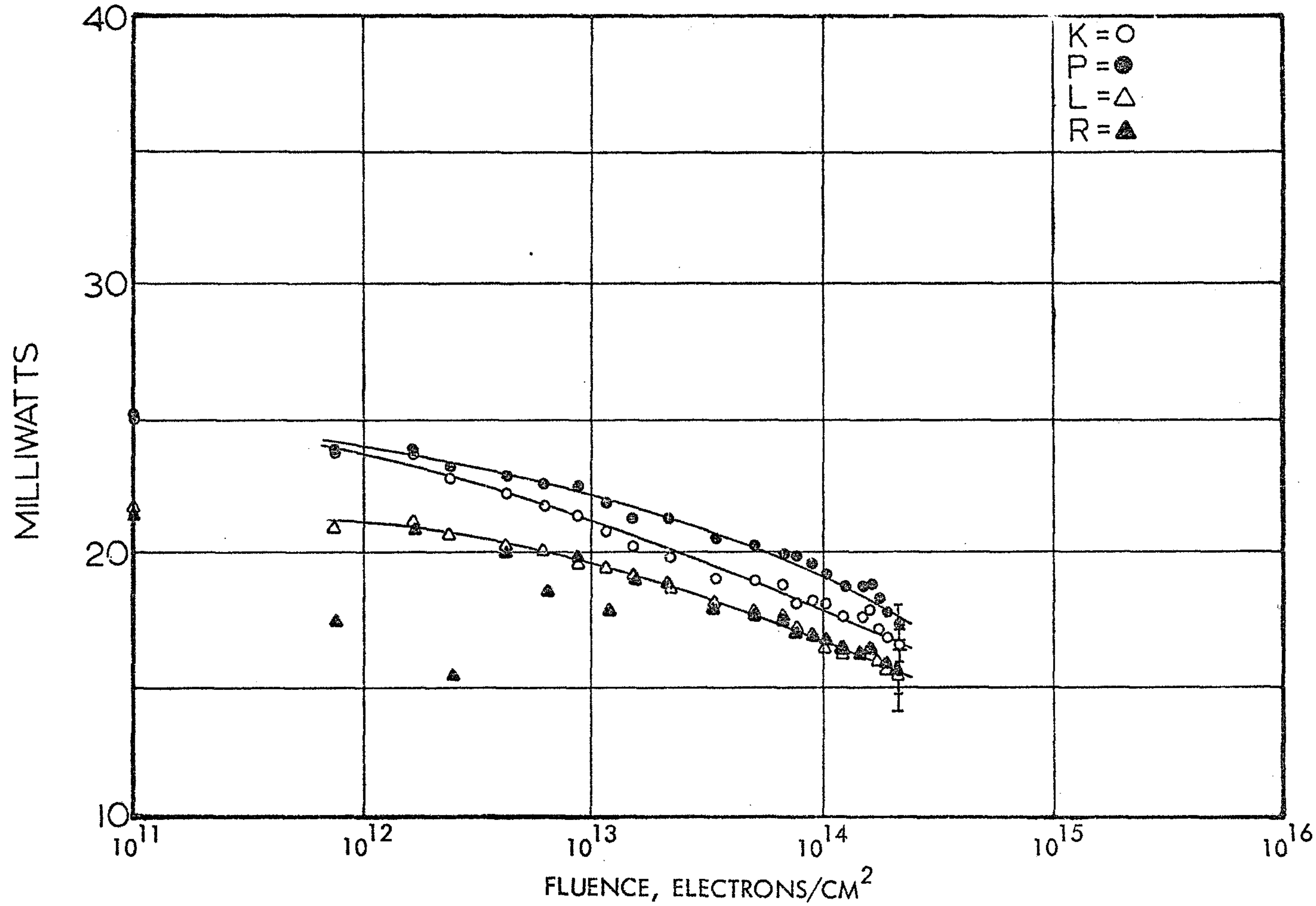

FIGURE 12
MAXIMUM POWER AT 333° K

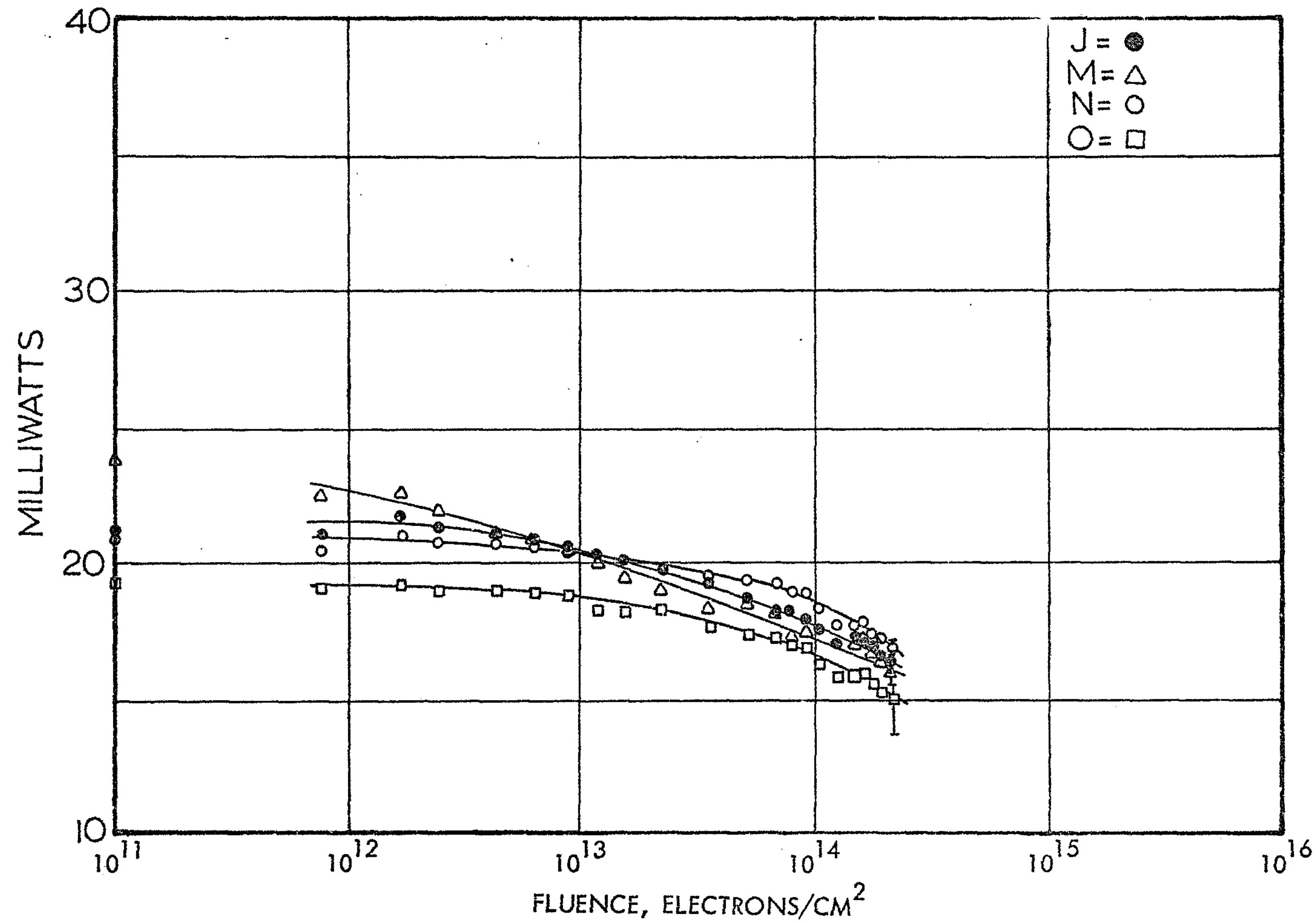

FIGURE 13
MAXIMUM POWER AT 333° K

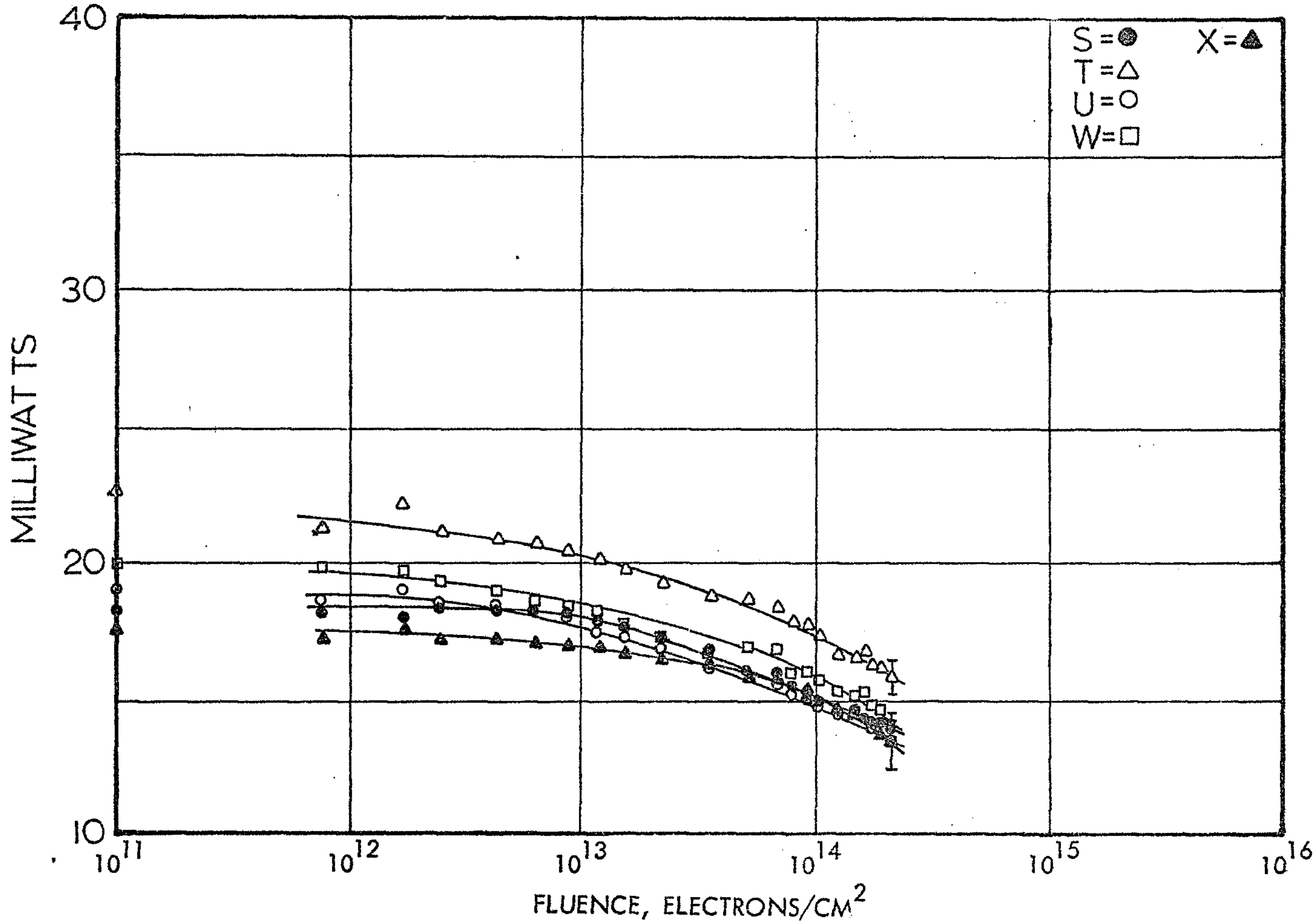

FIGURE 14

MAXIMUM POWER AT 353° K

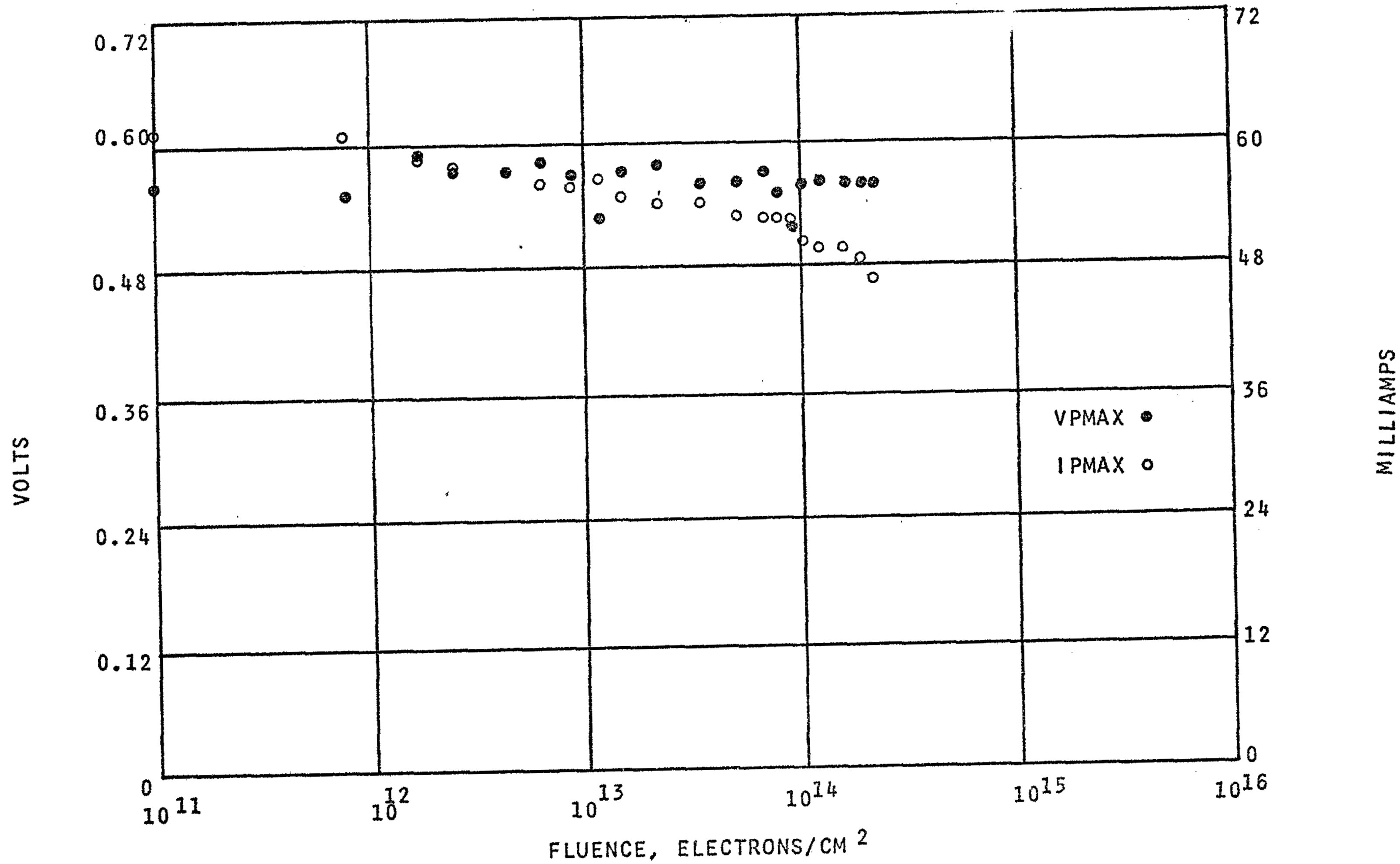

FIGURE 15 - GROUP A CURRENT AND VOLTAGE AT MAXIMUM POWER

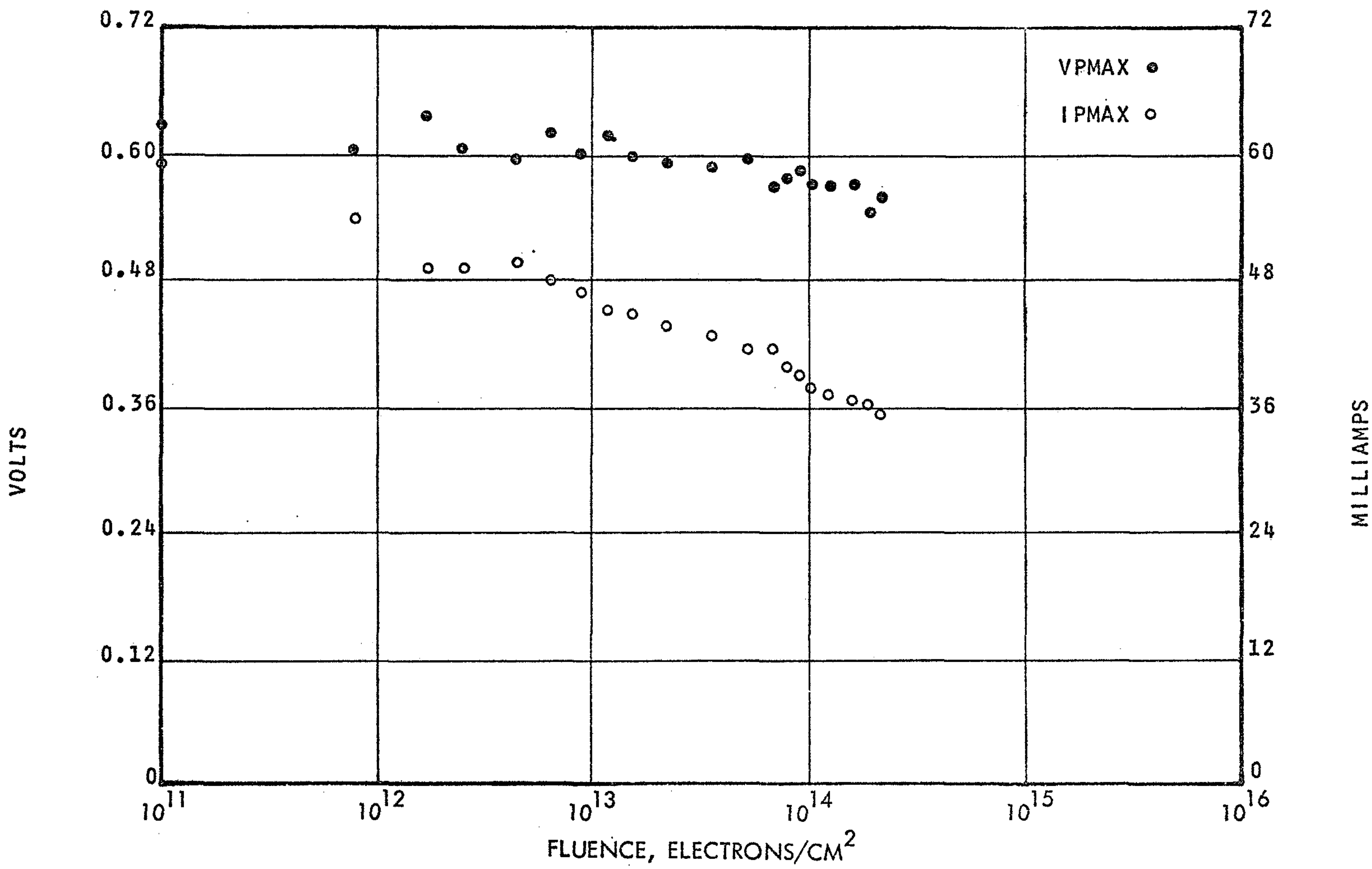

FIGURE 16 - GROUP B CURRENT AND VOLTAGE AT MAXIMUM POWER

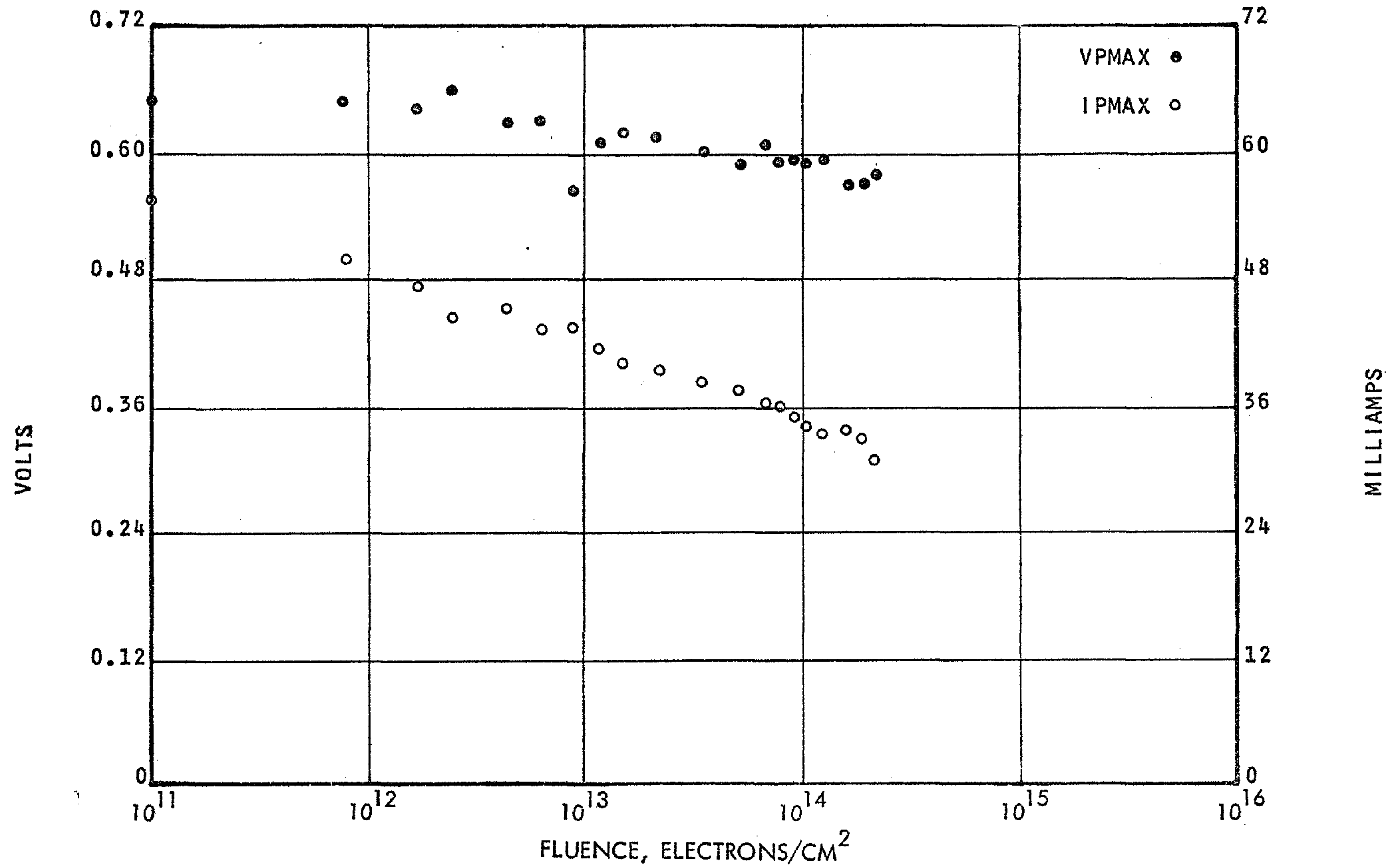

FIGURE 17 - GROUP C CURRENT AND VOLTAGE AT MAXIMUM POWER

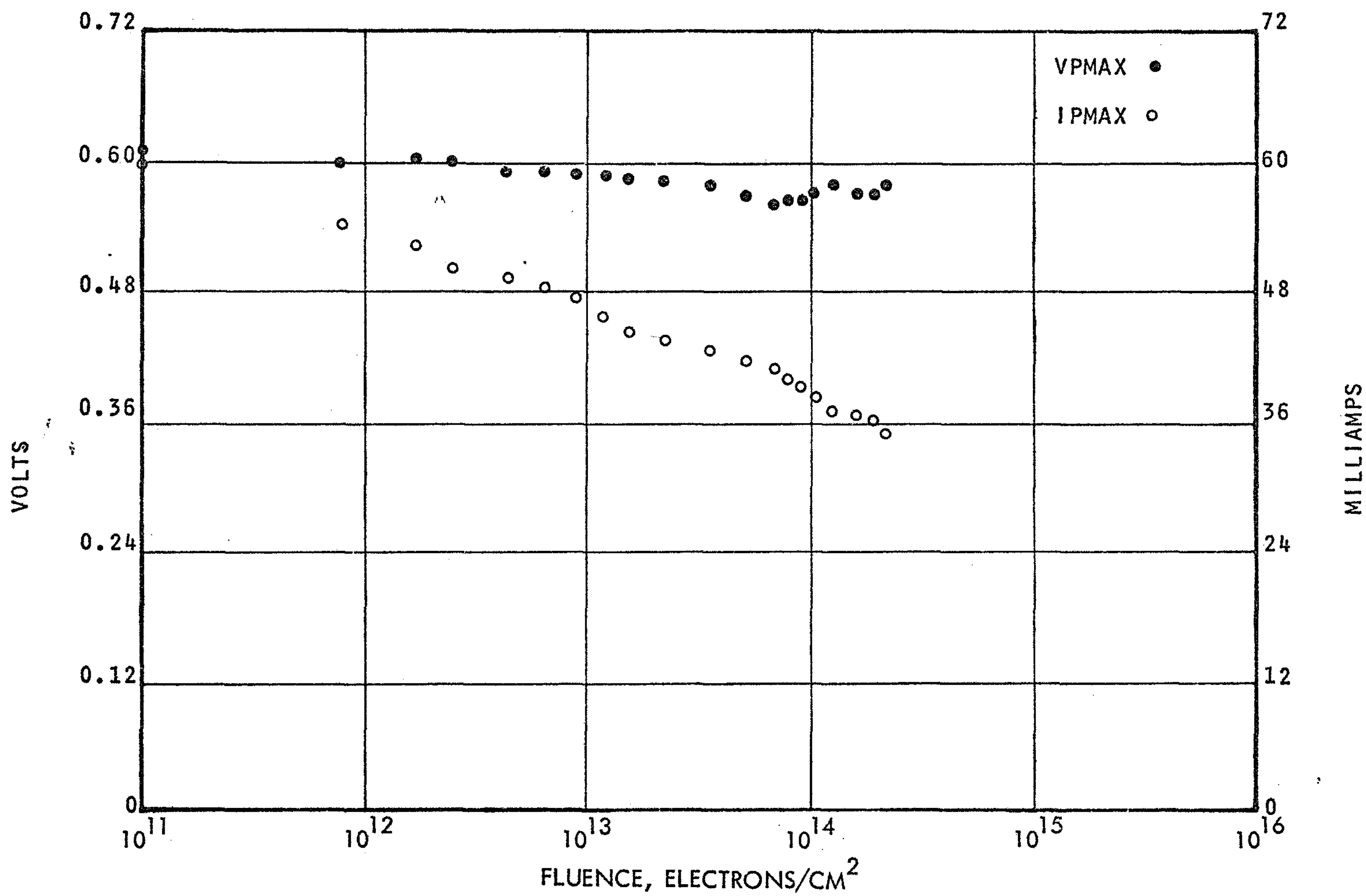

FIGURE 18 - GROUP D CURRENT AND VOLTAGE AT MAXIMUM POWER

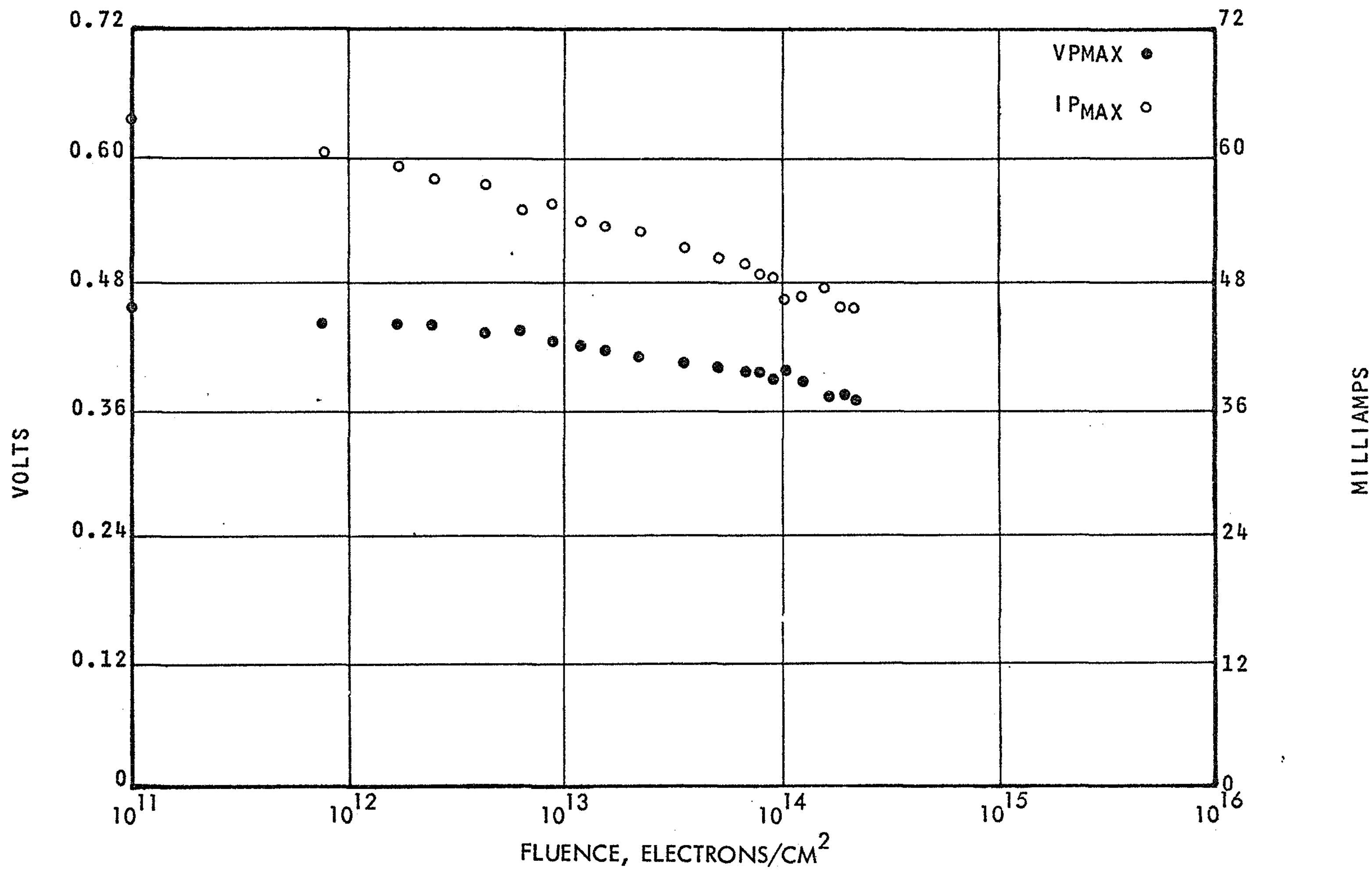

FIGURE 19 - GROUP E CURRENT AND VOLTAGE AT MAXIMUM POWER

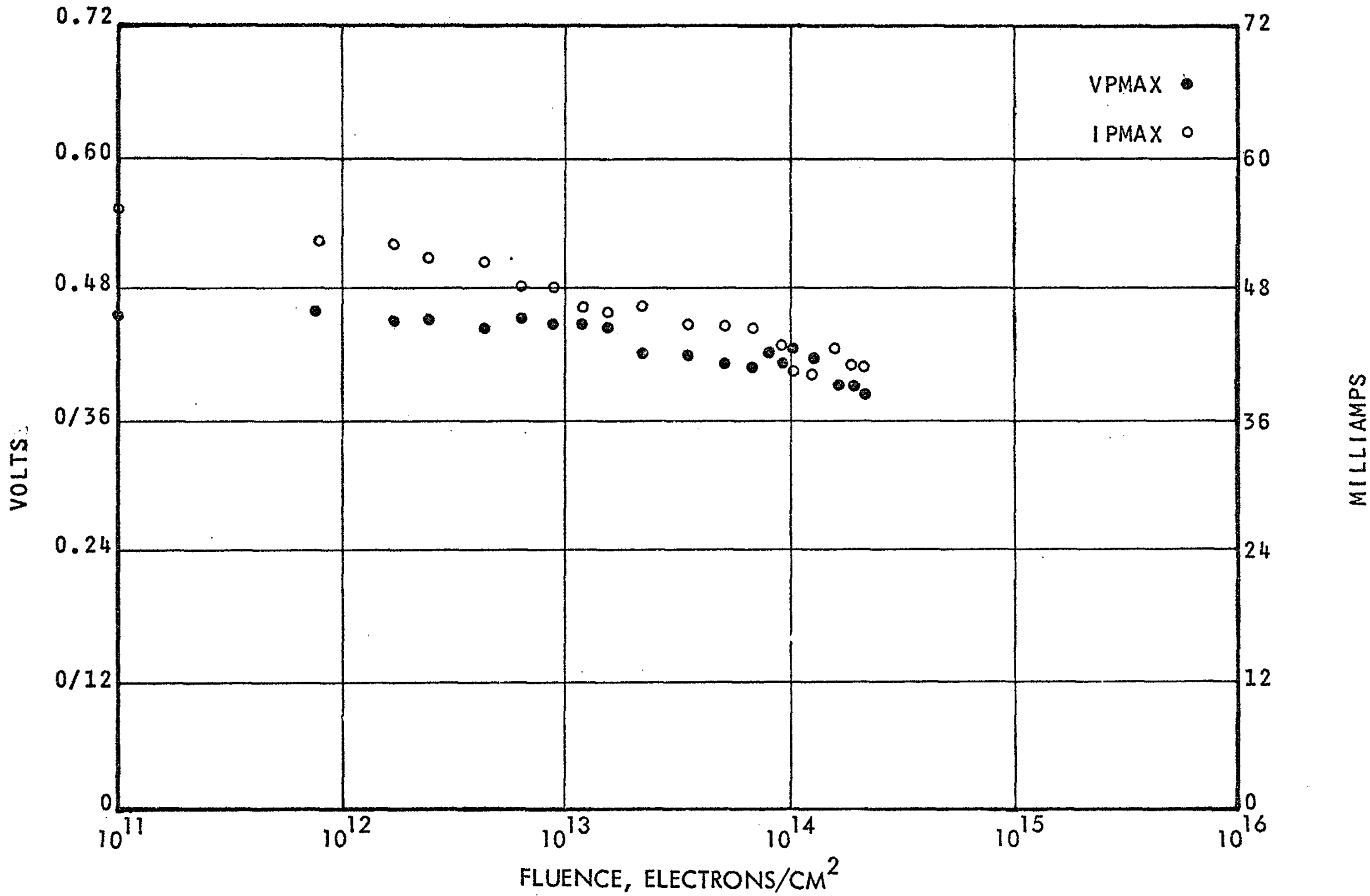

FIGURE 20 - GROUP F CURRENT AND VOLTAGE AT MAXIMUM POWER

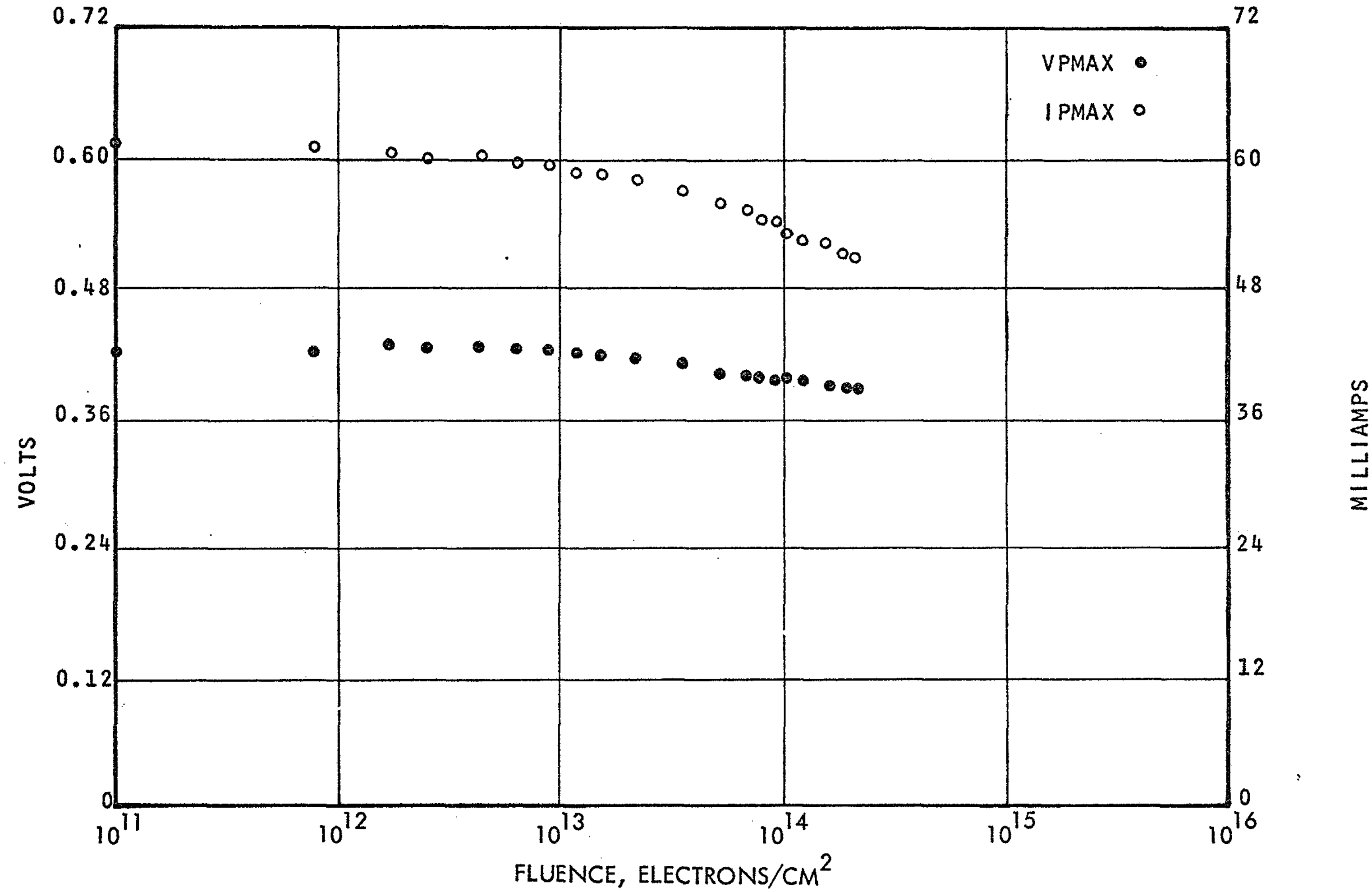

FIGURE 21 - GROUP G CURRENT AND VOLTAGE AT MAXIMUM POWER

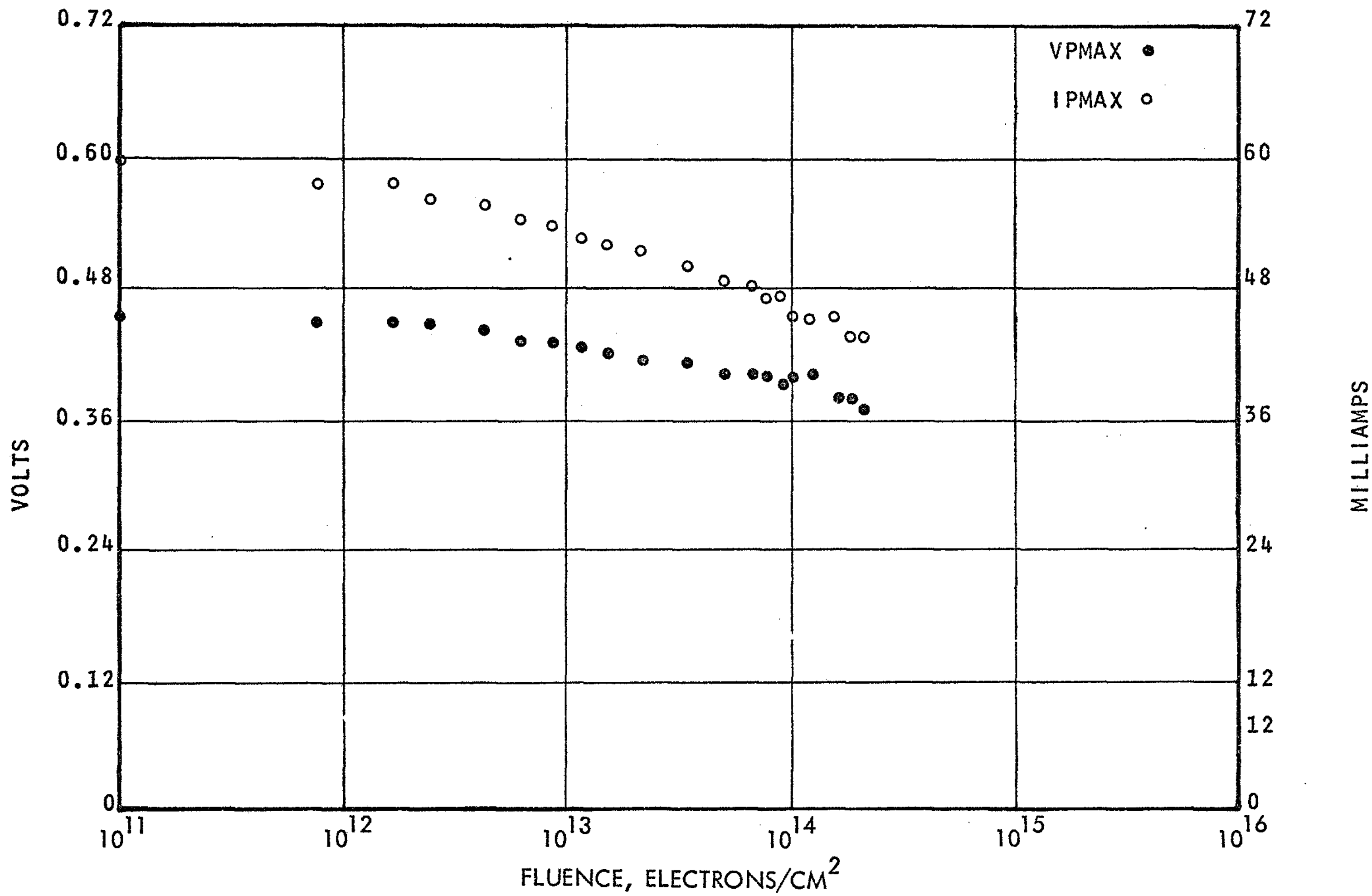

FIGURE 22 - GROUP H CURRENT AND VOLTAGE AT MAXIMUM POWER

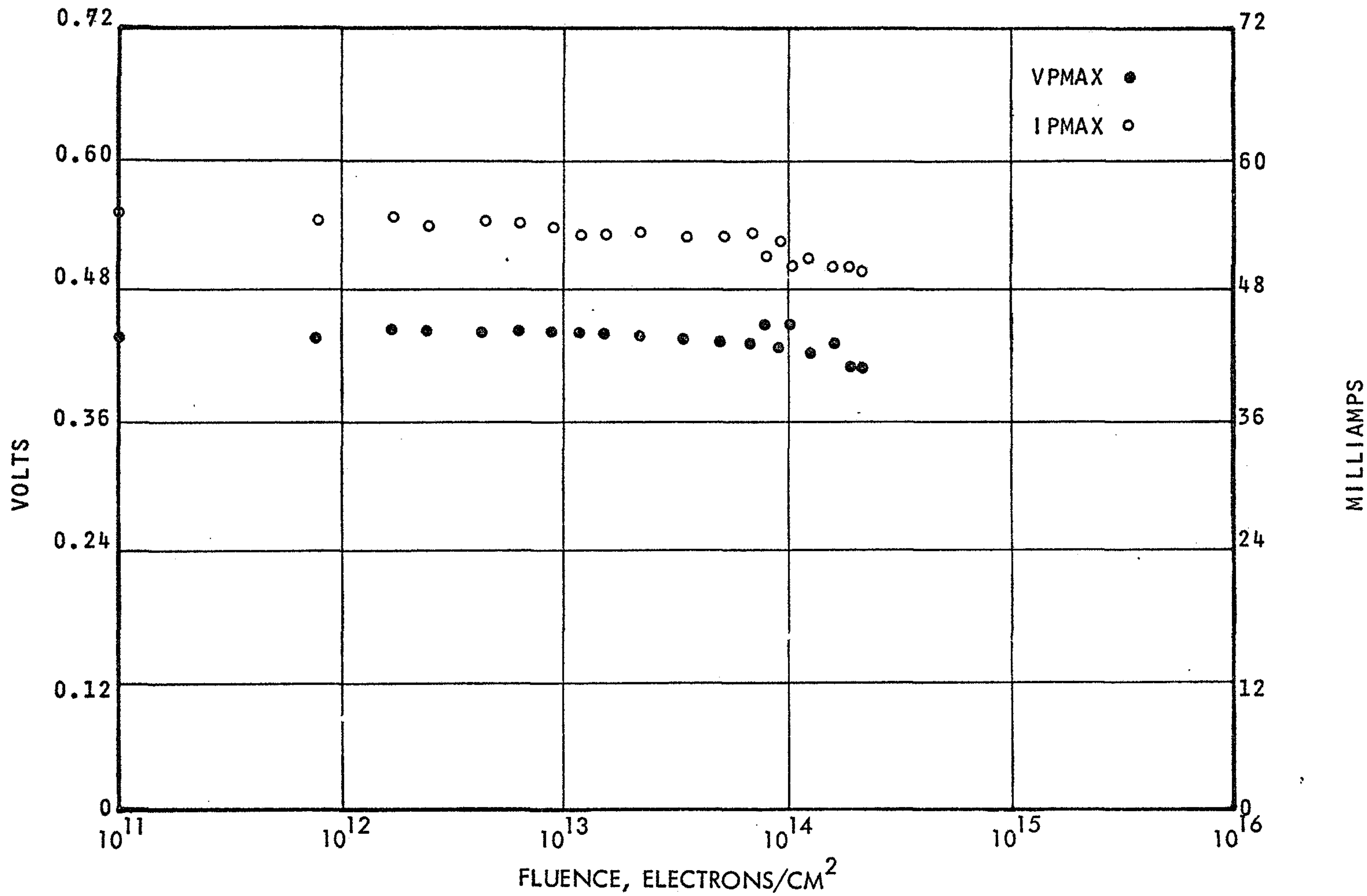

FIGURE 23 - GROUP I CURRENT AND VOLTAGE AT MAXIMUM POWER

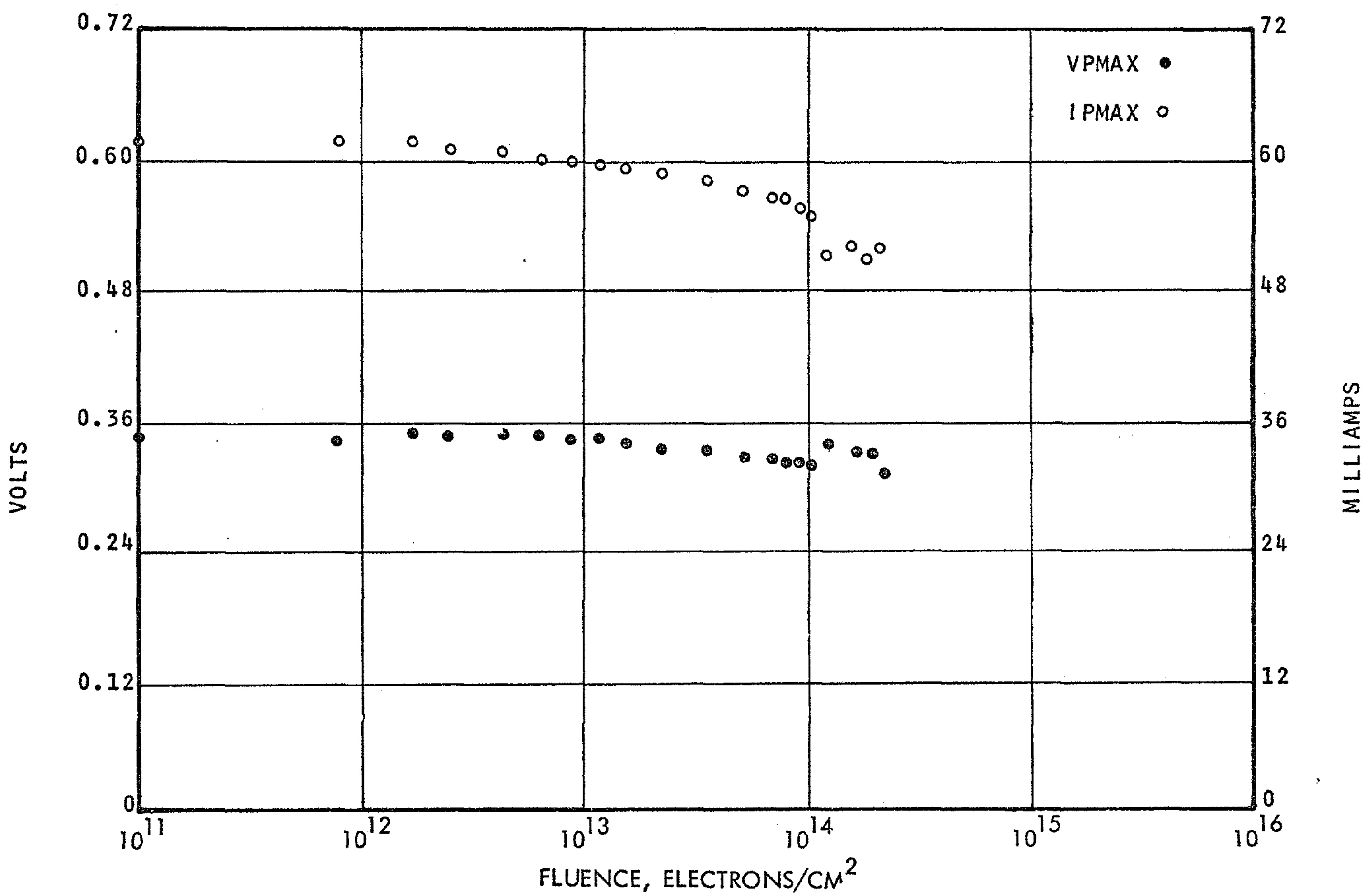

FIGURE 24 - GROUP J CURRENT AND VOLTAGE AT MAXIMUM POWER

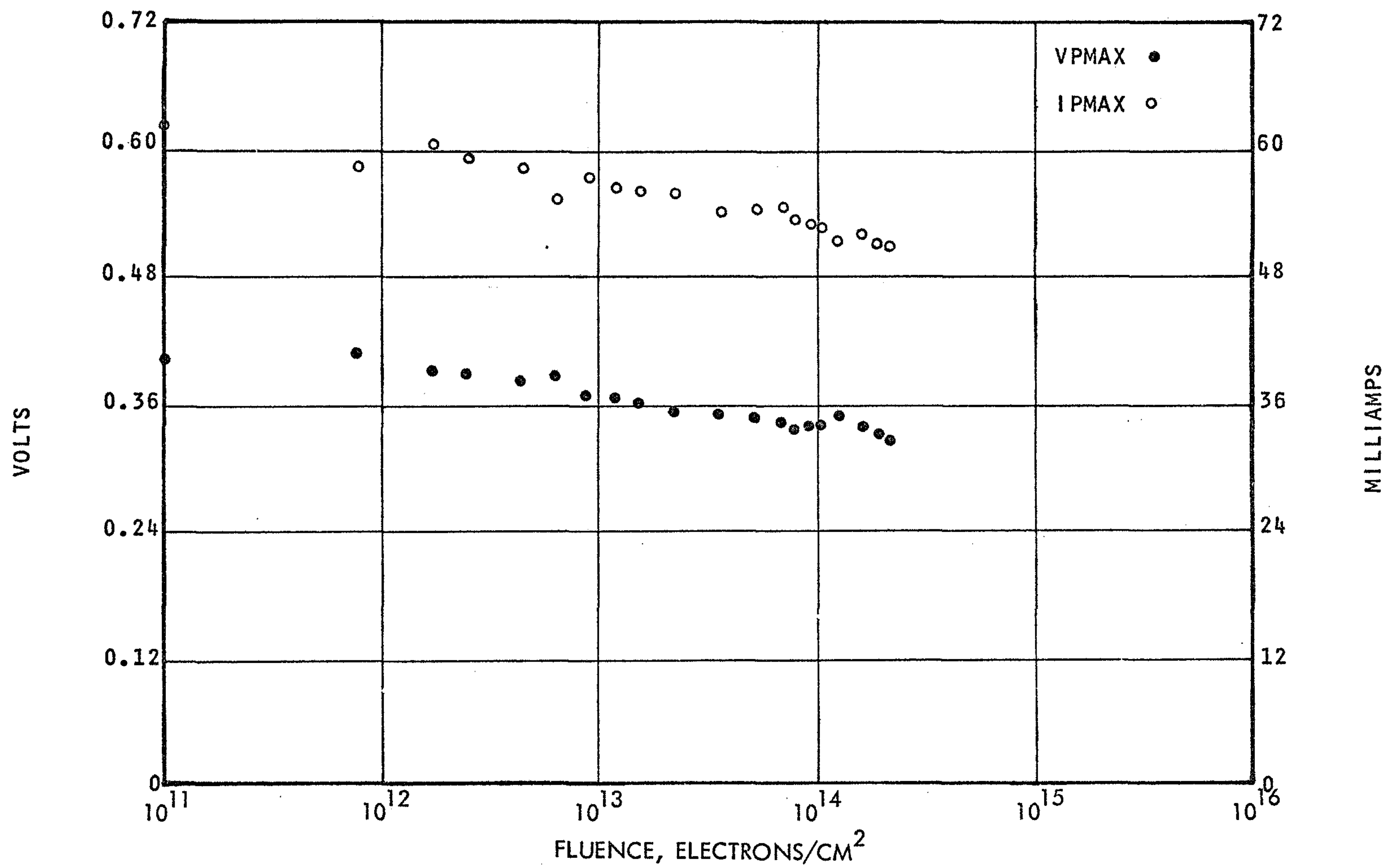

FIGURE 25 - GROUP K CURRENT AND VOLTAGE AT MAXIMUM POWER

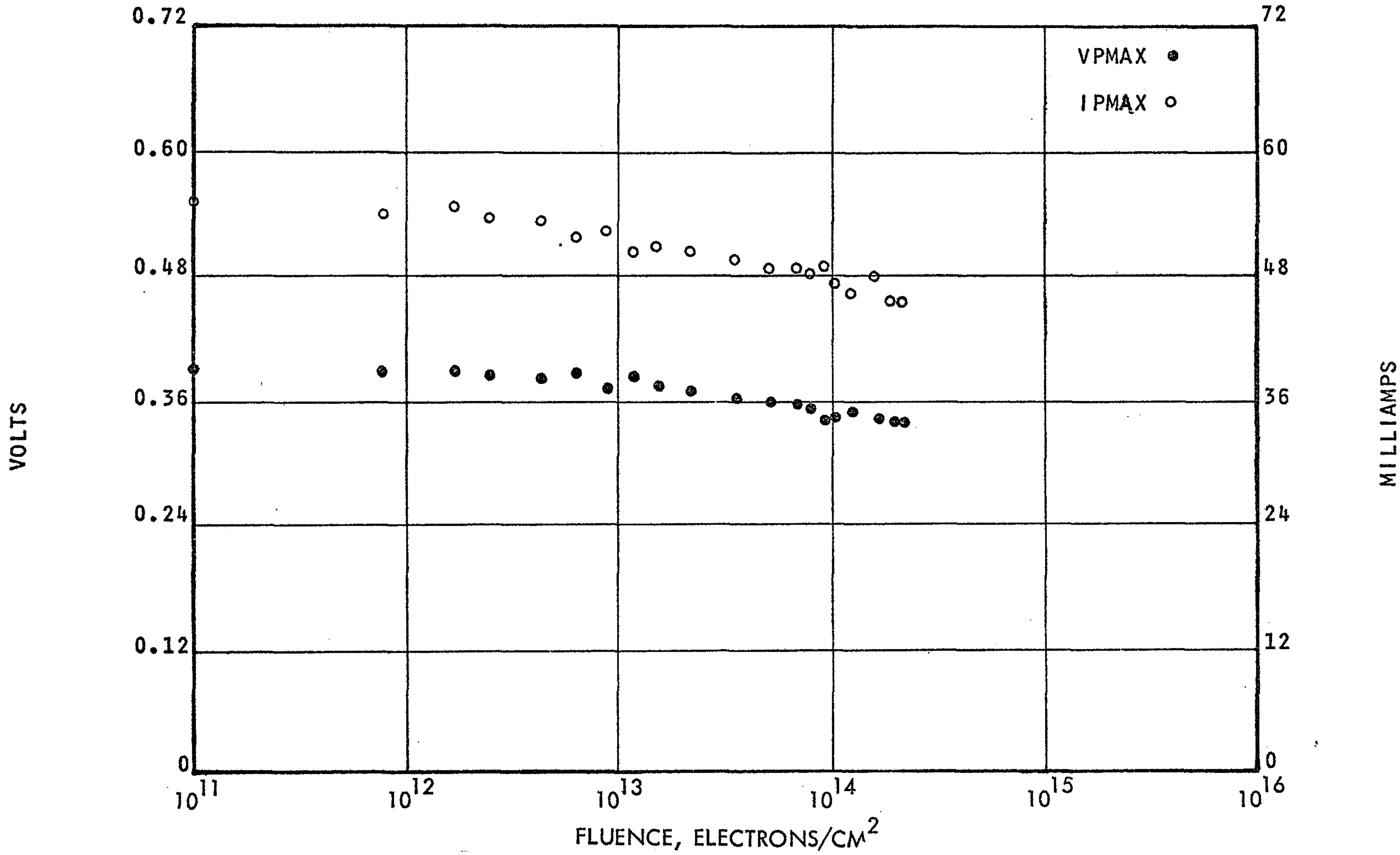

FIGURE 26 - GROUP L CURRENT AND VOLTAGE AT MAXIMUM POWER

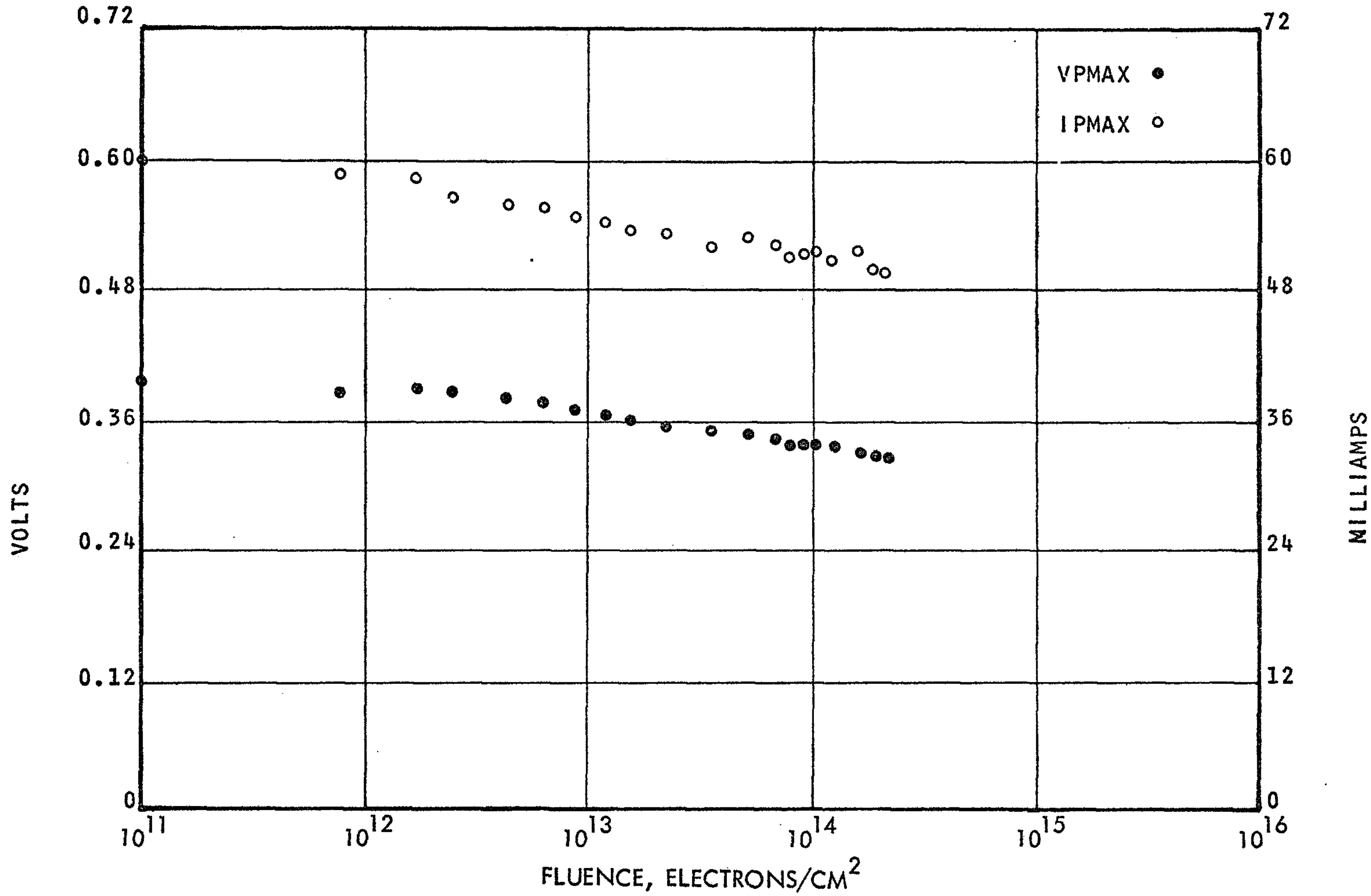

FIGURE 27 - GROUP M CURRENT AND VOLTAGE AT MAXIMUM POWER

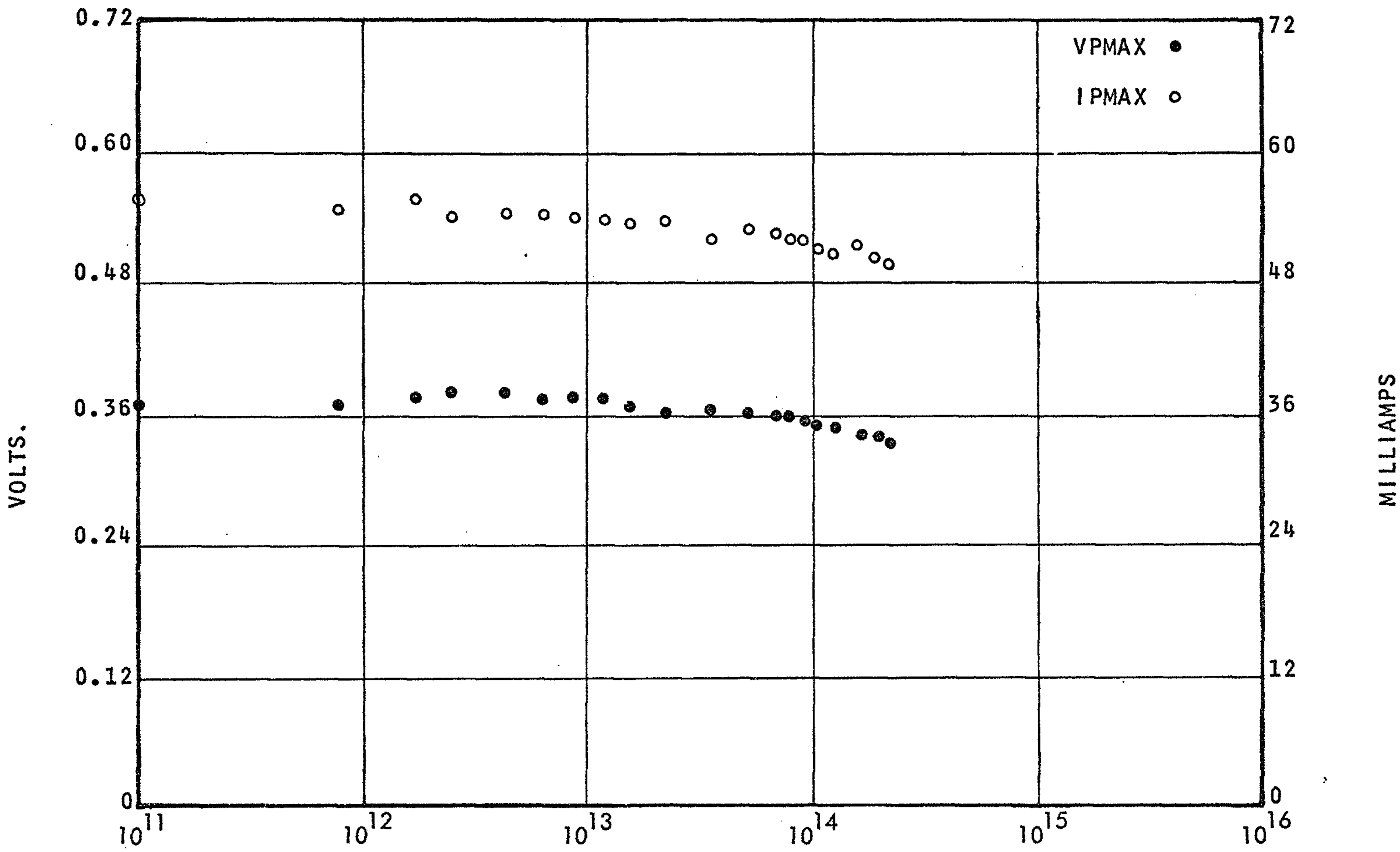

FIGURE 28 - GROUP N CURRENT AND VOLTAGE AT MAXIMUM POWER

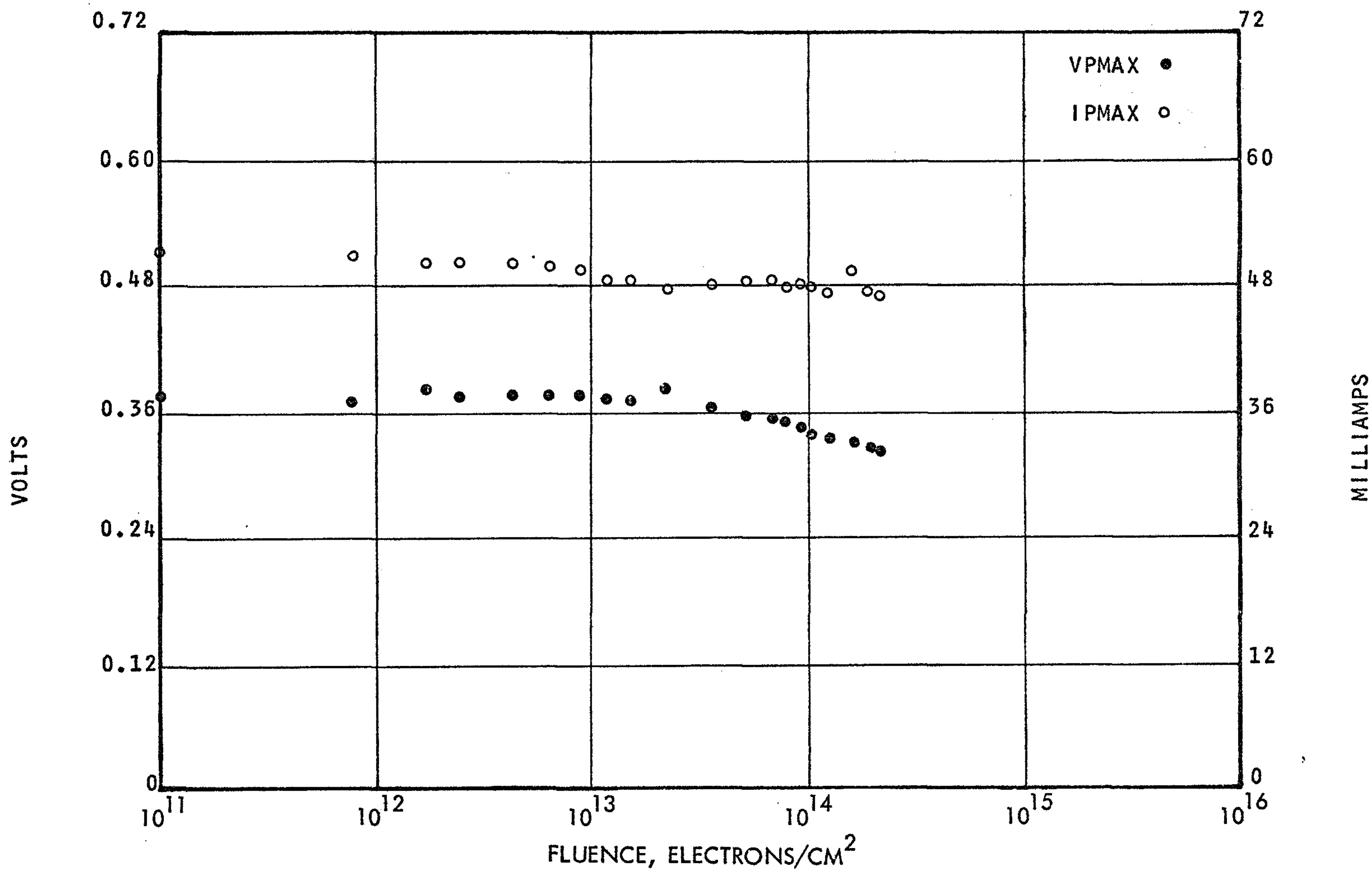

FIGURE 29 - GROUP O CURRENT AND VOLTAGE AT MAXIMUM POWER

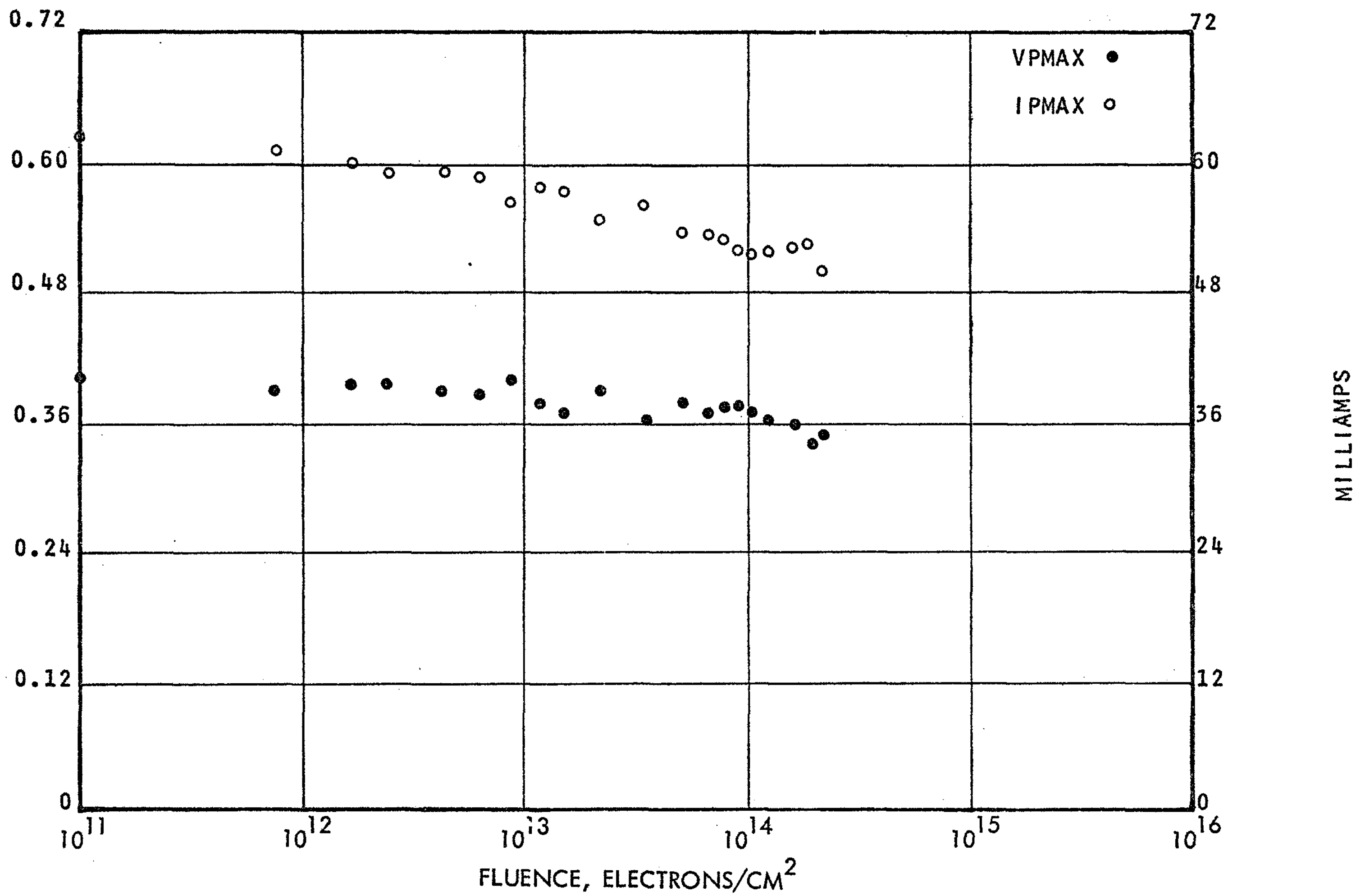

FIGURE 30 - GROUP P CURRENT AND VOLTAGE AT MAXIMUM POWER

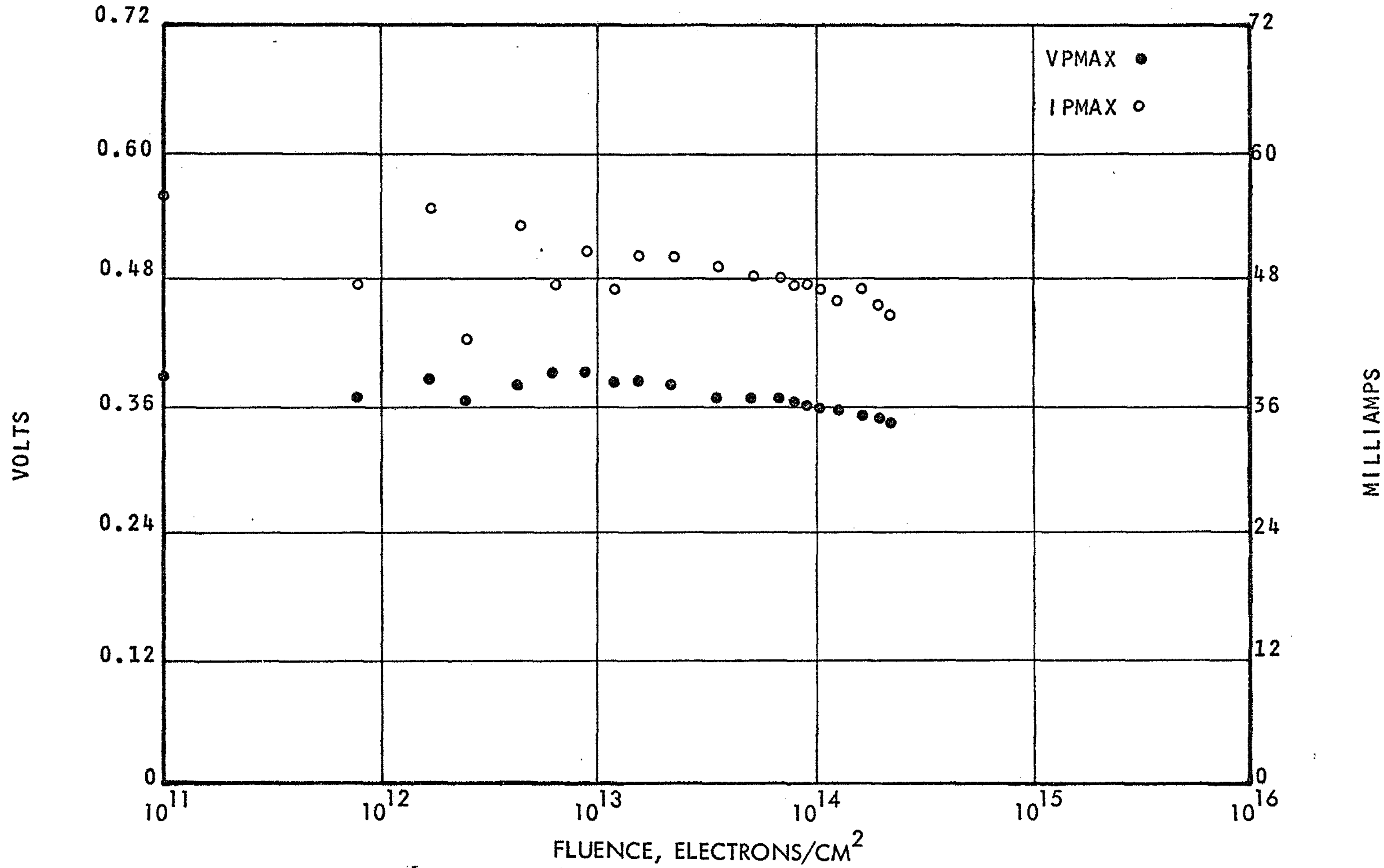

FIGURE 31 - GROUP R CURRENT AND VOLTAGE AT MAXIMUM POWER

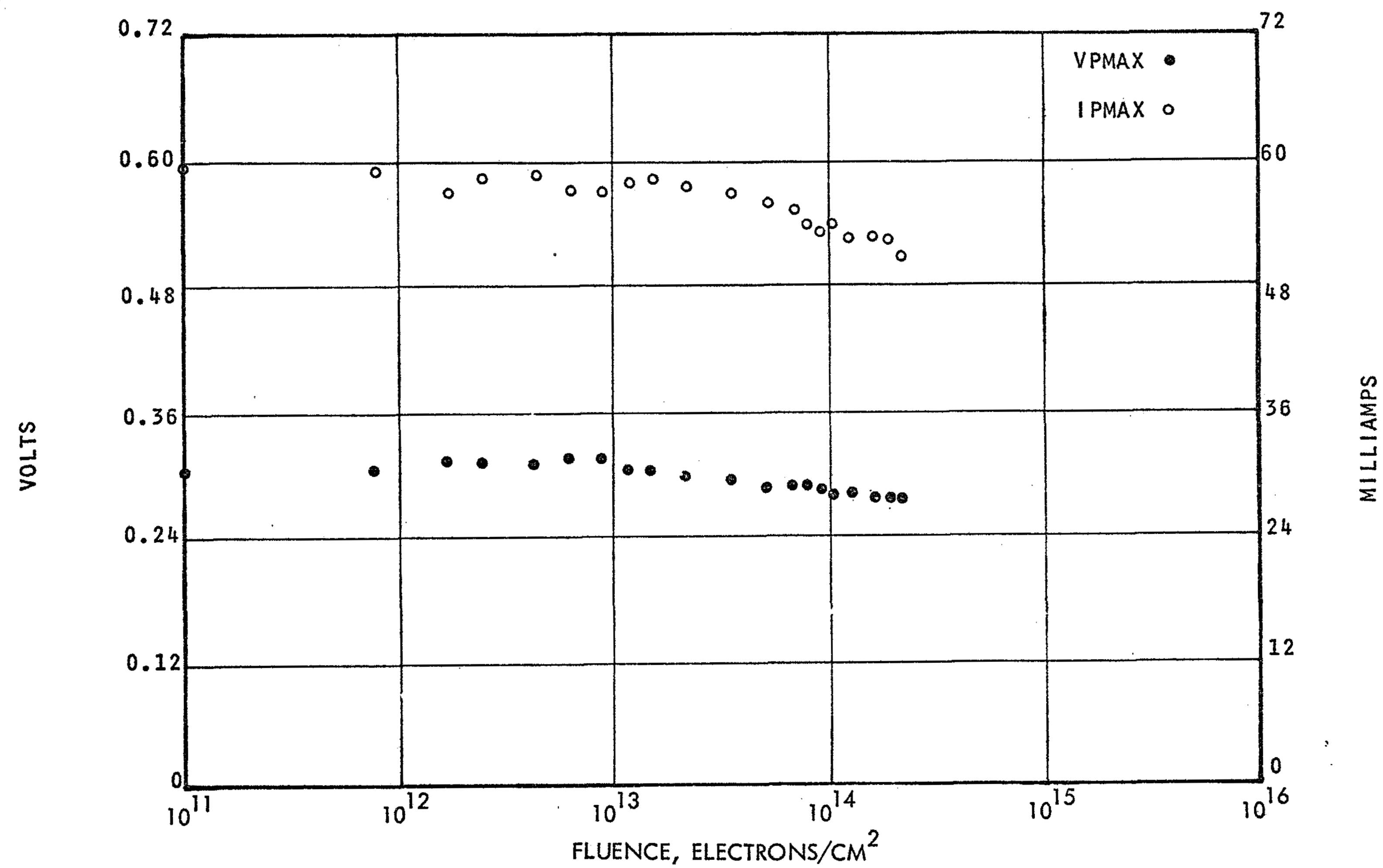

FIGURE 32 - GROUP S CURRENT AND VOLTAGE AT MAXIMUM POWER

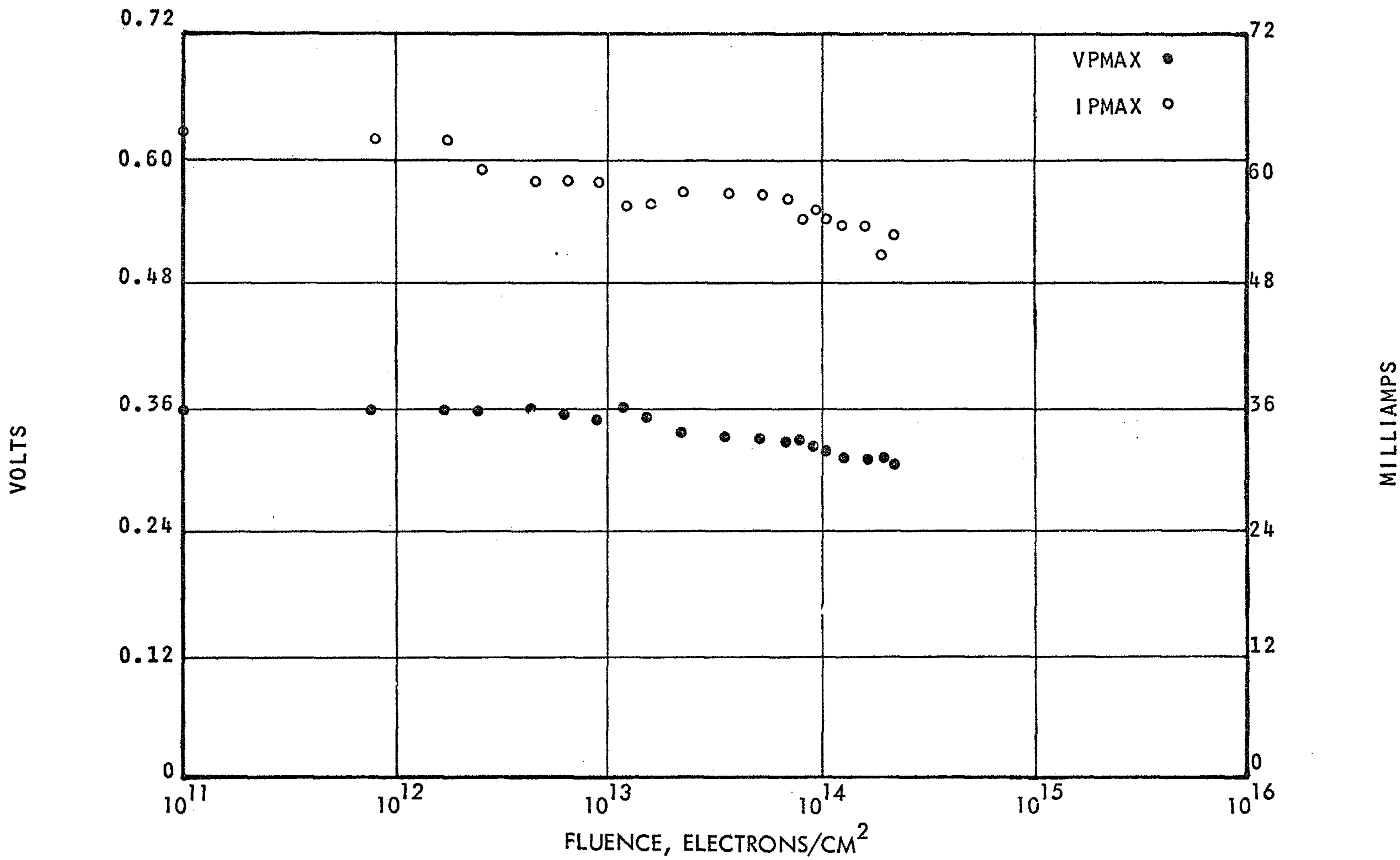

FIGURE 33 - GROUP T CURRENT AND VOLTAGE AT MAXIMUM POWER

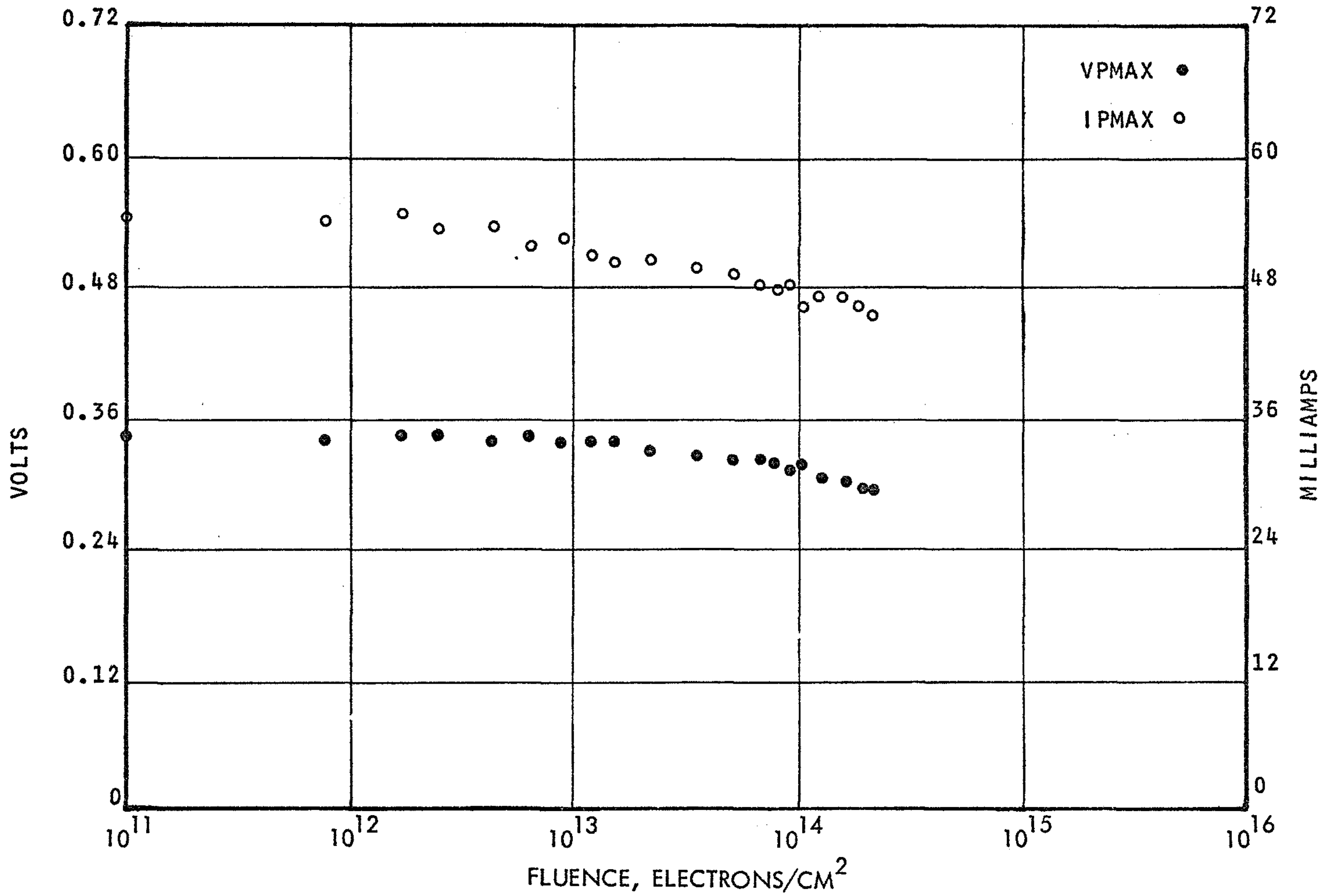

FIGURE 34 - GROUP U CURRENT AND VOLTAGE AT MAXIMUM POWER

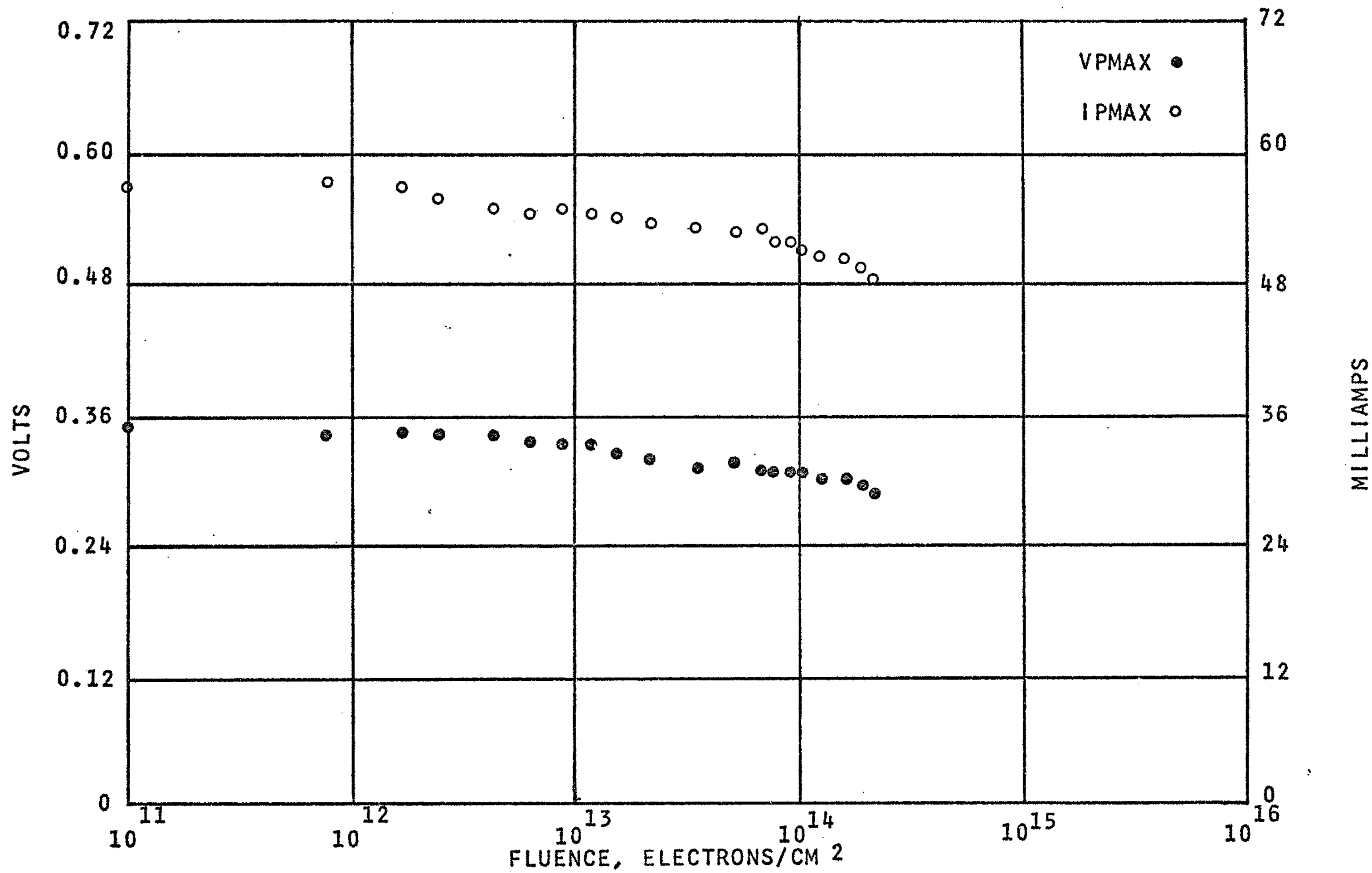

FIGURE 35 - GROUP W CURRENT AND VOLTAGE AT MAXIMUM POWER

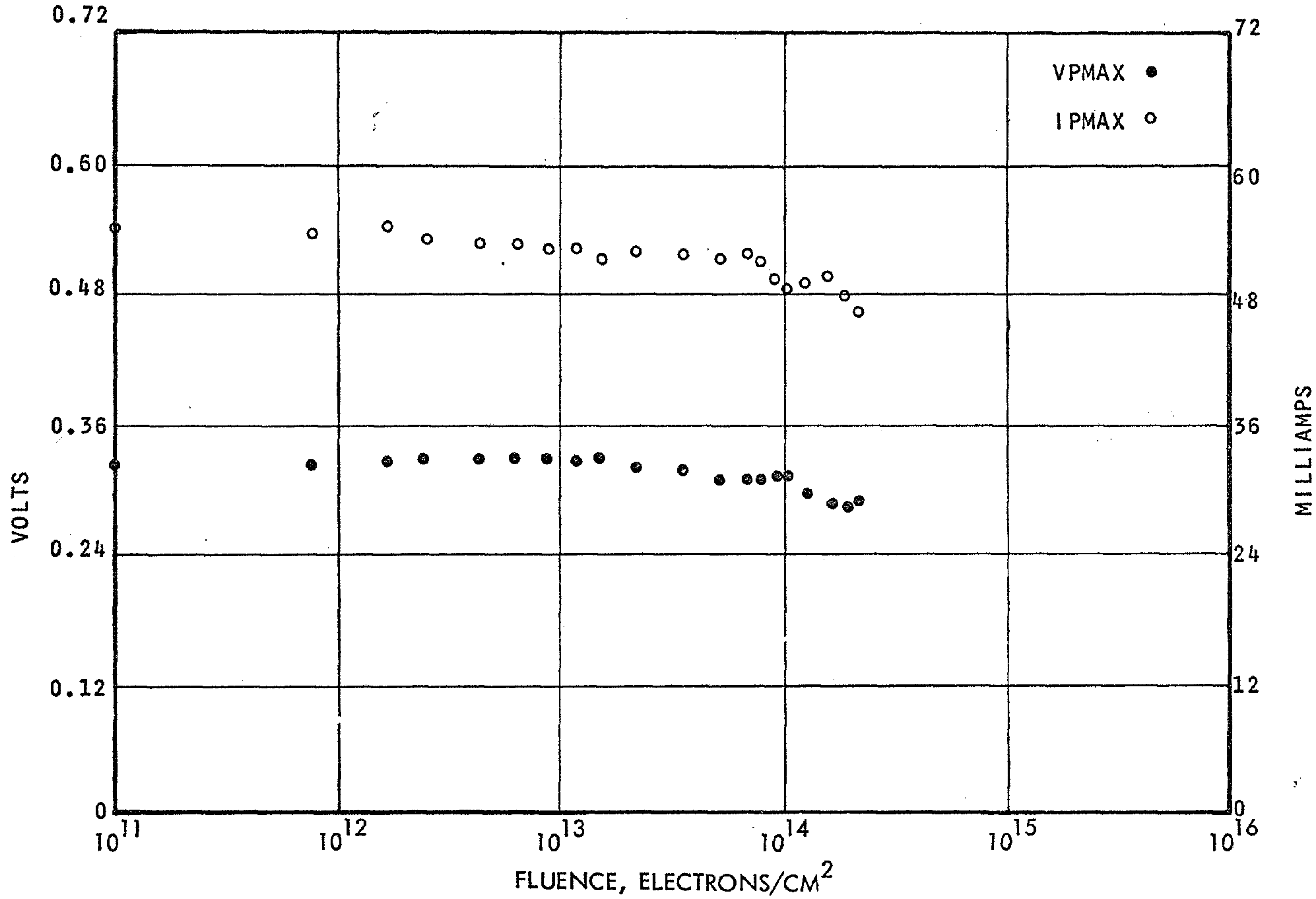

FIGURE 36 - GROUP X CURRENT AND VOLTAGE AT MAXIMUM POWER

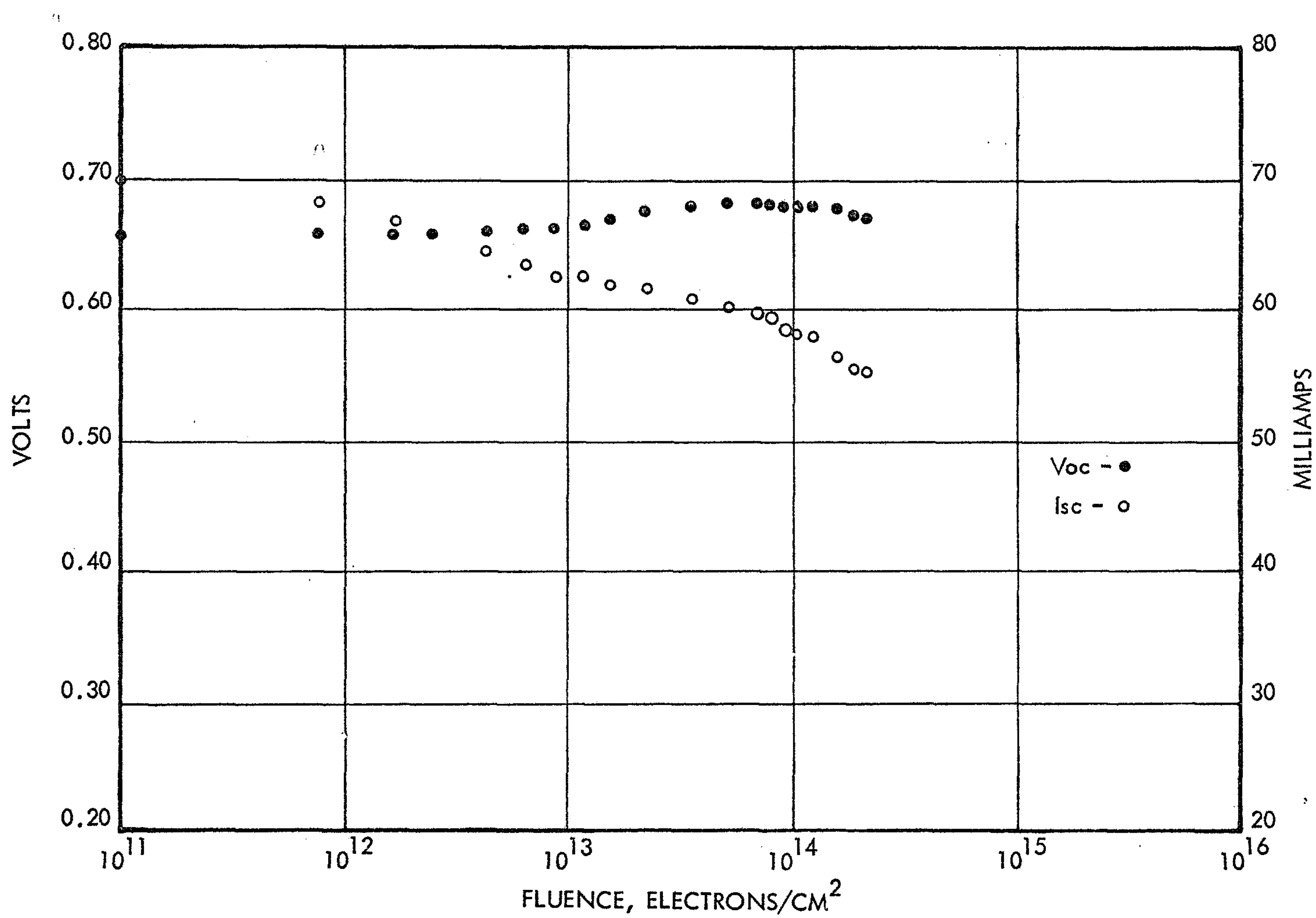

FIGURE 37 - GROUP A OPEN CIRCUIT VOLTAGE AND SHORT CIRCUIT CURRENT

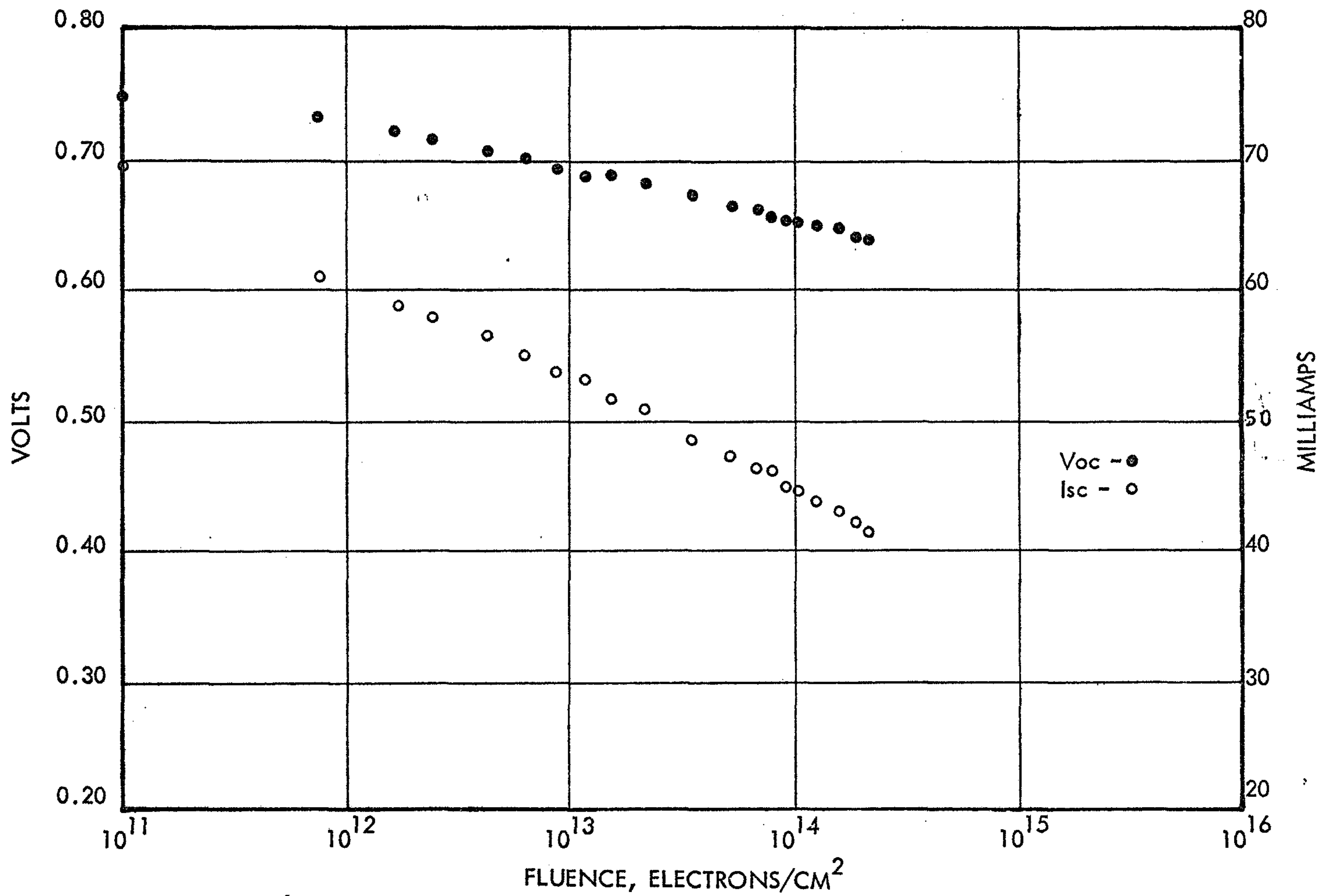

FIGURE 38 - GROUP B OPEN CIRCUIT VOLTAGE AND SHORT CIRCUIT CURRENT

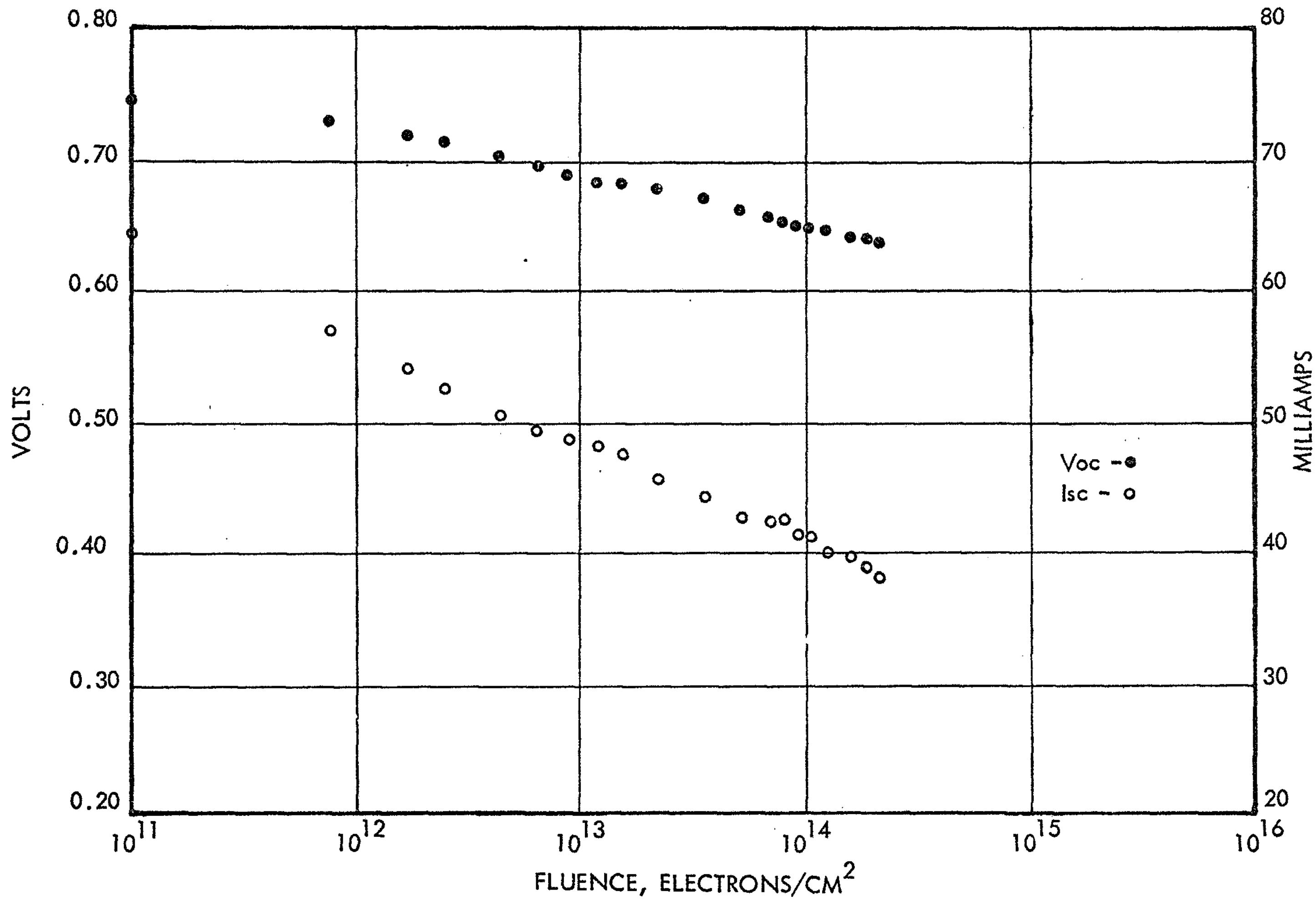

FIGURE 39 - GROUP C OPEN CIRCUIT VOLTAGE AND SHORT CIRCUIT CURRENT

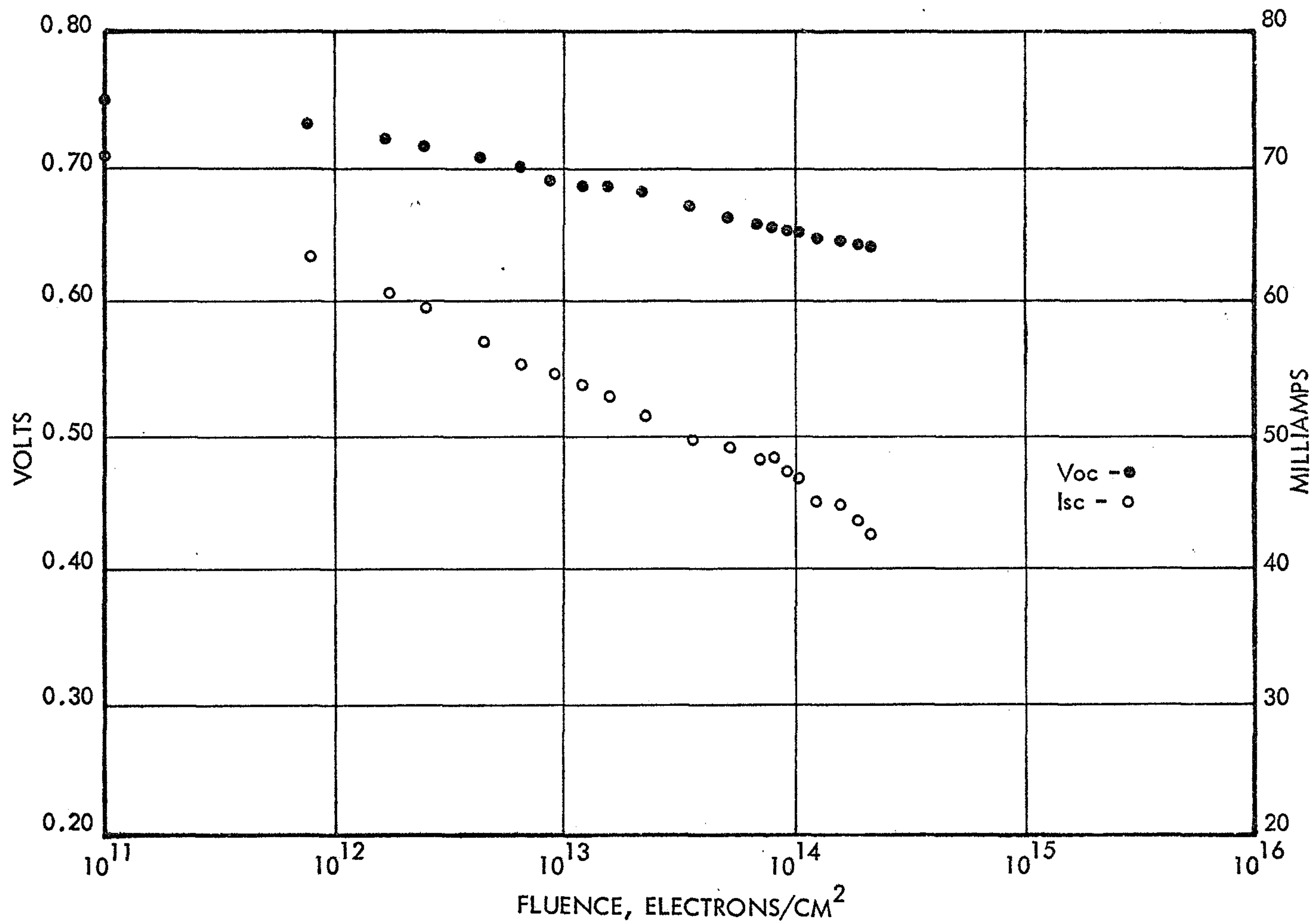

FIGURE 40 - GROUP D OPEN CIRCUIT VOLTAGE AND SHORT CIRCUIT CURRENT

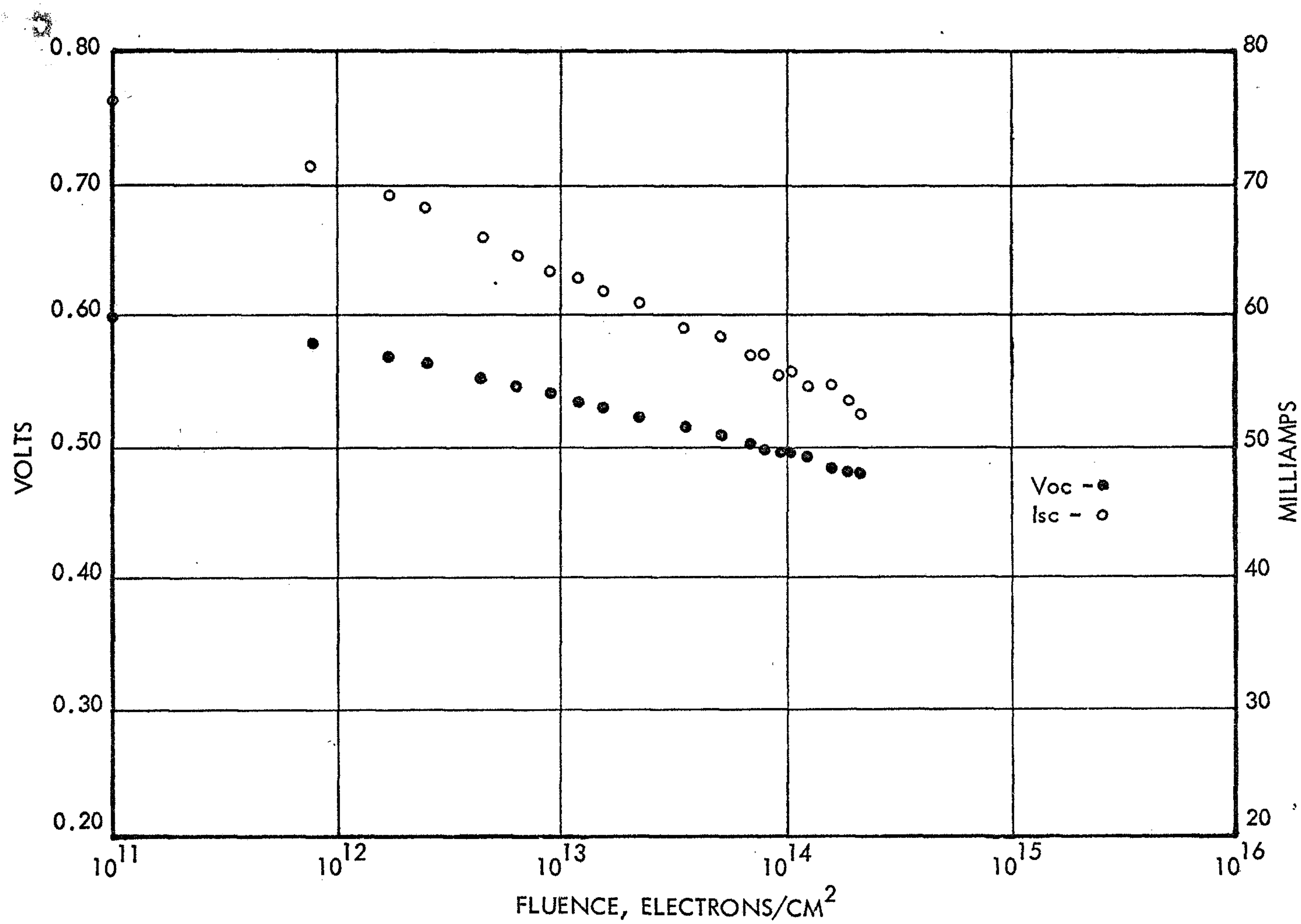

FIGURE 41 - GROUP E OPEN CIRCUIT VOLTAGE AND SHORT CIRCUIT CURRENT

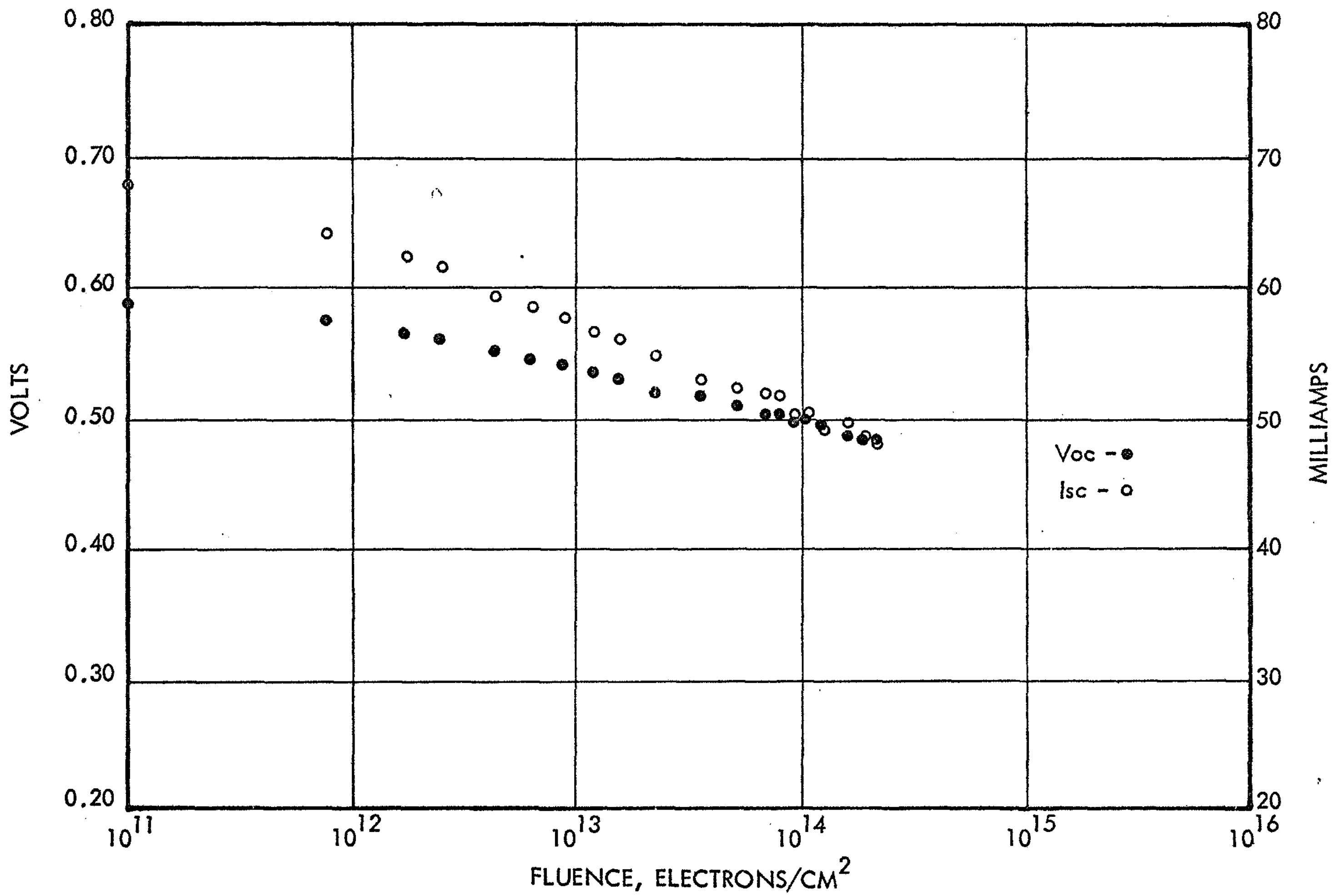

FIGURE 42 - GROUP F OPEN CIRCUIT VOLTAGE AND SHORT CIRCUIT CURRENT

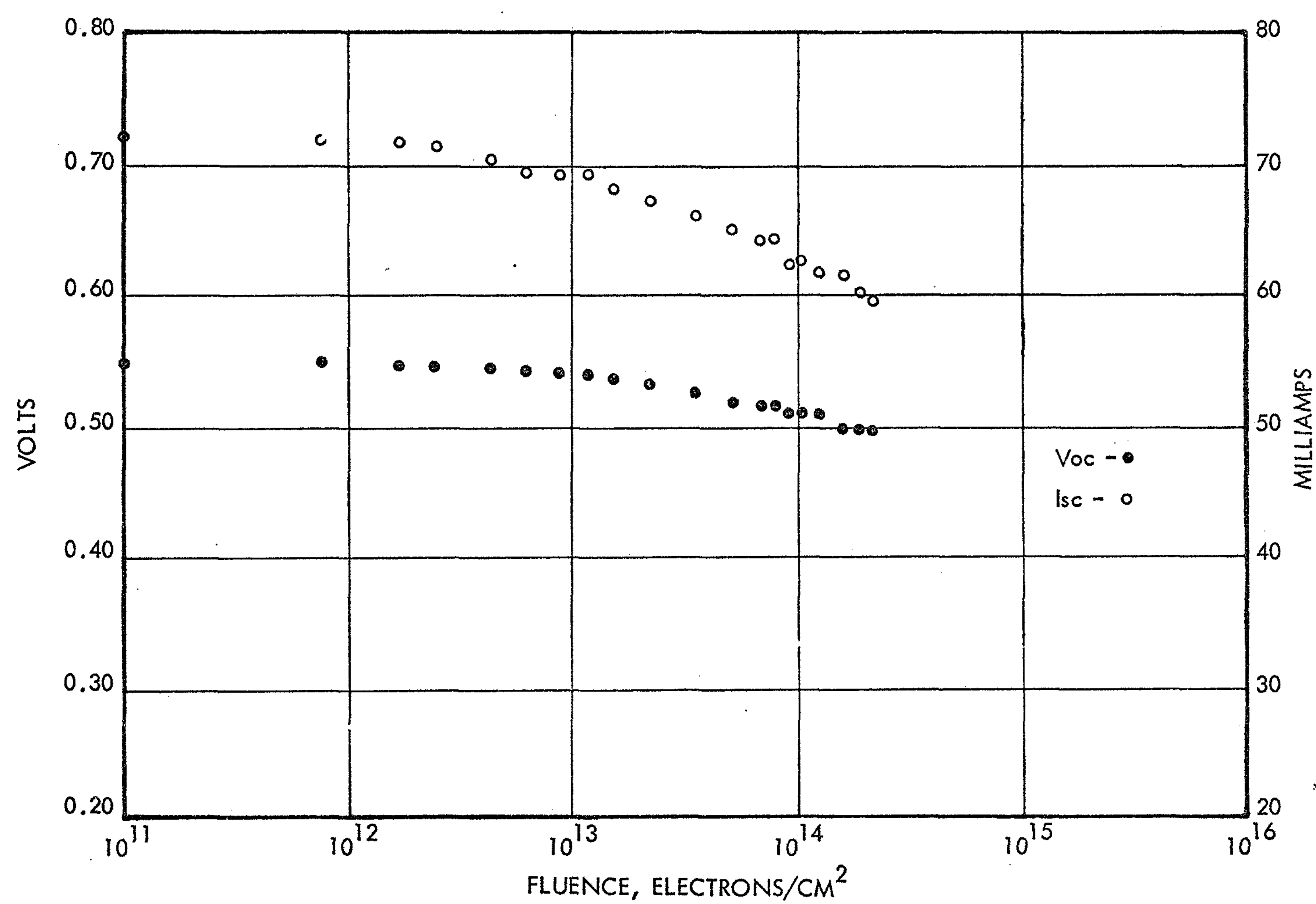

FIGURE 43 - GROUP G OPEN CIRCUIT VOLTAGE AND SHORT CIRCUIT CURRENT

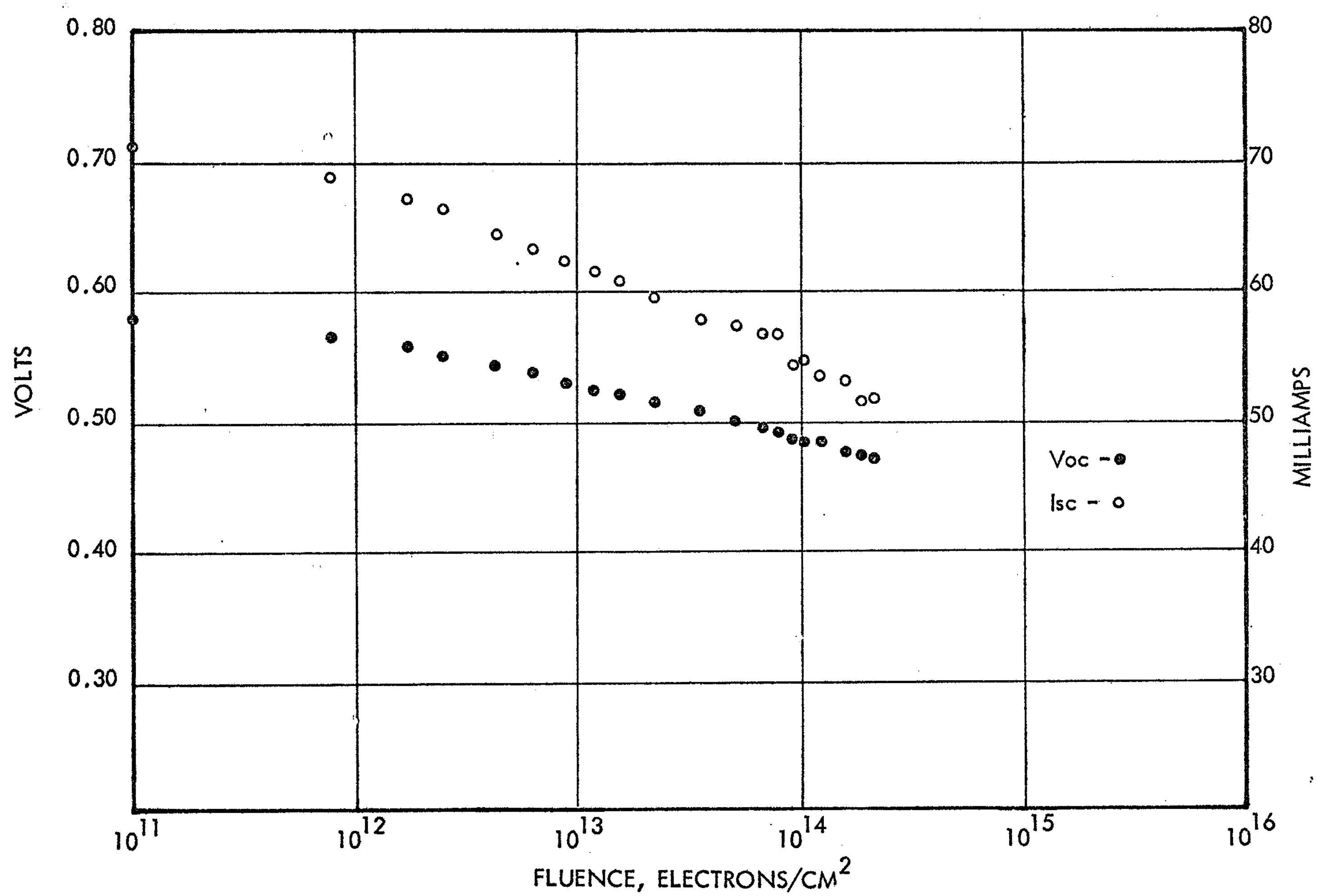

FIGURE 44 - GROUP H OPEN CIRCUIT VOLTAGE AND SHORT CIRCUIT CURRENT

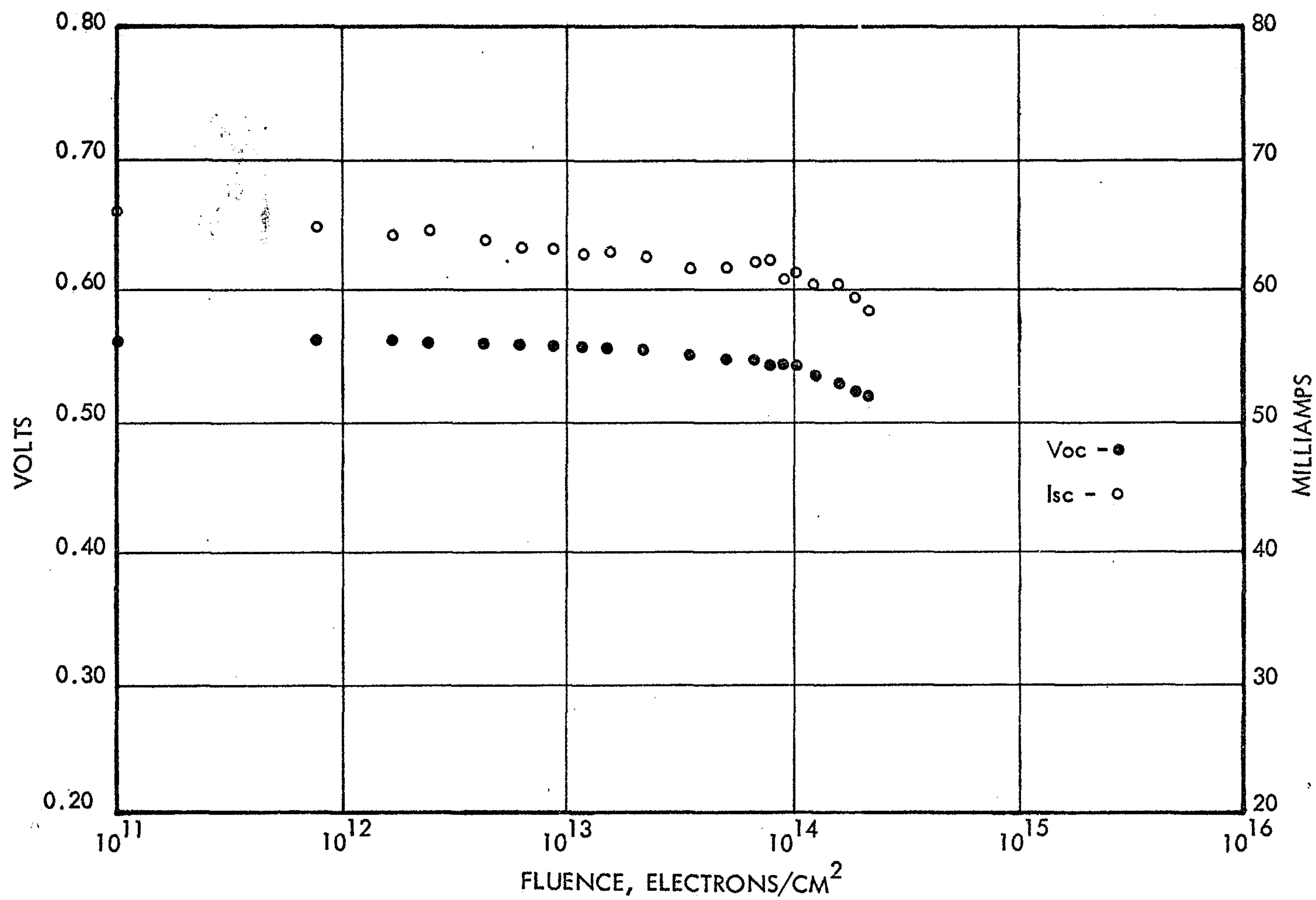

FIGURE 45 - GROUP I OPEN CIRCUIT VOLTAGE AND SHORT CIRCUIT CURRENT

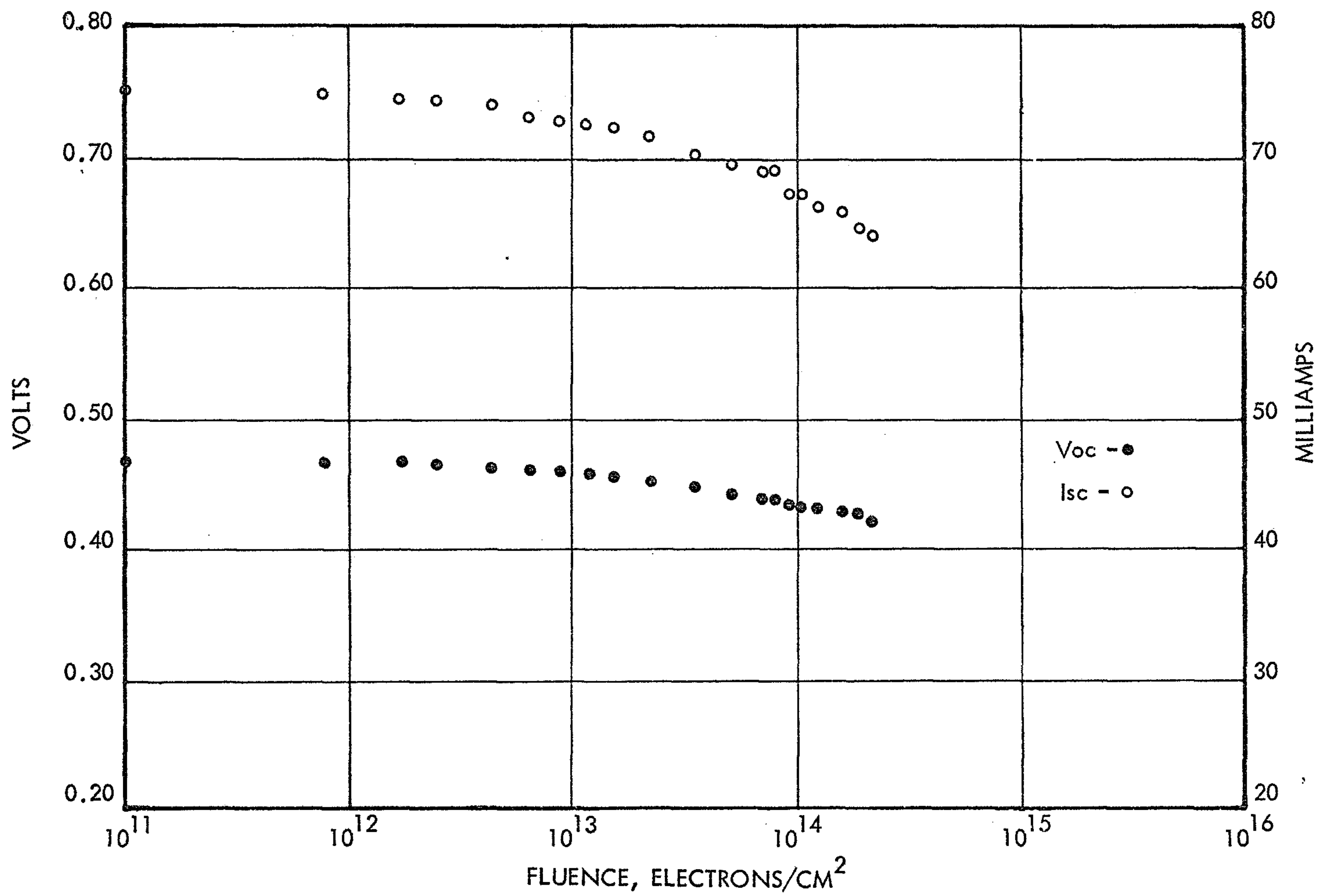

FIGURE 46 - GROUP J OPEN CIRCUIT VOLTAGE AND SHORT CIRCUIT CURRENT

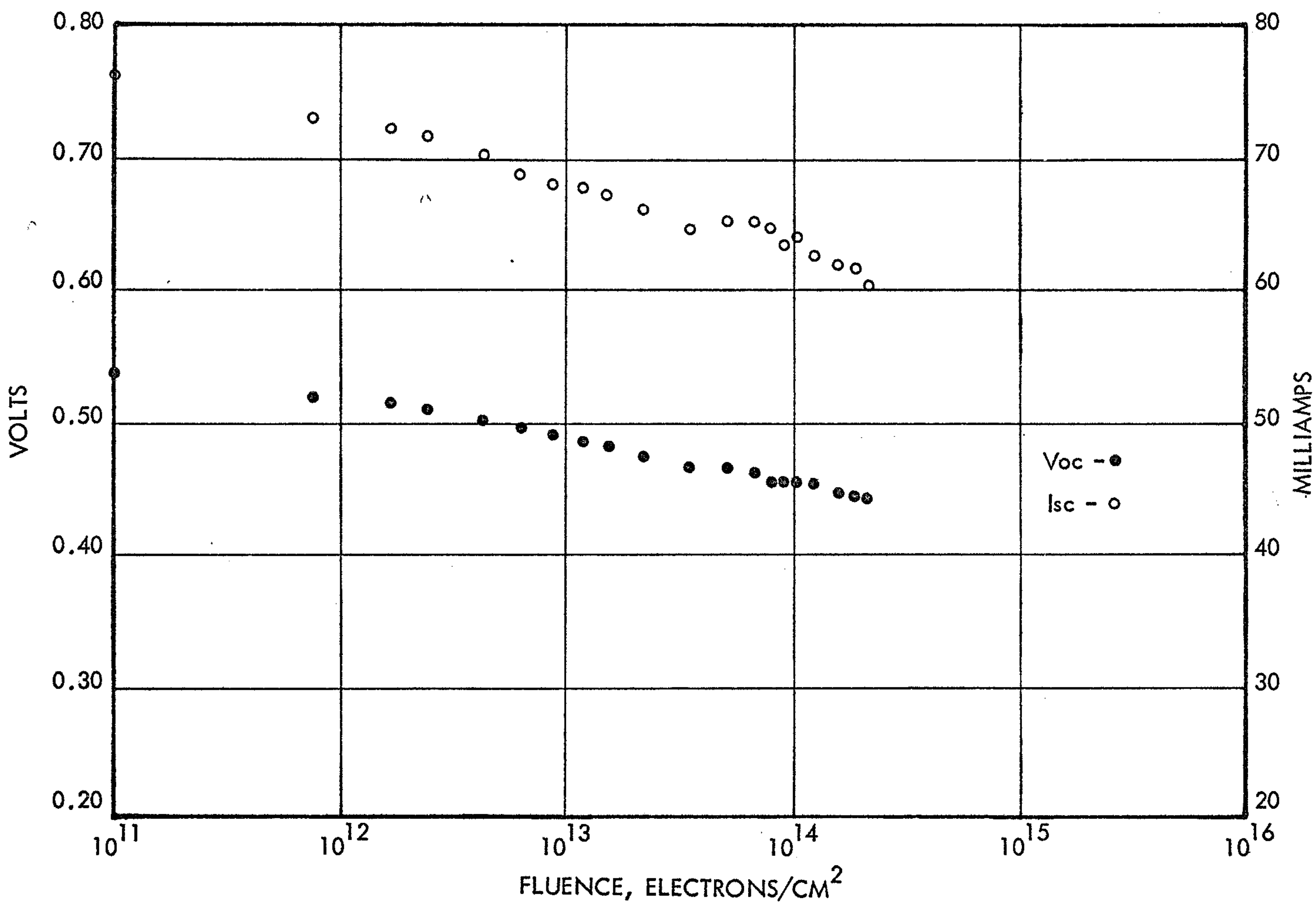

FIGURE 47 - GROUP K OPEN CIRCUIT VOLTAGE AND SHORT CIRCUIT CURRENT

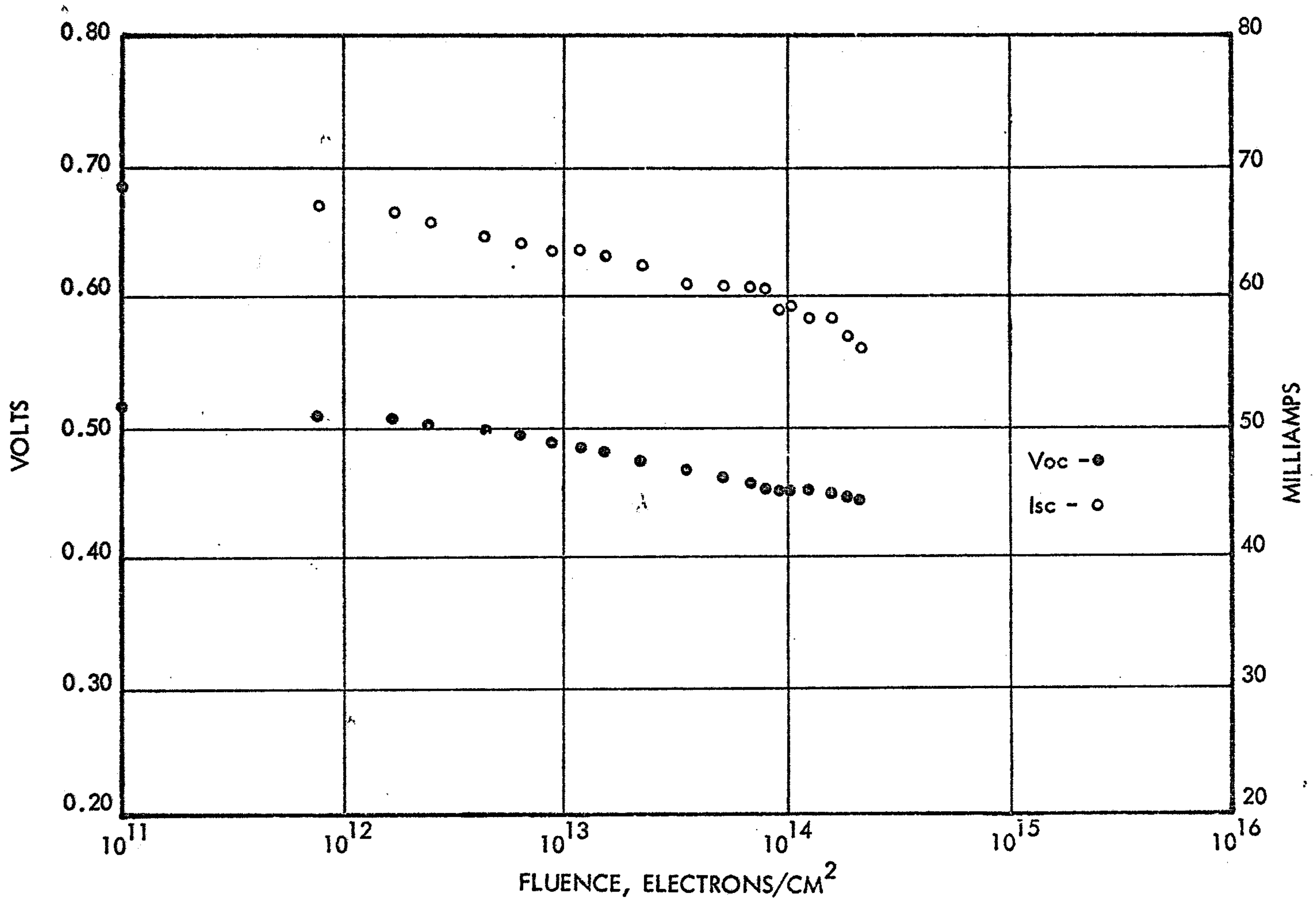

FIGURE 48 - GROUP L OPEN CIRCUIT VOLTAGE AND SHORT CIRCUIT CURRENT

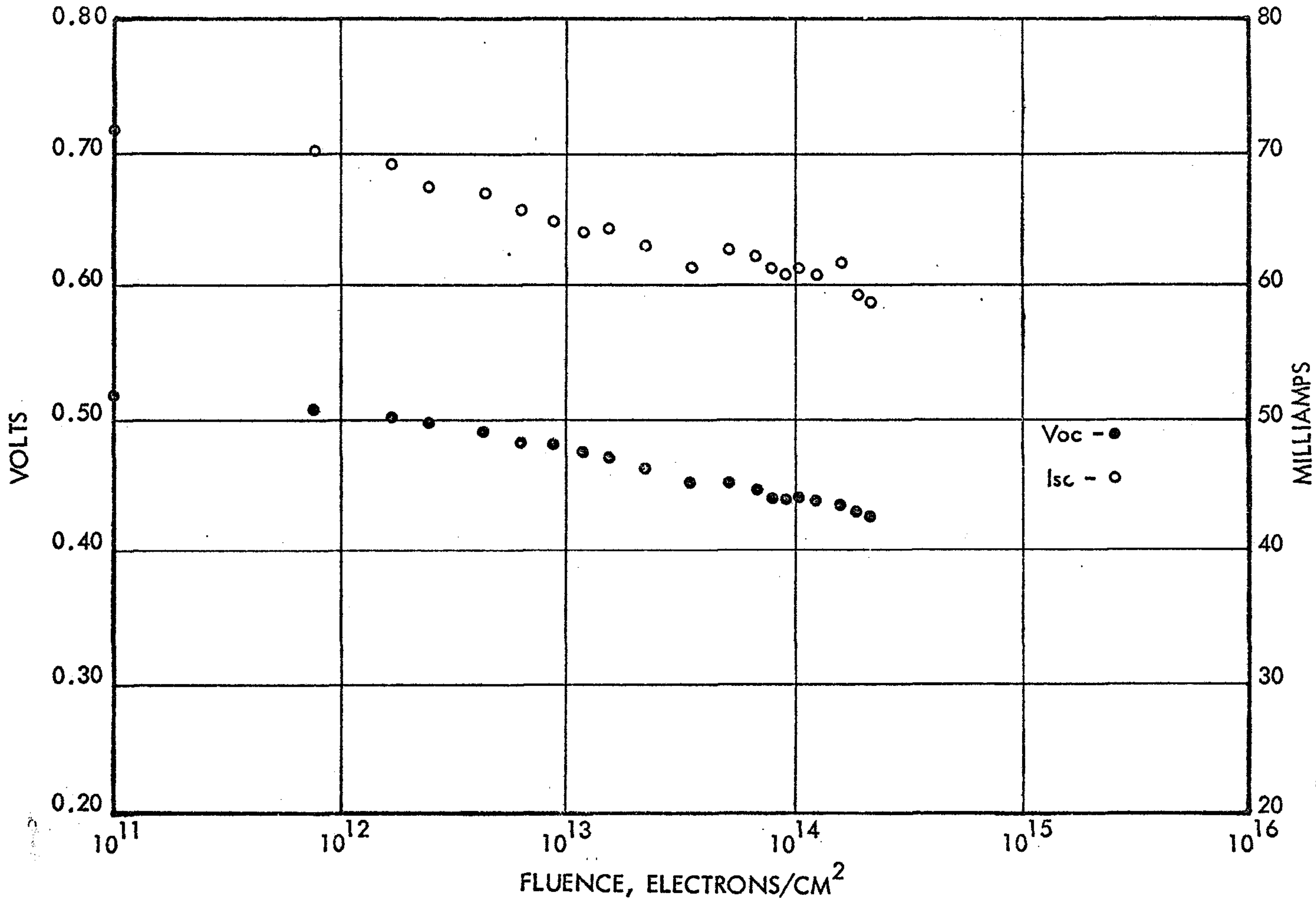

FIGURE 49 - GROUP M OPEN CIRCUIT VOLTAGE AND SHORT CIRCUIT CURRENT

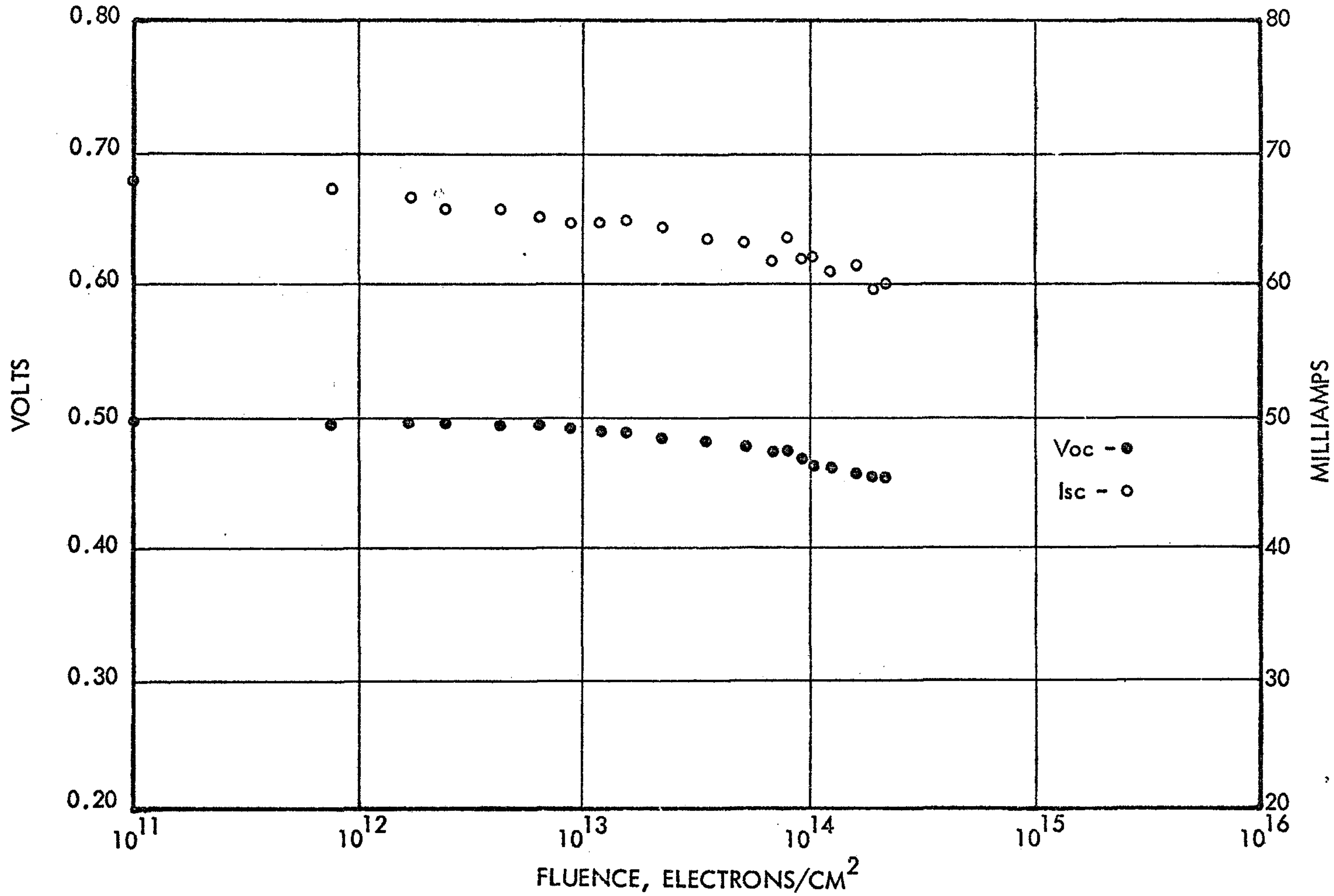

FIGURE 50 - GROUP N OPEN CIRCUIT VOLTAGE AND SHORT CIRCUIT CURRENT

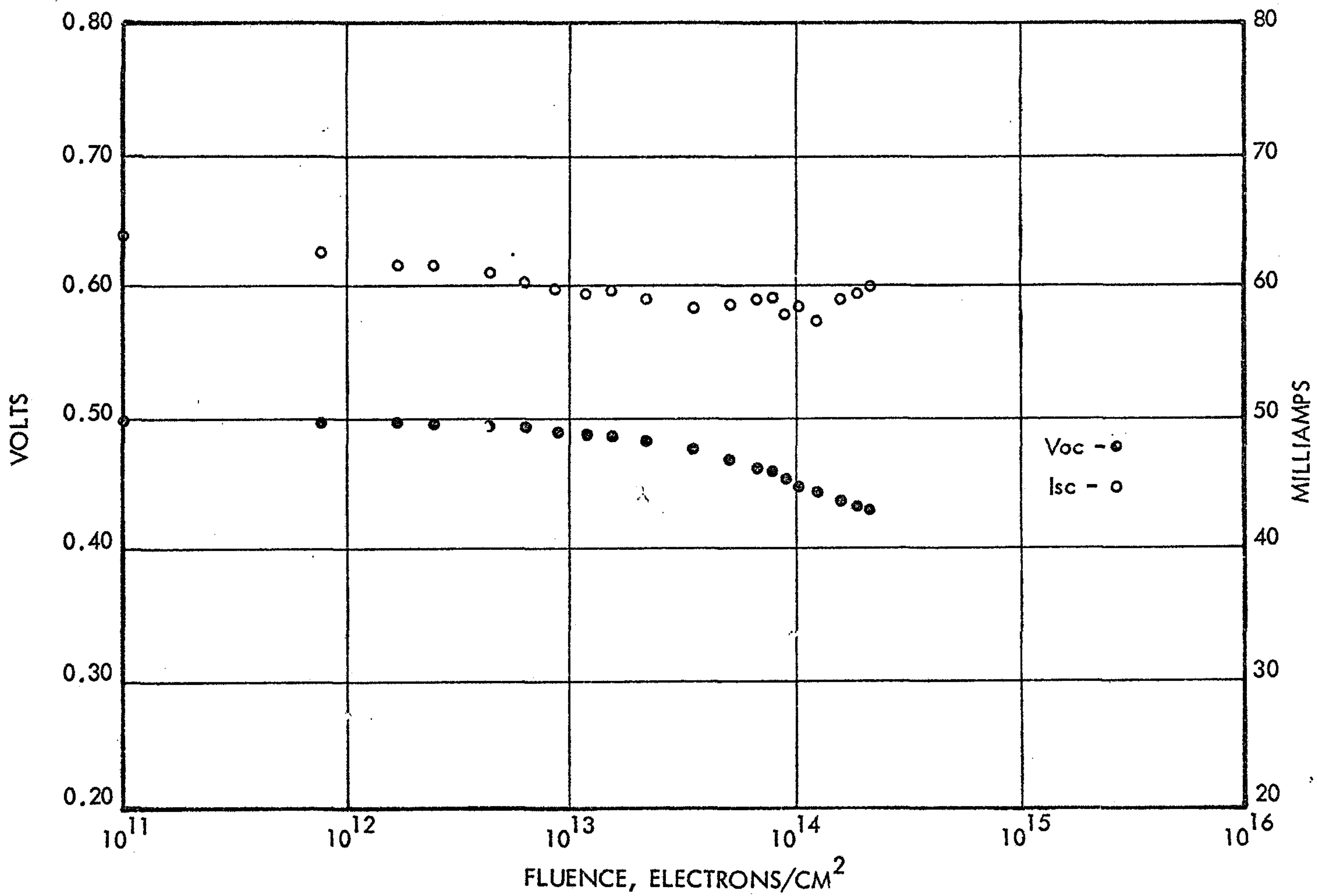

FIGURE 51 - GROUP O OPEN CIRCUIT VOLTAGE AND SHORT CIRCUIT CURRENT

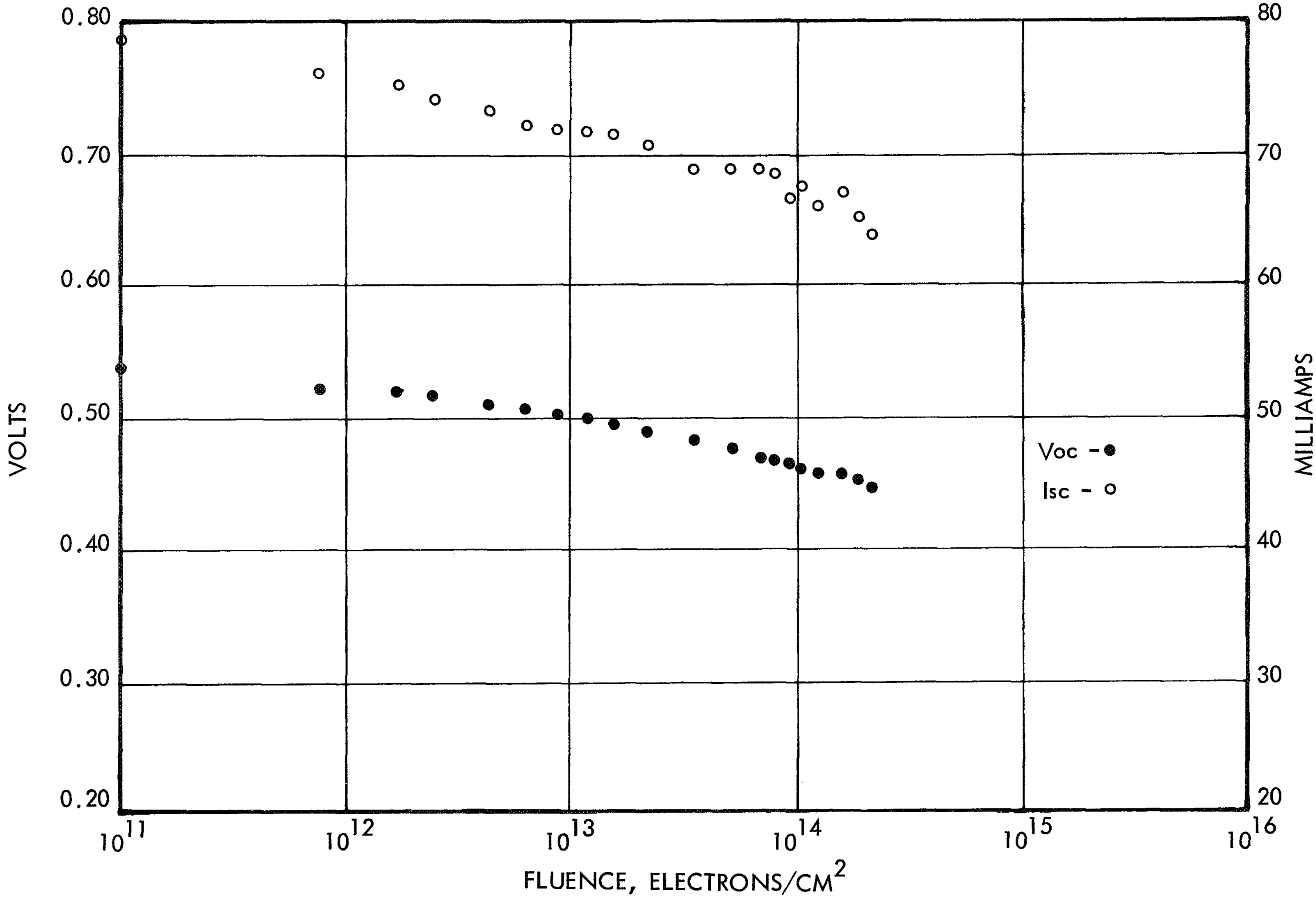

FIGURE 52 - GROUP P OPEN CIRCUIT VOLTAGE AND SHORT CIRCUIT CURRENT

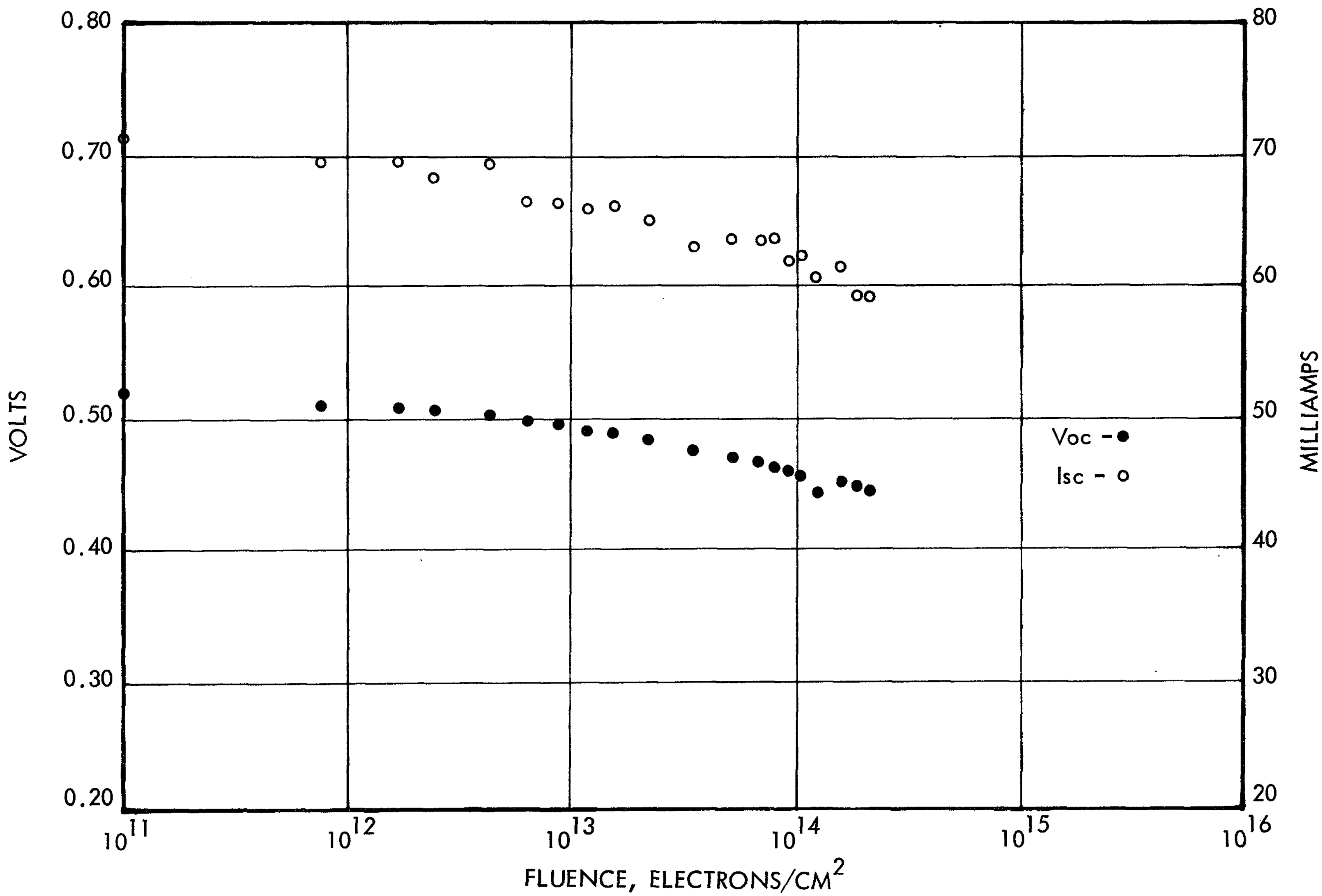

FIGURE 53 - GROUP R OPEN CIRCUIT VOLTAGE AND SHORT CIRCUIT CURRENT

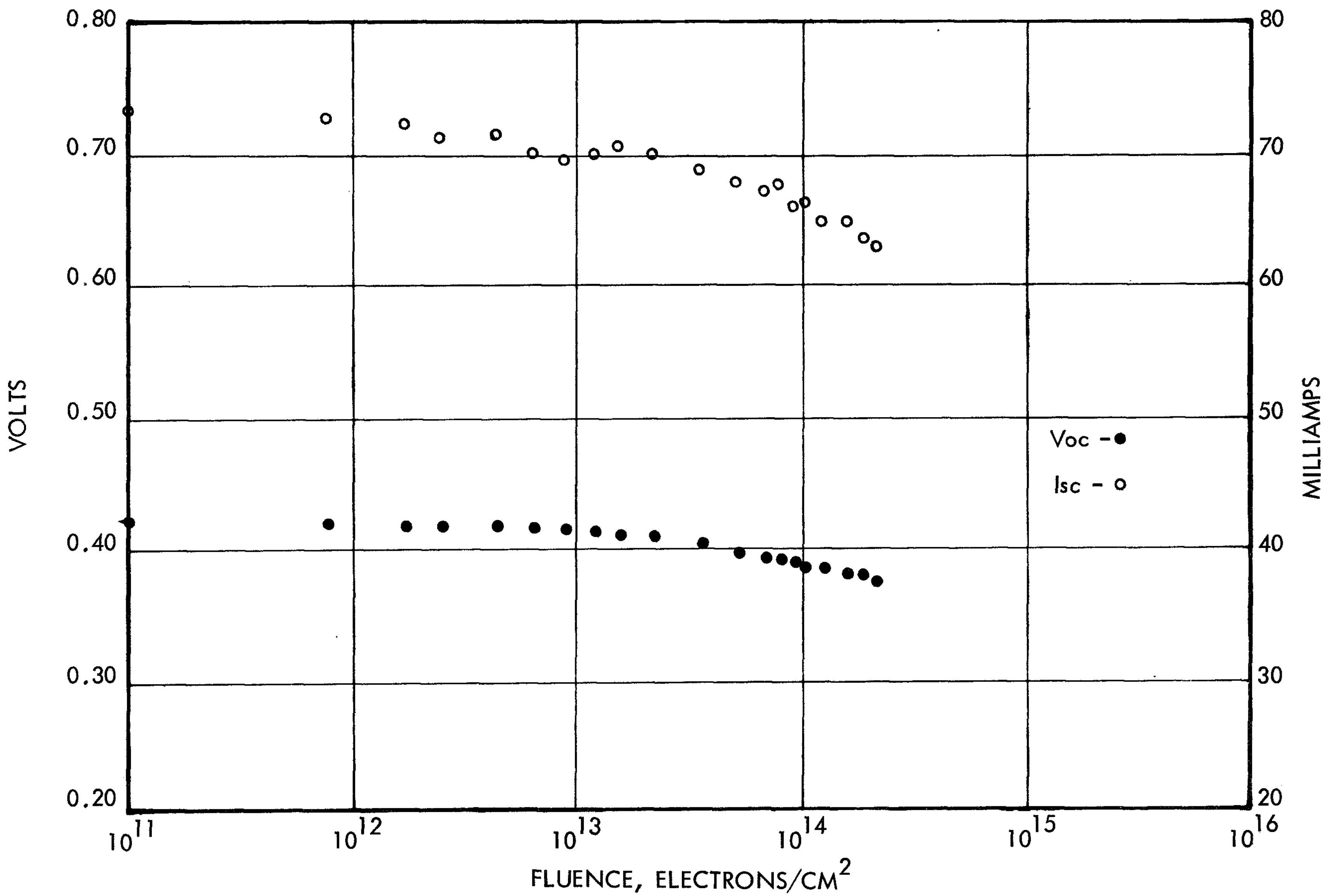

FIGURE 54 - GROUP S OPEN CIRCUIT VOLTAGE AND SHORT CIRCUIT CURRENT

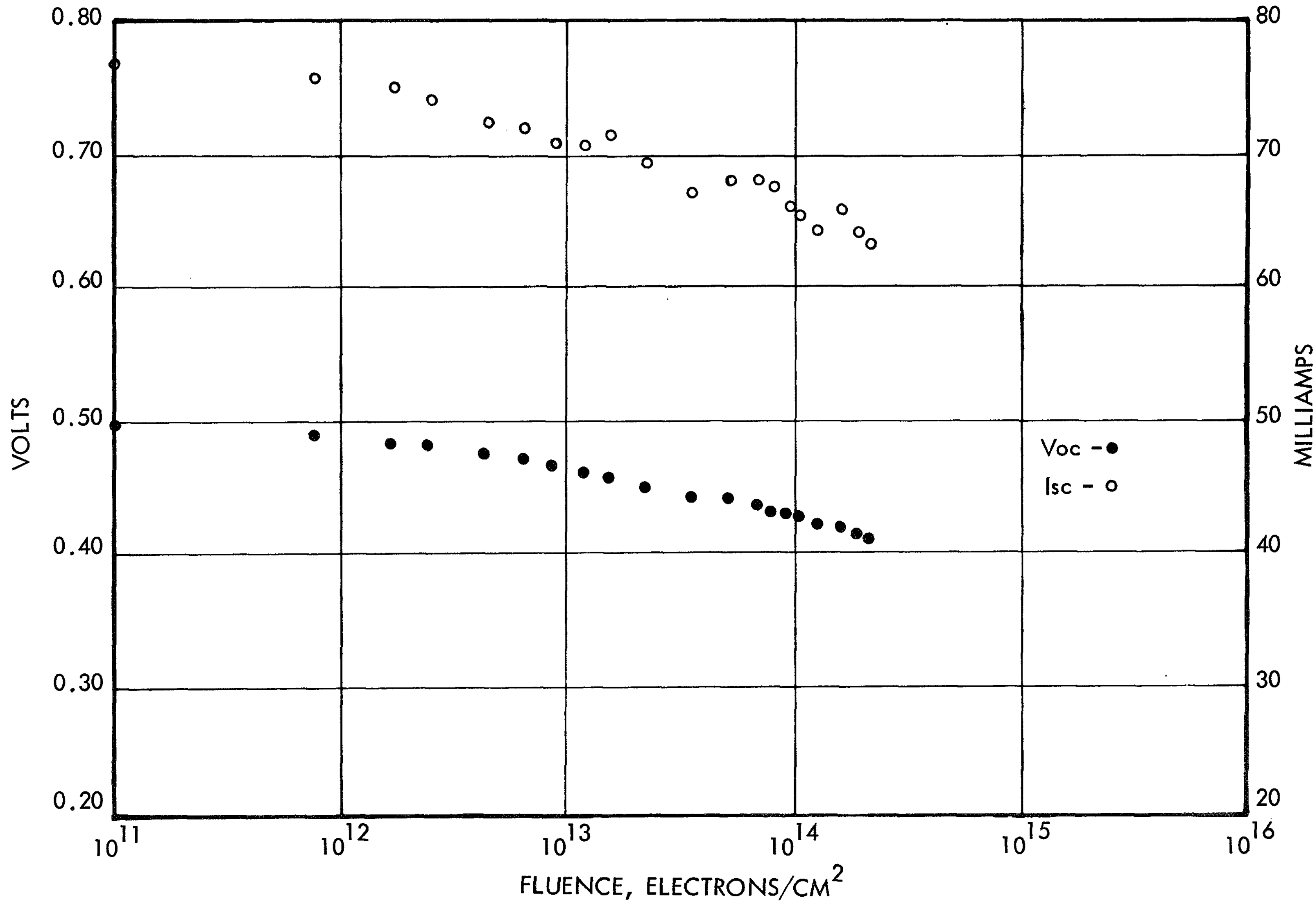

FIGURE 55 - GROUP T OPEN CIRCUIT VOLTAGE AND SHORT CIRCUIT CURRENT

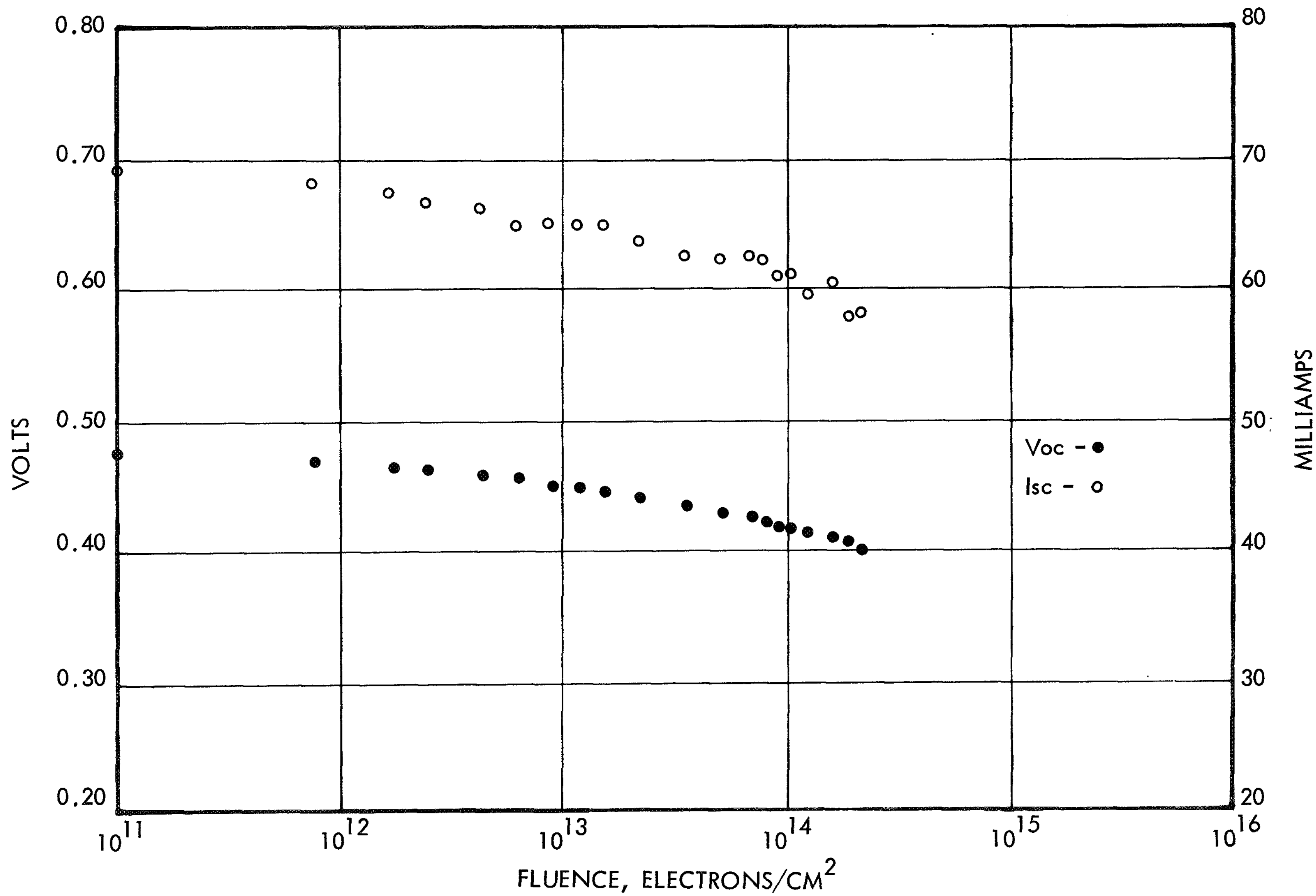

FIGURE 56 - GROUP U OPEN CIRCUIT VOLTAGE AND SHORT CIRCUIT CURRENT

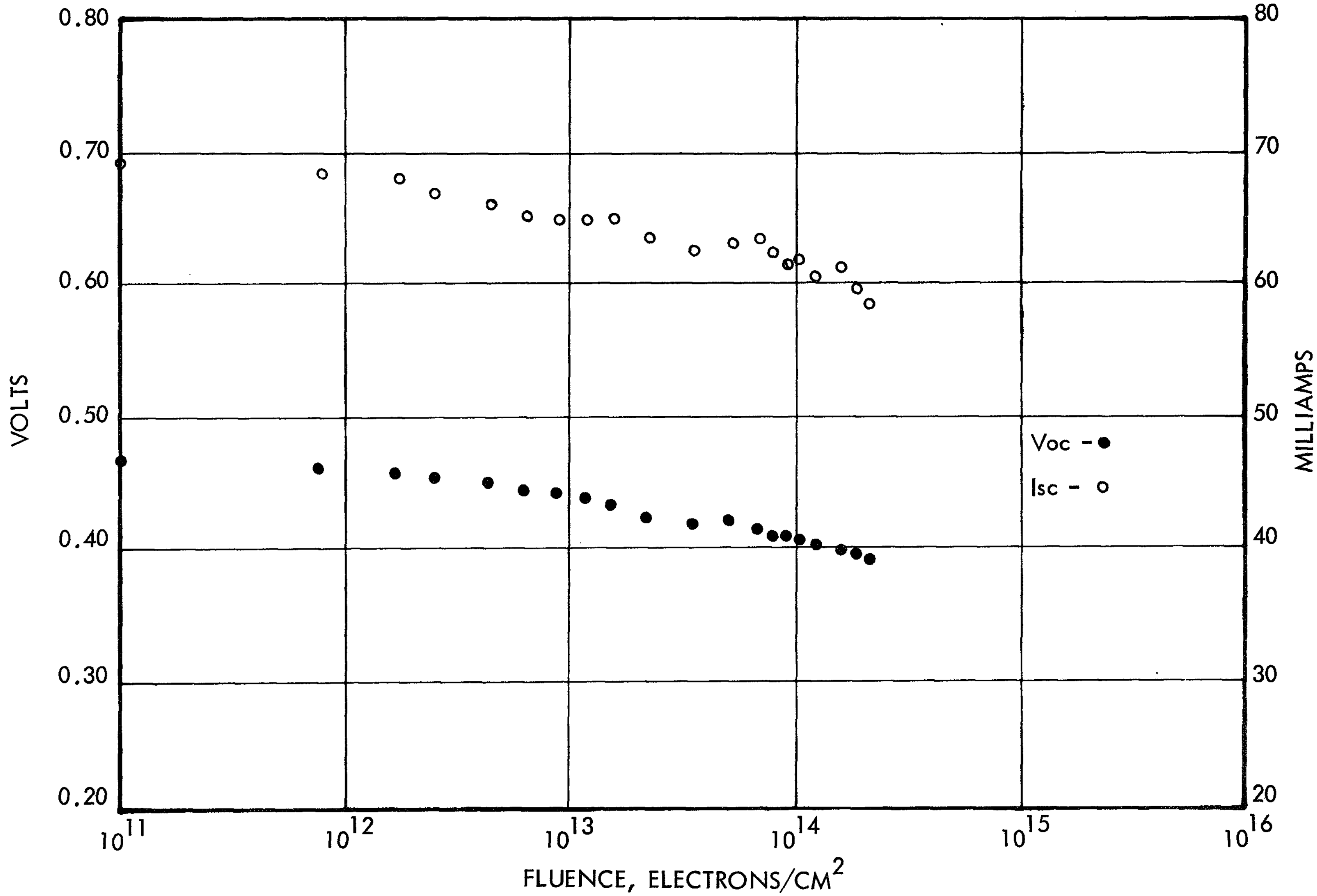

FIGURE 57 - GROUP W OPEN CIRCUIT VOLTAGE AND SHORT CIRCUIT CURRENT

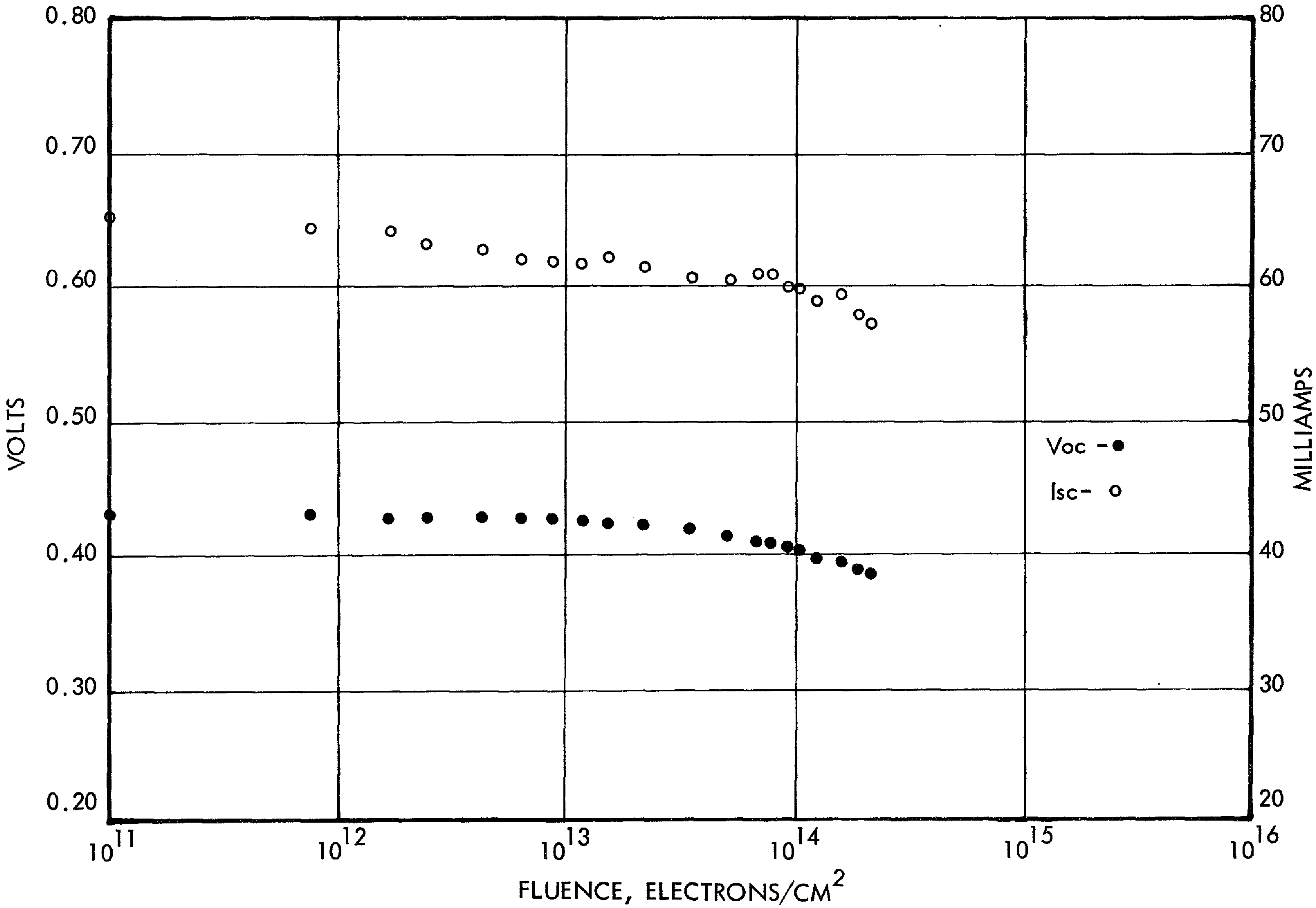

FIGURE 58 - GROUP X OPEN CIRCUIT VOLTAGE AND SHORT CIRCUIT CURRENT

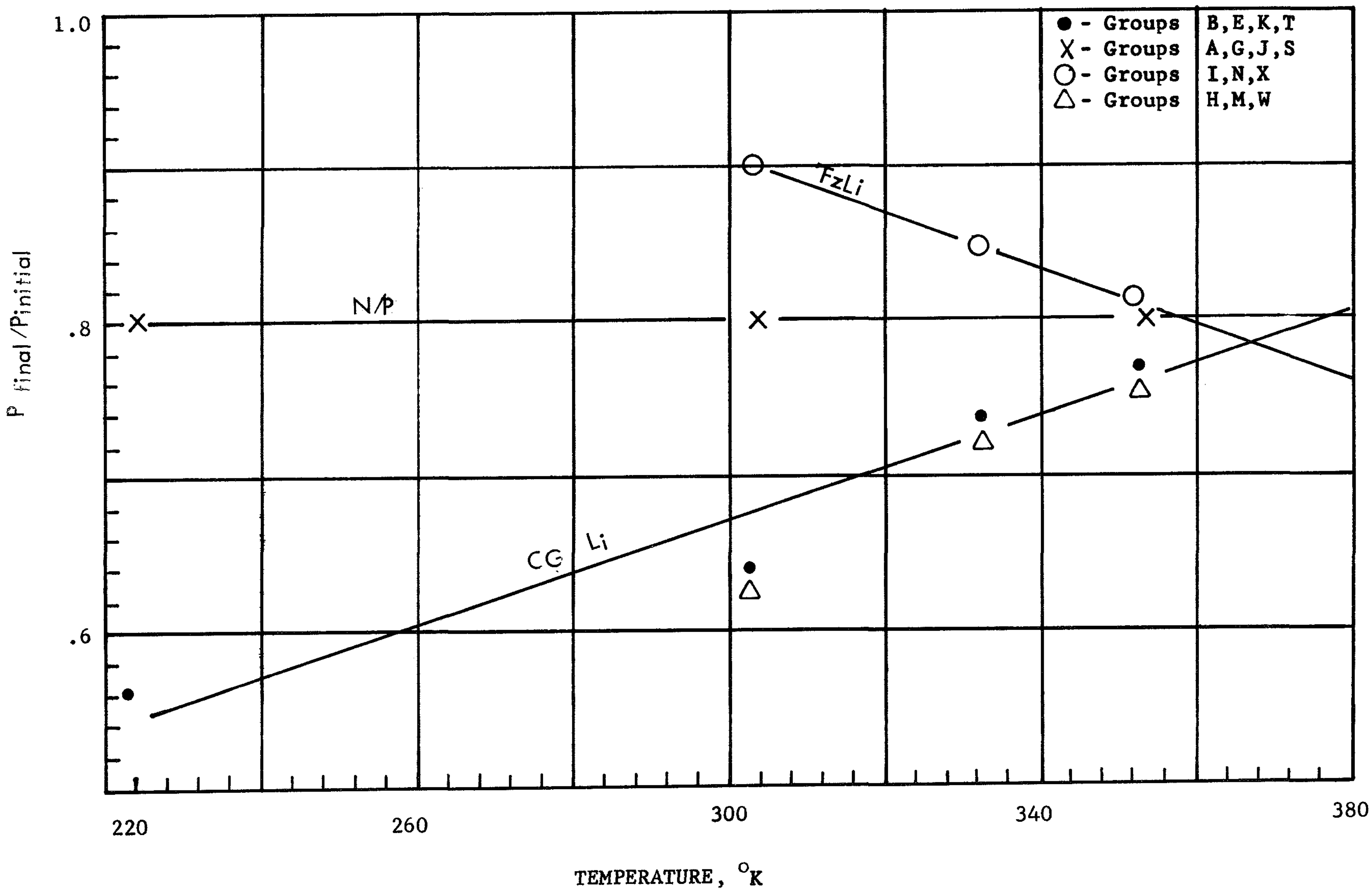

FIGURE 59 - NORMALIZED POWER VERSUS TEMPERATURE

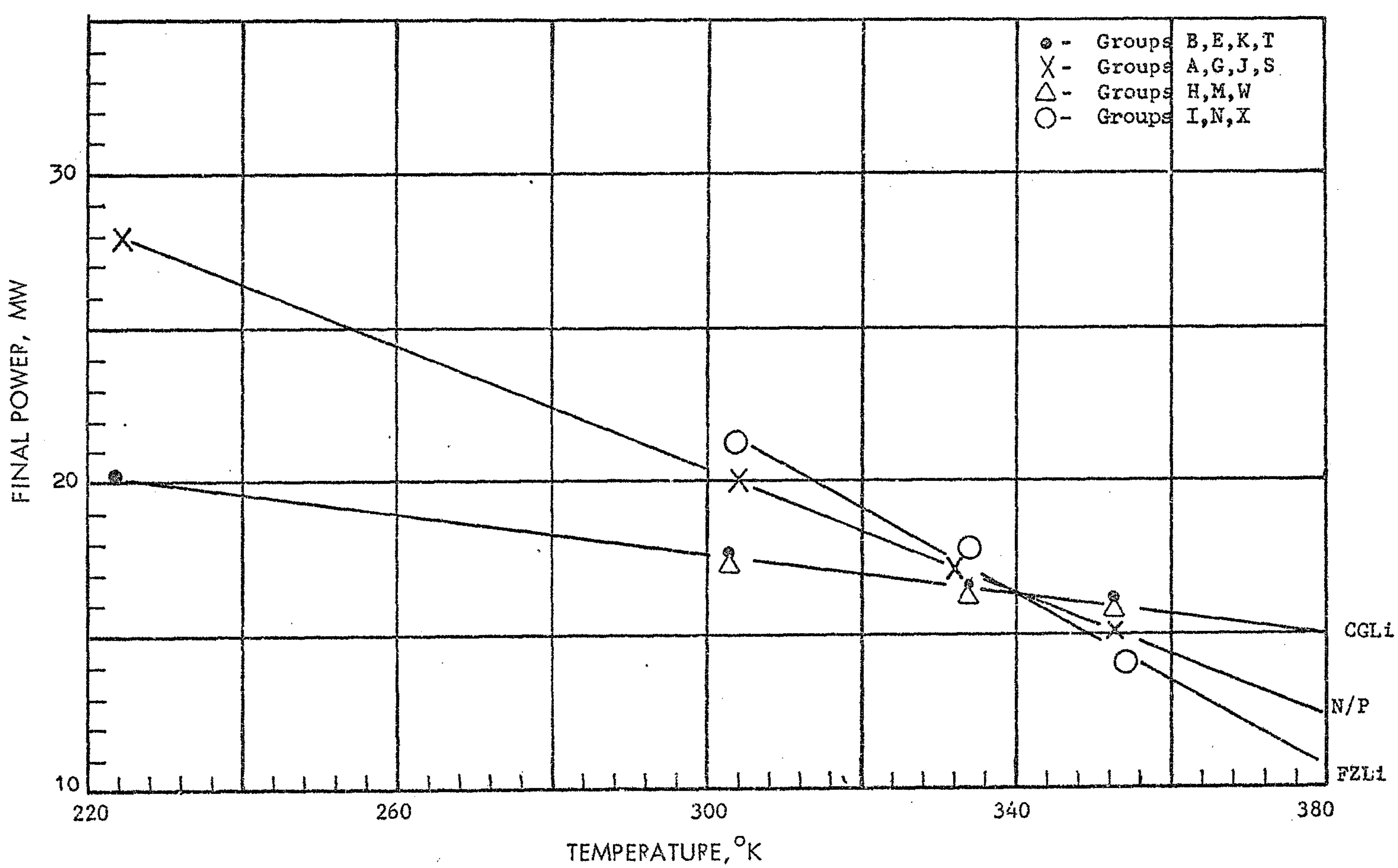

FIGURE 60 - FINAL POWER VERSUS TEMPERATURE

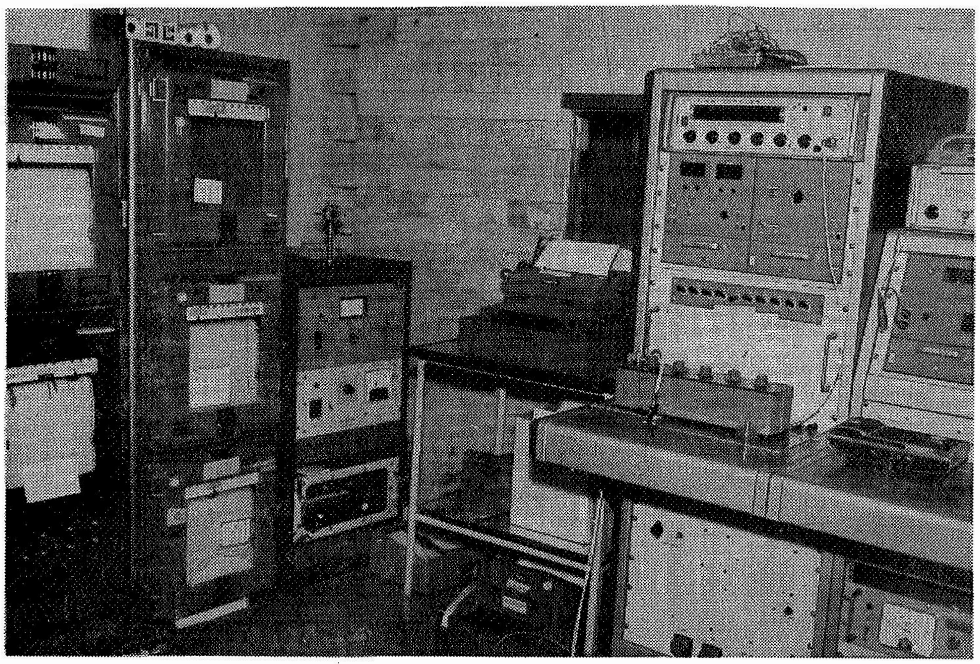

FIGURE 61 - ENVIROMENTAL CONTROL AND DATA ACQUISITION EQUIPMENT

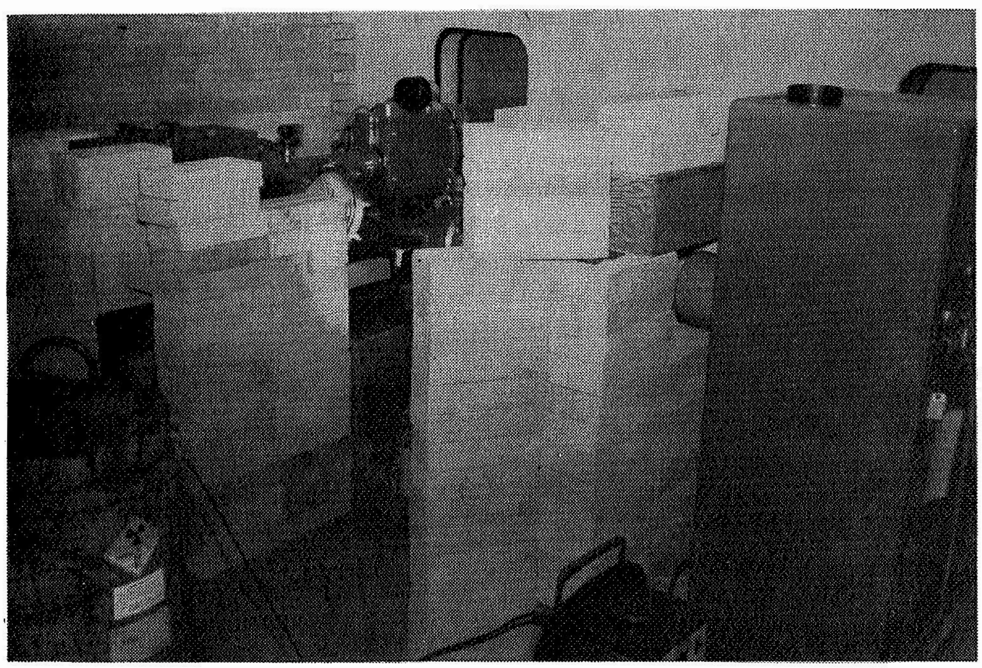

FIGURE 62 - TEST APPARATUS

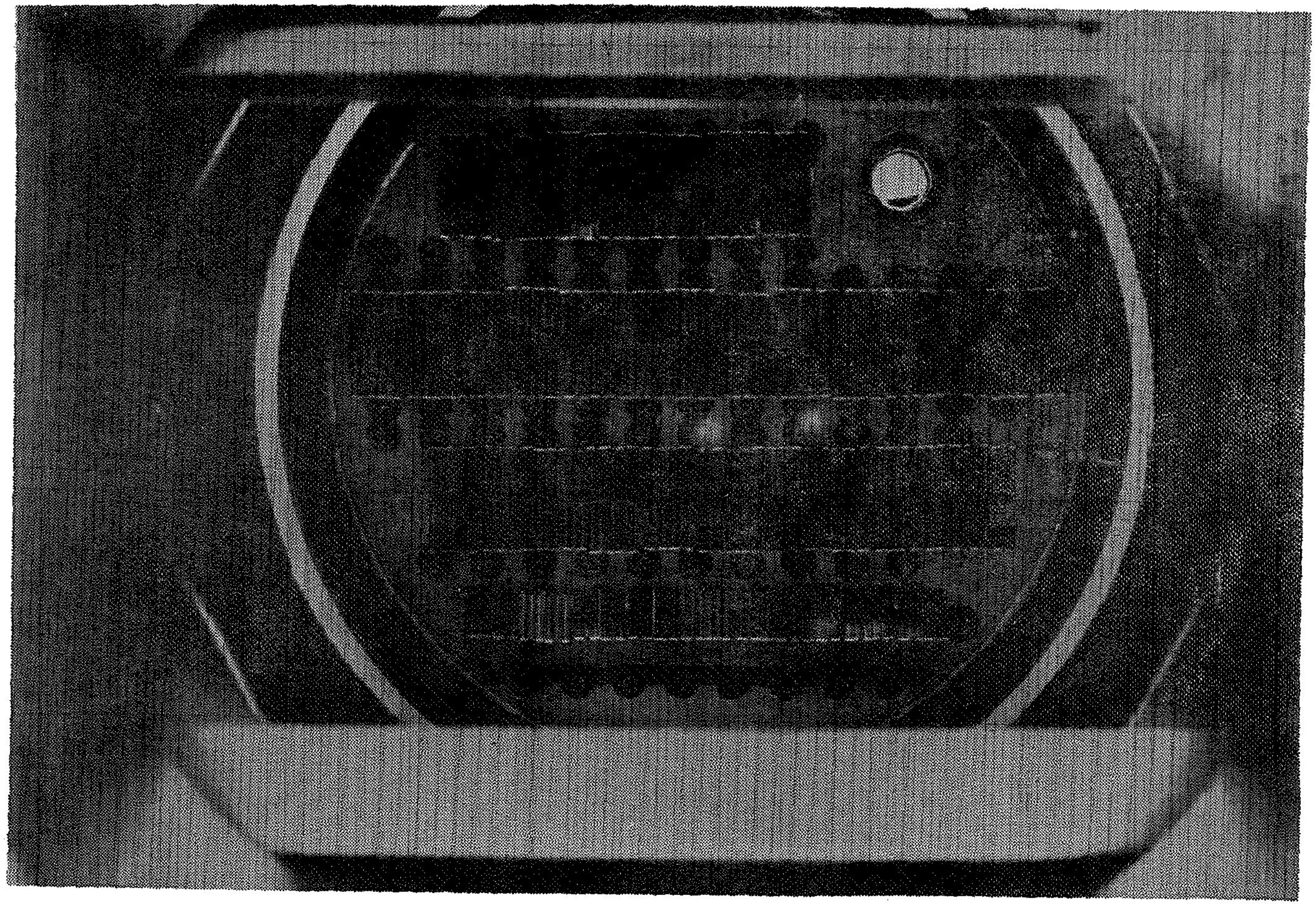

FIGURE 63 - SOLAR CELLS MOUNTED IN TEST POSITION

TABLE 1 - GROUP IDENTIFICATION AND ILLUMINATION

GROUP	CELL NO.	CELL SERIAL NUMBER	DATA CHANNEL	LIGHT LEVEL RELATIVE TO 140 WATTS/METER^2		
				PRE	POST	AVG.
A	1	C-1	010	-	.76	.715
	2	C-2	011	-	.73	
	3	C-3	012	-	.71	
B	1	C12-02	013	-	.70	.755
	2	C12-48	014	.77	.77	
	3	C12-04	015	.77	.80	
	4	C12-05	016	.79	.77	
	5	C12-06	017	.77	.79	
C	1	H8A-8396	018	.79	.80	.772
	2	H8A-8397	019	.78	.80	
	3	H8A-8400	020	.78	.82	
	4	H8A-8401	021	.76	.77	
	5	H8A-8402	022	.74	.77	
D	1	C12-07	023	.74	.74	.750
	2	C12-08	024	.76	.75	
	3	C12-09	025	.77	.76	
	4	C12-10	026	.74	.73	
	5	C12-11	027	.75	.75	
E	1	C12-12	028	1.01	1.02	1.009
	2	C12-13	029	1.00	1.02	
	3	C12-14	030	1.00	1.02	
	4	C12-16	031	1.00	1.02	
	5	C12-17	032	1.01	1.03	
	6	C12-18	038	1.00	1.04	
	7	C12-19	039	1.02	1.04	
	8	C12-20	040	1.02	1.04	
	9	C12-21	041	1.01	1.03	
	10	C12-22	042	1.01	1.03	

GROUP	CELL NO.	CELL SERIAL NUMBER	DATA CHANNEL	LIGHT LEVEL RELATIVE TO 140 WATTS/METER^2		
				PRE	POST	AVG.
F	1	H8A-8404	033	1.02	1.02	1.027
	2	H8A-8405	034	1.02	1.05	
	3	H8A-8407	035	1.01	1.04	
	4	H8A-8408	036	1.03	1.02	
	5	H8A-8409	037	1.03	1.03	
	6	H8A-8411	043	1.03	0.98	
	7	H8A-8412	044	1.04	1.00	
	8	H8A-8413	045	1.04	1.02	
	9	H8A-8477	046	1.02	1.04	
	10	H8A-8478	047	1.02	1.01	
G	1	C-4	048	1.02	1.00	1.015
	2	C-5	049	1.01	0.98	
	3	C-6	050	1.01	1.01	
	4	C-7	051	1.01	1.01	
	5	C-8	060	1.01	0.91	
	6	C-9	061	1.03	0.99	
H	1	C3-1	052	1.00	1.00	
	2	C3-2	053	1.01	1.03	
	3	C3-3	056	1.03	1.02	
	4	C3-4	057	1.03	1.01	
	5	C3-5	062	1.03	1.03	
	6	C3-6	063	1.02	1.04	
	7	C3-7	066	1.05	1.01	
	8	C3-8	067	1.04	1.02	
	9	C3-9	068	1.03	1.01	

TABLE 1 - GROUP IDENTIFICATION AND ILLUMINATION

GROUP	CELL NO.	CELL SERIAL NUMBER	DATA CHANNEL	LIGHT LEVEL RELATIVE TO 140 WATTS/METER^2		
				PRE	POST	AVG.
I	1	C1-1	054	1.01	1.01	1.028
	2	C1-2	055	1.03	1.01	
	3	C1-3	058	1.04	1.03	
	4	C1-4	059	1.04	1.01	
	5	C1-5	064	1.02	1.03	
	6	CJ-6	065	1.03	1.00	
	7	C1-7	069	0.95	1.04	
	8	C1-8	070	1.00	1.02	
	9	C1-11	071	0.96	1.02	
J	1	C-10	088	1.03	1.00	1.037
	2	C-11	089	1.03	0.97	
	3	C-12	098	1.00	1.00	
	4	C-13	099	1.01	1.04	
	5	C-14	108	1.07	1.11	
	6	C-15	109	1.07	1.07	
K	1	C12-23	076	1.02		1.033
	2	C12-24	077	1.00	1.02	
	3	C12-25	078	1.02	1.00	
	4	C12-26	079	1.02	1.00	
	5	C12-27	084	1.05	1.01	
	6	C12-28	085	1.05	1.00	
	7	C12-29	086	1.05	0.99	
	8	C12-47	087	1.05	0.99	
L	1	H8A-8482	072	1.02	1.05	1.035
	2	H8A-8483	073	1.02	1.05	
	3	H8A-8487	074	1.01	1.03	
	*4	H8A-8489	075	1.01	-	
	5	H8A-8491	080	1.02	1.05	
	6	H8A-8495	081	1.03	1.05	
	7	H8A-8497	082	1.05	1.06	
	8	H8A-8499	083	1.06	1.06	
M	1	C3-10	100	1.01	1.03	1.037
	2	C3-11	101	1.01	1.04	
	3	C3-12	104	1.03	1.02	
	4	C3-13	105	1.02	1.04	
	5	C3-24	110	1.07	1.08	
	6	C3-15	111	1.07	1.06	
	7	C3-16	114	1.04	1.04	
	8	C3-17	115	1.04	1.06	
N	1	C1-13	102	1.01	1.00	1.038
	2	C1-14	103	1.01	1.06	
	3	C1-9	112	1.07	1.07	
	4	C1-10	113	1.06	1.04	
O	1	C2-5	090	1.04	.93	1.049
	2	C2-2	106	1.05	1.03	
	3	C2-3	107	1.06	1.01	
	4	C2-4	116	1.05	1.03	
P	1	C12-32	094	1.02	1.00	1.013
	2	C12-33	095	1.02	1.00	
	3	C12-34	096	1.01	1.01	
	4	C12-35	097	1.01	1.02	
	5	C12-36	118	1.03	1.01	
	6	C12-37	119	1.02	1.03	
	7	C12-38	120	1.01	1.01	
	8	C12-39	121	1.00	1.01	

TABLE 1 - GROUP IDENTIFICATION AND ILLUMINATION

-87-

GROUP	CELL NO.	CELL SERIAL NUMBER	DATA CHANNEL	LIGHT LEVEL RELATIVE TO 140 WATTS/METER^2		
				PRE	POST	AVG.
R	1	H84-8490	091	1.05	0.99	1.032
	2	H8A-8501	092	1.03	0.98	
	3	H8A-8511	093	1.05	1.01	
	4	H8A-8506	125	1.02	1.05	
	5	H8A-8492	117	1.04	1.04	
	6	H84-8493	122	1.04	1.01	
	7	H3A-8500	123	1.03	-	
	8	H8A-8506	124	1.01	-	
S	1	C-16	138	1.07	1.05	1.070
	2	C-17	139	1.07	1.06	
	3	C-18	140	0.80	0.79	0.805
	4	C-19	141	0.80	0.74	
T	1	C12-40	126	1.01	1.02	1.051
	2	C12-41	127	1.01	1.03	
	3	C12-42	130	1.04	1.04	
	4	C12-43	131	1.06	1.07	
	5	C12-44	134	1.09	1.12	
	6	C12-46	135	1.11	1.11	
U	1	H8A-8494	128	1.04	1.05	1.084
	2	H8A-8496	129	1.06	1.03	
	3	H8A-8502	132	1.11	1.09	
	4	H8A-8504	133	1.11	1.09	
	5	H8A-8507	136	1.10	1.08	
	6	H8A-8509	137	1.08	1.09	
W	1	C3-18	144	0.83	0.79	0.857
	2	C3-19	145	0.84	0.84	
	3	C3-20	148	0.87	0.92	
	4	C3-21	149	0.88	0.92	
	5	C3-22	152	0.86	0.79	
	6	C3-23	153	0.85	0.80	
X	1	C1-16	142	0.83	0.86	0.867
	2	C1-17	143	0.85	0.89	
	3	C1-18	146	0.88	0.92	
	4	C1-19	147	0.89	0.88	
	5	C1-20	150	0.88	0.84	
	6	C1-21	151	0.87	0.82	

TABLE 1 - GROUP IDENTIFICATION AND ILLUMINATION

TEMPERATURE	223°K				303°K				333°K				353°K			
CELL NOMENCLATURE / FLUENCE	0	10	2x10	5x10	0	10	2x10	5x10	0	10	2x10	5x10	0	10	2x10	5x10
CENTRALAB Conventional n/p 0.10 ohm - Meter	34.6	28.7	27.6	25.9	25.8	21.2	19.9	17.9	21.3	17.9	16.9	15.4	18.1	15.3	14.3	12.8
CENTRALAB C-12 Crucible Grown 598°K, 8 Hour Diffusion	37.5	22.5	20.7	18.2	29.2	18.9	17.6	15.6	25.1	18.4	17.6	16.4	22.5	17.5	16.5	15.1
HELIOTEK H8A Crucible Grown 598°K, 8 Hour Diffusion	36.2	20.6	18.9	16.3	25.5	17.4	16.3	14.4	21.6	17.1	16.2	15.0	18.9	14.9	13.4	12.5
CENTRALAB Crucible Grown 698°K, 120 min Diffusion Plus 90 min Redistribution					27.2	18.4	17.0	15.1	23.8	17.6	16.9	15.7	19.9	15.9	15.0	13.6
CENTRALAB Float Zone Grown 698°K, 120 min. Diffusion Plus 90 min Redistribution					24.1	22.4	21.0	18.0	20.4	18.6	17.5	15.4	17.4	15.1	13.9	12.3
CENTRALAB Float Zone Grown 698°K, 120 min Diffusion									19.4	16.6	15.6	14.0				

TABLE 2 - POWER PERFORMANCE OF TEST CELLS

APPENDIX I

DATA REDUCTION COMPUTER PROGRAM

```
0000 R 010672 VMAX      0000 R 010475 V0      0000 R 005605 VOL      0000 R 010531 V1      0000 R 010532 V2
0000 R 010533 V3        0000 R 010534 V4      0000 R 010535 V5       0000 R 010536 V6      0000 R 010537 V7
0000 R 010625 XT        0000 R 010626 YT

00100    C     PROGRAM SRCELL FOR COMPUTING SOLAR CELL PARAMETERS
00101          DIMENSION KOUM(144),JOUM(23),HEAD(3,144),FLU(30),VLT(144,16),R(16)
00101         1,VOL(150),CUR(150),V(150),C(150),CURF(150),
00101         2P(150),PM(150),SE(150),PJMAX(23),CJMAX(23),VJMAX(23),AJTG(23),
00101         3AJTC(23),PJS(23),AJN(23),SJEF(23),VO(6),CU(6)
00103          DATA KOUM/1,2,3,4,5,6,7,8,9,10,11,12,13,14,15,16,17,18,19,20,21,
00103         122,23,29,30,31,32,33,24,25,25,27,28,34,35,36,37,38,39,40,41,42,51,
00103         252,43,44,47,48,53,54,57,58,59,45,46,49,50,55,56,60,61,62,73,80,89,
00103         390,99,100,67,68,69,70,75,76,77,78,63,64,65,66,71,72,73,74,91,92,
00103         495,96,101,102,105,106,33,94,103,104,97,98,81,107,85,86,87,88,109,
00103         5110,111,112,82,83,84,108,113,114,115,116,129,130,131,132,117,118,
00103         6121,122,125,126,119,120,123,124,127,128,135,136,139,140,143,144,
00103         7133,134,137,138,141,142/
00105          DATA JOUM/3,9,13,19,28,38,44,53,62,68,76,84,92,96,100,108,116,118,
00105         1120,126,132,138,144/
00107          READ(5,600)((HEAD(I,KO),I=1,3),KO=1,144)
00120      600 FORMAT(3A4)
00121          READ(5,605)(IRUN,FLU(IRUN))
00125      605 FORMAT(3X,I2,5X,E10.4)
00126          R(1)=0.4
00127          R(2)=2.4
00130          R(3)=4.4
00131          R(4)=6.4
00132          R(5)=8.4
00133          R(6)=10.4
00134          R(7)=12.4
00135          R(8)=14.4
00136          R(9)=17.4
00137          R(10)=20.4
00140          R(11)=24.4
00141          R(12)=28.4
00142          R(13)=39.4
00143          R(14)=56.4
00144          R(15)=93.4
00145          IF(IRUN.EQ.1)GO TO 4
00147          R(16)=999999999.
00150          GO TO 8
00151        4 R(16)=1000.4
00152        8 JJ=0
00153          KO=0
00154          JC=1
00155          DO 612 I=1,16
00160          KF=0
00161          DO 613 L=1,28
00164          KB=KF+1
00165          KE=KB+4
00166          READ(5,610)(VLT(KT,I),KT=KB,KE)
00174      610 FORMAT(16X,5(F5.5,7X),4X)
00175      613 CONTINUE
00177          READ(5,611)(VLT(KT,I),KT=141,144)
00205      611 FORMAT(16X,4(F5.5,7X),16X)
```

```
  512 CONTINUE
      WRITE(6,160)
  160 FORMAT(1H1,48X,16H JPL SOLAR CELLS,/////,40X,9H RUN NO.,10X,
     119H FLUENCE (E/SQ CM),/)
  110 WRITE(6,163)(IRUN,FLU(IRUN))
  163 FORMAT(1H ,43X,I2,15X,E10.4)
  115 KO=KO+1
      N=16
C     N IS THE NUMBER OF DATA POINTS USED TO CALCULATE THE CHARACTERISTICS
      INDIC=0
      IF(KO.LT.19)GO TO 21
      IF(KO.LT.63)GO TO 22
      IF(KO.LT.117)GO TO 23
      BETA=11605.43/353.165
      GO TO 24
   21 BETA=11605.43/223.165
      GO TO 24
   22 BETA=11605.43/303.165
      GO TO 24
   23 BETA=11605.43/333.165
   24 KI=KDUM(KO)
      DO 170 I=1,16
      VOL(I)=VLT(KI,I)
      CUR(I)=(VOL(I)/R(I))*1000.
      JJ=JJ+1
      V(JJ)=VOL(I)
      C(JJ)=CUR(I)
  170 CONTINUE
      WRITE(6,180)(HEAD(I,KO),I=1,3)
  180 FORMAT(1H1,50X,22H DATA FOR SPECIMEN NO.,2X,3A4,////)
   32 DO 190 L=1,2
      KISS=(L-1)*8+1
      LOVE=(L-1)*8+8
      IF(L.EQ.2)GO TO 191
      WRITE(6,181)
  181 FORMAT(1H ,3HRUN,4X,9H .4 OHMS,7X,9H 2.4 OHMS,7X,9H 4.4 OHMS,7X,
     19H 6.4 OHMS,7X,9H 8.4 OHMS,6X,10H 10.4 OHMS,6X,10H 12.4 OHMS,6X,
     210H 14.4 OHMS,/,1X,3HNO.,8(3X,13H MA       V      ))
      GO TO 193
  191 WRITE(6,182)
  182 FORMAT(1H ,3HRUN,2X,10H 17.4 OHMS,6X,10H 20.4 OHMS,6X,10H 24.4 OHM
     1S,5X,10H 29.4 OHMS,6X,10H 39.4 OHMS,5X,10H 55.4 OHMS,6X,10H 93.4 O
     2HMS,8X,5H OPEN,/,1X,3HNO.,8(3X,13H MA       V      ))
  193 WRITE(6,185)(IRUN,(CUR(I),VOL(I),I=KISS,LOVE))
  190 CONTINUE
  184 FORMAT(1H ,I2,8(3X,F5.2,2X,F6.5))
  185 FORMAT(1H ,I2,8(3X,F5.2,2X,F6.5),//////)
      DO 201 I=1,6
      CU(I)=CUR(I)
  201 VO(I)=VOL(I)
      DO 200 I=1,5,2
      CUR(I)=(CUR(I)+CUR(I+1))/2.
      CUR(I+1)=CUR(I)
      VOL(I)=(VOL(I)+VOL(I+1))/2.
      VOL(I+1)=VOL(I)
      C(JJ-16+I)=(C(JJ-16+I)+C(JJ-15+I))/2.
      C(JJ-15+I)=C(JJ-16+I)
      V(JJ-16+I)=(V(JJ-16+I)+V(JJ-15+I))/2.
```

```
      V(JJ-15+I)=V(JJ-15+I)
  200 CONTINUE
      GO TO 7
  520 INDIC=1
      AJ=JJ/15
C     AVERAGE THE VALUES OF VOLTAGE AND CURRENT FOR FIRST FEW DATA
C     POINTS IN BATCH COMPUTATION
      V1=0.0
      V2=0.0
      V3=0.0
      V4=0.0
      V5=0.0
      V6=0.0
      V7=0.0
      C1=0.0
      C2=0.0
      C3=0.0
      C4=0.0
      C5=0.0
      C6=0.0
      C7=0.0
      DO 89 I=1,JJ,15
      V1=V1+V(I)
      V2=V2+V(I+1)
      V3=V3+V(I+2)
      V4=V4+V(I+3)
      V5=V5+V(I+4)
      V6=V6+V(I+5)
      V7=V7+V(I+6)
      C1=C1+C(I)
      C2=C2+C(I+1)
      C3=C3+C(I+2)
      C4=C4+C(I+3)
      C5=C5+C(I+4)
      C6=C6+C(I+5)
      C7=C7+C(I+6)
   89 CONTINUE
      V1=V1/AJ
      V2=V2/AJ
      V3=V3/AJ
      V4=V4/AJ
      V5=V5/AJ
      V6=V6/AJ
      V7=V7/AJ
      C1=C1/AJ
      C2=C2/AJ
      C3=C3/AJ
      C4=C4/AJ
      C5=C5/AJ
      C6=C6/AJ
      C7=C7/AJ
      DO 90 I=1,JJ,15
      V(I)=V1
      V(I+1)=V2
      V(I+2)=V3
      V(I+3)=V4
      V(I+4)=V5
      V(I+5)=V6
```

```
00432        V(I+6)=V7
00433        C(I)=C1
00434        C(I+1)=C2
00435        C(I+2)=C3
00436        C(I+3)=C4
00437        C(I+4)=C5
00440        C(I+5)=C6
00441        C(I+6)=C7
00442     90 CONTINUE
00444        DO 432 I=1,JJ
00447        VOL(I)=V(I)
00450        CUR(I)=C(I)
00451    432 CONTINUE
00453        N=JJ
00454        JJ=0
00455      7 J=0
00456        DO 15 I=1,N
00461     15 PM(I)=CUR(I)*VOL(I)
00463     47 CURMX=CUR(1)
00464        DO 46 I=1,N
00467        BCC=CURMX-CUR(I)
00470        IF(BCC.GE.0.0)GO TO 46
00472        CURMX=CUR(I)
00473     46 CONTINUE
00475        BI=CURMX+.0001
00476        BOLD=1000000.
00477      2 SG11=0.0
00500        PSG11=0.0
00501        SG12=0.0
00502        PSG12=0.0
00503        SG13=0.0
00504        PSG13=0.0
00505        SG14=0.0
00506        PSG14=0.0
00507        SG22=0.0
00510        SG23=0.0
00511        SG21=0.0
00512        SG33=0.0
00513        SG44=0.0
00514        SG34=0.0
00515        SG24=0.0
00516        SG41=0.0
00517        SG31=0.0
00520        DO 3 I=1,N
00523        BC=BI-CUR(I)
00524    604 BL=ALOG(BC)
00525        CUBE(I)=CUR(I)**3
00526        CUR(I)=CUR(I)**2
00527        SG11=SG11+ (CUR(I)*VOL(I)/(BETA*BC))
00530        PSG11=PSG11-(CUR(I)*VOL(I)/(BETA*(BC**2)))
00531        SG12=SG12+(CUR(I)*BL/((BETA**2)*BC))
00532        PSG12=PSG12+(CUR(I)*(1.-BL)/((BETA**2)*(BC**2)))
00533        SG13=SG13+(CUBE(I)/(BETA*BC))
00534        PSG13=PSG13-(CUBE(I)/(BETA*(BC**2)))
00535        SG14=SG14+(CUR(I)/((BETA**2)*BC))
00536        SG41=SG41+(VOL(I)*CUR(I)/BETA)
00537        PSG14=PSG14-(CUR(I)/((BETA**2)*(BC**2)))
00540        SG22=SG22+(CUR(I)*(BL**2)/(BETA**2))
```

```
      SG23=SG23+(CURE(I)*BL/BETA)
      SG21=SG21+((CUR(I)*VOL(I)*BL)/BETA)
      SG33=SG33+(CUR(I)**2)
      SG44=SG44+(CUR(I)/(BETA**2))
      SG34=SG34+(CURE(I)/BETA)
      SG24=SG24+((CUR(I)*BL)/(BETA**2))
      SG31=SG31+(VOL(I)*(CUBE(I)))
    3 CONTINUE
      DO 555 I=1,N
      CURE(I)=0.0
  555 CUR(I)=SQRT(CUR(I))
      D1=SG22*SG33*SG44 +(2.*SG23*SG24*SG34)
      D1=D1-SG22*(SG34**2)-(SG33*(SG24**2))-(SG44*(SG23**2))
      DP1=2.*SG12*(SG33*SG44-(SG34**2))
      DP1=DP1+2.*SG13*((SG24*SG34)-(SG23*SG44))
      DP1=DP1+2.*SG14*((SG23*SG34)-(SG24*SG33))
      D2=(SG21*SG33*SG44)-SG21*(SG34**2)-(SG31*SG23*SG44)
      D2=D2+(SG31*SG24*SG34)+(SG41*SG23*SG34)-(SG41*SG24*SG33)
      DP2=SG11*(SG33*SG44-(SG34**2))+SG31*((SG14*SG34)-(SG13*SG44))
      DP2=DP2+(SG41*(SG13*SG34-(SG14*SG33)))
      D3=(SG22*SG34*SG41)-(SG22*SG31*SG44)+(SG23*SG21*SG44)
      D3=D3-(SG23*SG24*SG41)+((SG24**2)*SG31)-(SG24*SG21*SG34)
      DP3=2.*SG12*((SG34*SG41)-(SG31*SG44))
      DP3=DP3+SG13*((SG21*SG44)-(SG24*SG41))
      DP3=DP3+SG23*((SG11*SG44)-(SG41*SG14))
      DP3=DP3+SG14*((SG31*SG24)-(SG21*SG34))
      DP3=DP3+SG24*((SG31*SG14)-(SG11*SG34))
      D4=(SG22*SG31*SG34)-(SG22*SG33*SG41)+((SG23**2)*SG41)
      D4=D4-(SG23*SG21*SG34)-(SG24*SG23*SG31)+(SG24*SG21*SG33)
      DP4=2.*SG12*((SG31*SG34)-(SG33*SG41))
      DP4=DP4+SG21*((SG14*SG33)-(SG13*SG34))
      DP4=DP4+SG23*((SG13*SG41)-(SG14*SG31))
      DP4=DP4+SG13*((SG23*SG41)-(SG24*SG31))
      DP4=DP4+SG11*((SG24*SG33)-(SG23*SG34))
      B2=D2/D1
      B3=D3/D1
      B4=D4/D1
      B5=B4/B2
   75 AIC=EXP(B5)
      AIG=B1-AIC
      RS=B3
      AN=B2
      FB1=(SG11*D1)-(SG12*D2)+(SG13*D3)+SG14*D4
      FPB1=(PSG11*D1)+(SG11*DP1)-(PSG12*D2)-(SG12*DP2)
      FPB1=FPB1+(SG13*DP3)+(PSG13*D3)+(PSG14*D4)+(SG14*DP4)
      B1NEW=B1-(FB1/FPB1)
      B1NEW=ABS(B1NEW)
      R=0.0
      DO 17 I=1,N
      P(I)=(((B2*ALOG(B1-CUR(I)))-B4)*CUR(I)/BETA)-(B3*(CUR(I)**2))
      SE(I)=(P(I)-PM(I))**2
   17 R=R+SE(I)
      R=R/N
      R=SQRT(R)
      DIFF=R-ROLD
*DIAGNOSTIC*  THE TEST FOR EQUALITY BETWEEN NON-INTEGERS MAY NOT BE MEANINGFUL.
      IF(ROLD.EQ.1000000.)GO TO 78
      IF(DIFF)78,78,79
```

```
00644        78 WRITE(6,77)J,B,BOLD
00651        77 FORMAT(1H ,I2,2(5X,F8.4))
00652        78 DIFF=ABS(DIFF)
00653           DIFF=DIFF/BOLD
00654        70 IF(DIFF-.0001)5,6,6
00657         5 B1=B1NEW
00660           BOLD=B
00661           J=J+1
00662           IF(J-20)54,53,51
00665        53 IF(INDIC.EQ.1)GO TO 2
00667           DO 52 I=1,6
00672           CUR(I)=CU(I)
00673           VOL(I)=VO(I)
00674           C(JJ-16+I)=CU(I)
00675           V(JJ-16+I)=VO(I)
00676        52 PM(I)=CUR(I)*VOL(I)
00700           GO TO 47
00701        51 IF(J-50)54,55,55
00704        55 WRITE(6,135)
00706       135 FORMAT(1H1,50X,21H CONVERGES TOO SLOWLY,///,30X,17H CALCULATED POW
00706          1ER,5X,15H MEASURED POWER,5X,8H CURRENT,/,38X,3H MW,17X,3H MW,13X,
00706          23H MA,//)
00707           WRITE(6,136)(P(I),PM(I),CUR(I),I=1,N)
00717       136 FORMAT(1H ,34X,F8.4,10X,F8.4,11X,F6.3)
00720           GO TO 997
00721        54 GO TO 2
00722         6 SEE=B
00723           XI=CUR(1)
00724           YI=0.0
00725        16 TI=(XI+YI)/2.
00726           DP=B2*(ALOG(B1-TI))/BETA
00727           DP=DP-((B2*TI)/(BETA*(B1-TI)))
00730           DP=DP-(B4/BETA)-(2.*B3*TI)
00731           IF(ABS(DP)-0.0001)14,14,11
00734        11 IF(DP)12,14,13
00737        12 XI=TI
00740           GO TO 16
00741        13 YI=TI
00742           GO TO 16
00743        14 CMAX=TI
00744           VMAX=(B2*(ALOG(B1-CMAX)))-B4
00745           VMAX=(VMAX/BETA)-(B3*CMAX)
00746           PMAX=CMAX*VMAX
00747           IF(INDIC.EQ.1)GO TO 322
00751           WRITE(6,245)(HEAD(I,KO),I=1,3)
00757       245 FORMAT(1H1,50X,33H CHARACTERISTICS FOR SPECIMEN NO.,2X,3A4,////)
00760           WRITE(6,244)
00762       244 FORMAT(1H0,4H RUN,5X,5H PMAX,5X,5H IMAX,6X,5H VMAX,9X,3H IG,13X,
00762          13H IO,13X,3H RS,14X,2H N,12X,4H SEE,/,1X,4H NO.,6X,3H MW,7X,3H MA,
00762          28X,2H V,11X,3H MA,13X,7H MA,12X,6H KOHMS,26X,3H MW,/)
00763       235 WRITE(6,247)(IRUN,PMAX,CMAX,VMAX,AIG,AIO,RS,AN,SEE)
00776 *DIAGNOSTIC*  A . OR P IS NOT FOLLOWED BY A DIGIT IN THE FORMAT.
00776       247 FORMAT(1H ,2X,I2,5X,F6.3,5X,F5.2,5X,F6.5,4(5X,1PE11.4),5X,0P,F8.5)
00777           KJ=JNUM(JO)
01000           IF(KO.EQ.KJ)GO TO 520
01002           GO TO 115
01003       322 PJMAX(JO)=PMAX
01004           CJMAX(JO)=CMAX
```

```
01005          VJMAX(JO)=VMAX
01006          AJTG(JO)=ATG
01007          AJTO(JO)=ATO
01010          PJS(JO)=PS
01011          AJN(JO)=AN
01012          SJFE(JO)=SFE
01013          IF(JO.EQ.23)GO TO 700
01015          JO=JO+1
01016          GO TO 115
01017      700 DO 701 JJO=1,27
01022          IF(JJO.EQ.1)GO TO 702
01024          JB=JE+1
01025          JE=JDUM(JJO)
01026          GO TO 703
01027      702 JB=1
01030          JE=3
01031      703 WRITE(5,745)
01033      745 FORMAT(1H1,50X,30H CHARACTERISTICS FOR COMPOSITE)
01034          DO 704 JK=JB,JE
01037          WRITE(6,746)(HEAD(1,JK),HEAD(2,JK),HEAD(3,JK))
01044      704 CONTINUE
01046      746 FORMAT(1H0,60X,3A4)
01047          WRITE(5,244)
01051      735 WRITE(5,247)(IRUN,PJMAX(JJO),CJMAX(JJO),VJMAX(JJO),AJTG(JJO),
01051         1AJTO(JJO),PJS(JJO),AJN(JJO),SJFE(JJO))
01064      701 CONTINUE
01066      997 CONTINUE
01067      999 STOP
01070          END

     END OF COMPILATION:          2 DIAGNOSTICS.

***** CORE RESIDENCE TIME IN SEC = 72     CORE USED = 37376  *****
```

APPENDIX 2

CHARACTERISTICS FOR COMPOSITES UNCORRECTED FOR LIGHT LEVEL

These run/fluence data may be applied to all data included in the appendix.

Run No.	Hours	Fluence	Run No.	Hours	Fluence
01	Preirradiation		13	1645	6.85×10^{13}
02	18	0.75×10^{12}	14	1881	7.84×10^{13}
03	40	1.67×10^{12}	15	2209	9.20×10^{13}
04	58	2.42×10^{12}	16	2443	1.02×10^{14}
05	101	4.21×10^{12}	17	3013	1.26×10^{14}
06	149	6.21×10^{12}	18	3611	1.51×10^{14}
07	212	8.83×10^{12}	19	3915	1.63×10^{14}
08	279	1.16×10^{13}	20	4172	1.74×10^{14}
09	364	1.52×10^{13}	21	4480	1.87×10^{14}
10	528	2.20×10^{13}	22	4840	2.07×10^{14}
11	837	3.49×10^{13}			
12	1217	5.07×10^{13}			

Composite A Consisting of: C- 1 -5, C- 2 -5, C- 3 -5

RUN NO.	PMAX MW	IMAX MA	VMAX VOLTS	VOC VOLTS	ISC MA
1	24.761	44.00	.56279	.65722	50.10
2	24.284	43.82	.55422	.65962	48.97
3	24.885	42.06	.59167	.66028	48.02
4	24.003	41.66	.57622	.66085	47.28
5	23.904	41.47	.57638	.66210	46.49
6	23.648	40.35	.58605	.66384	45.55
7	22.866	39.99	.57185	.66557	44.91
8	21.537	40.63	.53008	.66732	44.91
9	22.560	39.31	.57396	.67298	44.50
10	22.647	38.93	.58169	.67686	44.26
11	21.901	38.94	.56242	.68069	43.65
12	21.436	37.99	.56419	.68204	43.24
13	21.605	37.78	.57185	.68319	42.70
14	20.838	37.80	.55121	.68243	42.48
15	19.600	37.68	.52020	.68131	41.82
16	20.255	36.06	.56165	.68186	41.66
17	20.031	35.53	.56372	.68034	41.44
18	19.658	35.89	.54772	-	-
19	19.909	35.48	.56106	.67804	40.50
20	19.334	34.92	.55368	-	-
21	19.496	34.71	.56161	.67469	39.53
22	18.870	33.59	.56184	.67349	38.74

Composite B Consisting of: C12- 02 -5, C12- 48 -5, C12- 04 -5, C12- 05 -5, C12- 06 -5

RUN NO.	PMAX MW	IMAX MA	VMAX VOLTS	VOC VOLTS	ISC MA
1	28.302	44.83	.63130	.75108	52.51
2	24.720	40.77	.60637	.73331	46.11
3	23.829	37.41	.63698	.72338	44.24
4	22.741	37.39	.60821	.71764	43.41
5	22.499	37.70	.59675	.70829	42.27
6	22.634	36.41	.62165	.70207	41.17
7	21.529	35.65	.60395	.69459	40.35
8	21.258	34.37	.61849	.68985	39.92
9	20.419	33.93	.60185	.68996	38.98
10	19.591	33.04	.59302	.68411	38.33
11	19.132	32.35	.59148	.67529	36.79
12	18.735	31.38	.59700	.66740	35.83
13	17.953	31.48	.57023	.66276	35.19
14	17.495	30.21	.57904	.65930	35.05
15	17.306	29.52	.58621	.65581	34.20
16	16.582	28.78	.57613	.65565	34.02
17	16.266	28.41	.57254	.65227	33.19
18	16.094	27.99	.57496	-	-
19	16.020	27.90	.57425	.64641	32.39
20	15.470	27.01	.57279	-	-
21	15.070	27.63	.54550	.64344	31.75
22	11.502	20.38	.56444	.63909	31.18

CHARACTERISTICS FOR COMPOSITES

UNCORRECTED FOR LIGHT LEVEL

Composite C Consisting of: H8A-8396-5, H8A-8397-5, H8A-8400-5, H8A-8401-5, H8A-8402-5

RUN NO.	PMAX MW	IMAX MA	VMAX VOLTS	VOC VOLTS	ISC MA
1	27.941	43.00	.64981	.74664	49.94
2	24.895	38.39	.64854	.73002	44.19
3	23.535	36.61	.64280	.71982	41.86
4	22.683	34.41	.65930	.71376	40.66
5	21.965	34.98	.62796	.70417	39.19
6	21.079	33.50	.62922	.69784	38.19
7	19.006	33.66	.56460	.69034	37.43
8	19.684	32.13	.61262	.68550	37.05
9	19.283	31.08	.62053	.68569	36.47
10	18.895	30.60	.61741	.67971	35.14
11	17.837	29.56	.60339	.67130	34.01
12	17.155	29.19	.58766	.66373	32.96
13	17.258	28.20	.61205	.65930	32.67
14	16.607	27.97	.59366	.65593	32.83
15	16.150	27.13	.59523	.65266	31.95
16	15.843	26.68	.59388	.65287	31.79
17	15.427	25.82	.59751	.64934	31.02
18	15.051	25.84	.58237	-	-
19	15.051	26.29	.57245	.64400	30.76
20	14.738	25.26	.58344	-	-
21	14.478	25.49	.56806	.69099	29.86
22	14.009	24.02	.58324	.63972	29.12

Composite D Consisting of: C12- 07-5D, C12- 08 -5D, C12- 09 -5D, C12- 10 -5D, C12- 11 -5D

RUN NO.	PMAX MW	IMAX MA	VMAX VOLTS	VOC VOLTS	ISC MA
1	27.397	44.78	.61185	.74990	53.22
2	24.500	40.74	.60132	.73219	47.54
3	23.791	39.31	.60528	.72246	45.42
4	22.634	37.72	.60003	.71674	44.67
5	21.967	37.03	.59327	.70678	42.89
6	21.584	36.38	.59329	.70077	41.63
7	21.027	35.63	.59009	.69281	41.05
8	20.289	34.44	.58907	.68804	40.36
9	19.490	33.23	.58651	.68779	39.68
10	19.212	32.86	.58465	.68176	38.64
11	18.610	32.02	.58126	.67316	37.28
12	17.707	31.09	.56952	.66536	36.70
13	17.161	30.71	.55885	.66065	35.99
14	16.948	30.09	.56330	.65752	36.10
15	16.635	29.40	.56573	.65421	35.32
16	16.500	28.79	.57320	.65395	34.89
17	16.080	27.89	.57662	.65063	34.10
18	15.708	27.90	.56292	-	-
19	15.968	27.71	.57620	.69528	33.53
20	15.450	27.02	.57177	-	-
21	11.949	20.94	.57052	.64198	32.35
22	15.316	26.26	.58334	.64079	31.85

CHARACTERISTICS FOR COMPOSITES
UNCORRECTED FOR LIGHT LEVEL

Composite E Consisting of: C12- 12 -3, C12- 13 -3, C12- 14 -3, C12- 16 -3, C12- 17 -3, C12- 18 -3, C12- 19 -3, C12- 20 -3, C12- 21 -3, C12- 22 -3

RUN NO.	PMAX MW	IMAX MA	VMAX VOLTS	VOC VOLTS	ISC MA
1	29.468	64.45	.45723	.59865	76.52
2	26.973	61.16	.44100	.57511	71.80
3	26.516	59.99	.44198	.56498	69.99
4	25.756	58.60	.43950	.55997	68.90
5	25.080	57.88	.43330	.55021	66.78
6	24.220	55.60	.43559	.54415	65.30
7	23.774	56.22	.42287	.53844	64.15
8	22.926	54.47	.42089	.53389	63.58
9	22.468	54.07	.41555	.52841	62.57
10	21.861	53.45	.40901	.52212	61.43
11	21.041	51.85	.40578	.51562	59.65
12	20.388	51.03	.39955	.50883	58.89
13	19.946	50.34	.39624	.50329	57.80
14	19.504	49.49	.39405	.50071	57.79
15	19.085	48.98	.38966	.49604	56.21
16	18.874	47.11	.40062	.49878	56.61
17	18.196	47.01	.38703	.49275	55.16
18	17.969	46.94	.38280	-	-
19	18.025	47.97	.37574	.48331	55.28
20	17.605	46.86	.37571	-	-
21	17.362	46.17	.37609	.47935	53.75
22	17.201	46.14	.37278	.47828	52.94

Composite F Consisting of: H8A-8404-3, H8A-8405-3, H8A-8407-3, H8A-8408-3, H8A-8409-3, H8A-8411-3, H8A-8412-3, H8A-8413-3, H8A-8477-3, H8A-8478-3

RUN NO.	PMAX MW	IMAX MA	VMAX VOLTS	VOC VOLTS	ISC MA
1	26.142	57.02	.45851	.58794	69.83
2	24.735	53.79	.45988	.57177	65.67
3	24.135	53.67	.44968	.56339	64.24
4	23.442	52.18	.44923	.55949	63.36
5	22.944	51.91	.44199	.55055	60.84
6	22.500	49.64	.45327	.54440	60.01
7	22.152	49.45	.44797	.53908	59.03
8	21.330	47.90	.44532	.53530	57.86
9	20.946	47.42	.44167	.53019	57.30
10	20.098	47.95	.41916	.52362	56.17
11	19.175	46.08	.41609	.51748	54.34
12	18.781	45.79	.41016	.51172	53.86
13	18.554	45.57	.40717	.50629	53.25
14	18.227	43.55	.41855	.50453	53.06
15	18.001	43.87	.41029	.49987	51.88
16	17.703	41.74	.42414	.50185	52.02
17	17.405	41.85	.41586	.49717	50.62
18	17.003	41.24	.41228	-	-
19	16.982	43.56	.38985	.48747	51.15
20	16.682	40.82	.40871	-	-
21	16.364	42.04	.38929	.48472	49.81
22	16.120	42.13	.38259	.48311	49.29

CHARACTERISTICS FOR COMPOSITES
UNCORRECTED FOR LIGHT LEVEL

Composite G Consisting of: C- 4 -3, C- 5 -3, C- 6 -3, C- 7 -3, C- 8 -3, C- 9 -3

RUN NO.	PMAX MW	IMAX MA	VMAX VOLTS	VOC VOLTS	ISC MA
1	26.216	62.55	.41915	.54582	73.50
2	25.939	61.88	.41916	.54532	72.89
3	26.287	61.47	.42764	.54495	72.72
4	25.866	61.08	.42349	.54386	72.43
5	26.037	61.32	.42463	.54156	71.50
6	25.769	60.98	.42257	.53970	70.59
7	25.474	60.53	.42083	.53687	70.36
8	25.087	59.83	.41930	.53600	70.28
9	24.768	59.65	.41524	.53341	69.21
10	24.395	59.23	.41185	.53004	68.32
11	23.656	57.90	.40861	.52503	67.26
12	22.800	56.69	.40219	.51825	66.12
13	22.570	56.27	.40113	.51507	65.27
14	22.069	55.18	.39997	.51392	65.56
15	21.746	54.92	.39599	.50986	63.42
16	21.433	53.88	.39780	.51109	63.72
17	21.112	53.51	.39451	.51013	62.83
18	21.252	51.86	.40981	-	-
19	20.705	53.52	.38683	.50009	62.64
20	20.002	52.29	.38826	-	-
21	20.107	51.90	.38738	.49857	61.15
22	19.967	51.69	.38626	.49474	60.23

Composite H Consisting of: C3- 1 -3, C3- 2 -3, C3- 3 -3, C3- 4 -3, C3- 5 -3, C3- 6 -3, C3- 7 -3, C3- 8 -3, C3- 9 -3

RUN NO.	PMAX MW	IMAX MA	VMAX VOLTS	VOC VOLTS	ISC MA
1	27.924	61.50	.45404	.57791	73.17
2	26.529	59.25	.44772	.56377	70.64
3	26.400	59.35	.44480	-	69.20
4	25.551	57.67	.44305	.55624	68.43
5	24.955	57.14	.43670	.55121	66.24
6	24.157	56.05	.43095	.54262	65.05
7	23.658	55.29	.42790	.53753	64.02
8	22.937	54.17	.42346	.53129	63.25
9	22.450	53.67	.41833	.52669	62.40
10	21.802	53.05	.41098	.52153	61.06
11	21.016	51.45	.40845	.51621	59.03
12	20.187	50.14	.40265	.50795	58.56
13	19.798	49.52	.39976	.50140	57.73
14	19.256	48.45	.39740	.49660	57.70
15	19.009	48.69	.39040	.49333	55.48
16	18.540	46.69	.39712	.48890	55.85
17	17.960	46.31	.38785	.48789	54.57
18	17.936	45.01	.39849	-	-
19	17.658	46.70	.37809	.47532	54.53
20	17.486	44.41	.39376	-	-
21	16.976	44.68	.37999	.47180	53.00
22	16.438	44.77	.36721	.46934	53.42

CHARACTERISTICS FOR COMPOSITES

UNCORRECTED FOR LIGHT LEVEL

Composite I Consisting of: C1- 1 -3, C1- 2 -3, C1- 3 -3, C1- 4 -3, C1- 5 -3, C1- 6 -3, C1- 7 -3, C1- 8 -3, C1- 11 -3

RUN NO.	PMAX MW	IMAX MA	VMAX VOLTS	VOC VOLTS	ISC MA
1	24.754	56.87	.43530	.55951	67.86
2	24.234	55.94	.43319	.55847	66.58
3	24.965	56.63	.44089	.55836	65.97
4	24.532	55.51	.44194	.55762	66.34
5	24.641	55.97	.44025	.55635	65.50
6	24.450	55.84	.43789	.55637	65.03
7	24.434	55.47	.44046	.55500	64.96
8	24.030	54.66	.43964	.55382	64.67
9	23.975	54.80	.43748	.55242	64.75
10	23.911	54.98	.43487	.55213	64.43
11	23.666	54.51	.43418	.54963	63.48
12	23.475	54.56	.43025	.54605	63.55
13	23.608	54.82	.43068	.54627	64.02
14	23.419	52.58	.44540	.54213	64.20
15	23.002	54.17	.42465	.54002	62.58
16	23.087	51.76	.44601	.53917	63.10
17	22.047	52.42	.42058	.53837	62.15
18	21.715	52.07	.41703	-	-
19	22.116	51.41	.42969	.52732	62.54
20	21.736	50.22	.43281	-	-
21	21.098	51.66	.40837	.52304	61.27
22	20.835	51.14	.40740	.52197	60.18

Composite J Consisting of: C- 10 -6, C- 11 -6, C- 12 -6, C- 13 -6, C- 14 -6, C- 15 -6,

RUN NO.	PMAX MW	IMAX MA	VMAX VOLTS	VOC VOLTS	ISC MA
1	22.108	63.68	.34717	.47135	78.30
2	21.981	64.13	.34273	.46824	77.85
3	22.620	64.22	.35221	.46957	77.39
4	22.272	63.48	.35083	.46808	77.23
5	22.083	63.39	.34837	.46609	76.83
6	21.816	59.26	.36817	.46441	75.94
7	21.398	58.72	.36440	.46223	75.68
8	21.230	58.31	.36411	.46009	75.34
9	20.960	61.72	.33958	.45834	75.08
10	20.469	61.15	.33474	.45435	74.41
11	20.075	60.54	.33161	.44958	72.85
12	19.364	59.48	.32558	.44293	72.12
13	18.800	55.22	.34047	.43946	71.70
14	18.819	58.54	.32148	.43831	71.85
15	18.490	57.75	.32016	.43569	70.04
16	18.208	57.22	.31819	.43437	69.94
17	17.837	53.03	.33635	.43242	69.04
18	17.741	53.05	.33441	-	-
19	17.624	54.19	.31520	.42745	68.46
20	17.362	51.92	.33442	-	-
21	17.154	51.67	.33201	.42612	66.91
22	16.307	54.28	.31152	.41989	66.31

CHARACTERISTICS FOR COMPOSITES

UNCORRECTED FOR LIGHT LEVEL

Composite K Consisting of: C12- 23 -6, C12- 24 -6, C12- 25 -6, C12- 26 -6, C12- 27 -6, C12- 28 -6, C12- 29 -6, C12- 47 -6

RUN NO.	PMAX MW	IMAX MA	VMAX VOLTS	VOC VOLTS	ISC MA
1	25.973	64.76	.40107	.53786	79.02
2	24.608	60.56	.40634	.52142	75.57
3	24.503	62.82	.39005	.51582	74.99
4	23.739	61.35	.38696	.51039	74.18
5	23.091	60.54	.38142	.50326	72.64
6	22.435	58.39	.38420	.49738	71.30
7	22.151	59.59	.37174	.49173	70.55
8	21.523	58.57	.36747	.48653	70.06
9	20.984	58.00	.36181	.48104	69.50
10	20.465	57.71	.35462	.47386	68.48
11	19.678	56.21	.35010	.46542	66.91
12	19.551	56.34	.34703	.46406	67.57
13	19.351	56.38	.34323	.46006	67.56
14	18.542	55.34	.33507	.45159	67.03
15	18.639	55.05	.33859	.45120	65.57
16	18.610	54.75	.33991	.45364	66.30
17	18.441	52.94	.34832	.45191	64.85
18	17.991	52.11	.34525	-	-
19	18.299	53.78	.34028	.44579	64.15
20	17.692	51.54	.34329	-	-
21	17.308	52.75	.32814	.44030	63.68
22	16.981	52.38	.32420	.43782	62.64

Composite L Consisting of: H8A-8482-6, H8A-8483-6, H8A-8487-6, H8A-8489-6, H8A-8491-6, H8A-8495-6, H8A-8497-6, H8A-8499-6

RUN NO.	PMAX MW	IMAX MA	VMAX VOLTS	VOC VOLTS	ISC MA
1	22.330	57.41	.38894	.52105	71.09
2	21.676	56.16	.38600	.51146	69.48
3	21.920	56.97	.38476	.509.01	69.22
4	21.332	55.68	.38312	.50457	68.28
5	20.961	55.36	.37861	.49952	67.15
6	20.795	53.89	.38589	.49571	66.43
7	20.231	54.43	.37171	.49042	65.92
8	20.028	52.24	.38338	.48682	65.94
9	19.678	52.73	.37317	.48259	65.45
10	19.214	52.17	.36826	.47618	64.65
11	18.648	51.37	.36300	.46863	63.22
12	18.269	50.73	.36010	.46468	63.07
13	18.112	50.63	.35772	.46138	63.10
14	17.591	49.91	.35244	.45596	62.82
15	17.325	50.97	.33991	.45478	60.99
16	16.940	49.28	.34372	.45500	61.42
17	16.840	48.21	.34931	.45279	60.26
18	16.574	48.39	.34252	-	-
19	16.832	49.61	.33917	.44854	60.79
20	16.357	47.04	.34773	-	-
21	16.020	47.43	.33774	.44321	58.73
22	15.849	47.13	.33629	.44076	57.90

CHARACTERISTICS FOR COMPOSITES

UNCORRECTED FOR LIGHT LEVEL

Composite M Consisting of: C3- 10 -6, C3- 11 -6, C3- 12 -6, C3- 13 -6, C3- 24 -6, C3- 15 -6, C3- 16 -6, C3- 17 -6

RUN NO.	PMAX MW	IMAX MA	VMAX VOLTS	VOC VOLTS	ISC MA
1	24.701	62.42	.39574	.52052	74.76
2	23.448	61.10	.38375	.50738	72.87
3	23.590	60.82	.38786	.50286	71.90
4	22.808	59.00	.38657	.49799	70.36
5	22.156	58.22	.38058	.49102	69.71
6	21.786	58.00	.37560	.48576	68.46
7	21.233	57.13	.37165	.48013	67.67
8	20.702	56.43	.36683	.47501	66.58
9	20.216	55.82	.36218	.47061	67.05
10	19.682	55.40	.35529	.46254	65.51
11	18.932	54.17	.34950	.45379	63.83
12	19.139	55.14	.34712	.45290	65.24
13	18.833	54.54	.34531	.44836	65.00
14	17.883	53.05	.33713	.43940	63.71
15	18.048	53.53	.33716	.43939	63.02
16	18.161	53.70	.33820	.44178	63.80
17	17.749	52.74	.33655	.43962	63.09
18	17.340	52.49	.33033	-	-
19	17.743	53.99	.32860	.43292	64.24
20	17.055	52.28	.32620	-	-
21	16.815	51.64	.32562	.42698	61.49
22	16.555	51.21	.32325	.42467	60.95

Composite N Consisting of: C1- 13 -6, C1- 14 -6, C1- 9 -6, C1- 10 -6,

RUN NO.	PMAX MW	IMAX MA	VMAX VOLTS	VOC VOLTS	ISC MA
1	21.682	58.17	.37271	.49816	70.51
2	21.253	57.49	.36968	.49529	69.86
3	21.940	58.39	.37576	.49693	69.30
4	21.485	56.78	.37841	.49543	68.42
5	21.547	57.12	.37719	.49414	68.37
6	21.381	56.90	.37576	.49345	67.74
7	21.251	56.51	.37605	.49168	67.04
8	21.065	56.19	.37486	.49026	67.13
9	20.870	56.04	.37241	.48935	67.40
10	20.494	56.20	.36464	.48649	66.72
11	20.153	54.67	.36863	.48309	65.84
12	20.111	55.37	.36322	.47844	65.72
13	19.918	55.14	.36123	.47368	64.06
14	19.671	54.60	.36030	.47419	65.93
15	19.479	54.48	.35758	.47047	64.22
16	18.895	53.53	.35295	.46620	64.44
17	18.456	52.89	.34897	.46382	63.33
18	18.153	52.27	.34728	-	-
19	18.417	53.65	.34331	.45855	64.13
20	17.897	52.85	.33862	-	-
21	17.828	52.27	.34104	.45443	61.88
22	17.492	51.74	.33805	.45279	62.26

CHARACTERISTICS FOR COMPOSITES

UNCORRECTED FOR LIGHT LEVEL

Composite O Consisting of: C2- 2 -6, C2- 3 -6, C2- 5 -6, C2- 4 -6

RUN NO.	PMAX MW	IMAX MA	VMAX VOLTS	VOC VOLTS	ISC MA
1	20.309	54.00	.37608	.49979	66.92
2	19.842	53.51	.37083	.49721	65.59
3	20.120	52.69	.38188	.49791	64.63
4	19.861	52.84	.37587	.49692	64.28
5	19.844	52.61	.37716	.49508	63.90
6	19.706	52.40	.37605	.49405	63.22
7	19.561	51.99	.37628	.49189	62.64
8	19.053	50.98	.37376	.48994	62.17
9	19.017	50.99	.37294	.48815	62.60
10	19.077	49.79	.38317	.48409	61.98
11	18.415	50.26	.36641	.47826	61.08
12	18.172	50.68	.35856	.47007	61.35
13	18.031	50.92	.35408	.46378	61.71
14	17.687	50.20	.35233	.46172	61.84
15	17.539	50.53	.34708	.45625	60.75
16	17.105	50.18	.34090	.45226	61.38
17	16.742	49.64	.33724	.44595	60.22
18	16.447	49.80	.33024	-	-
19	16.715	48.78	.32667	.43540	62.01
20	16.275	50.04	.32526	-	-
21	16.138	49.99	.32285	.43042	60.33
22	15.827	49.40	.32040	.42755	60.30

Composite P Consisting of: C12- 32 -6D, C12- 33 -6D, C12- 34 -6D, C12- 35 -6D, C12- 36 -6D, C12- 37 -6D, C12- 38 -6D, C12- 39 -6D

RUN NO.	PMAX MW	IMAX MA	VMAX VOLTS	VOC VOLTS	ISC MA
1	25.590	63.51	.40291	.53987	79.99
2	24.246	62.16	.39006	.52600	77.24
3	24.241	61.29	.39553	.52074	76.27
4	23.670	60.04	.39425	.51852	75.31
5	23.353	60.07	.38880	.51158	74.31
6	22.955	59.67	.38473	.50840	73.28
7	22.925	57.13	.40125	.50330	72.90
8	22.224	58.72	.37847	.50031	72.50
9	21.642	58.27	.37140	.49548	72.52
10	21.617	55.74	.38781	.49106	71.59
11	20.847	57.03	.36554	.48407	69.81
12	20.597	54.44	.37835	.47874	69.89
13	20.218	54.27	.37251	.47235	69.81
14	20.135	53.61	.37559	.47019	69.47
15	19.815	52.82	.37517	.46816	67.76
16	19.384	52.20	.37137	.46578	68.41
17	19.029	52.40	.36315	.46184	66.99
18	18.738	51.48	.36398	-	-
19	19.031	52.91	.35927	.45631	67.95
20	18.406	51.28	.35892	-	-
21	17.966	53.13	.33816	.45066	65.79
22	17.491	50.47	.34660	.44923	64.40

CHARACTERISTICS FOR COMPOSITES

UNCORRECTED FOR LIGHT LEVEL

Composite R Consisting of: H8A-8490-6D, H8A-8501-6D, H8A-8511-6D, H8A-8492-6D, H8A-8493-6D, H8A-8505-6D, H8A-8500-6D, H8A-8506-6D

RUN NO.	PMAX MW	IMAX MA	VMAX VOLTS	VOC VOLTS	ISC MA
1	22.325	57.51	.38820	.52289	71.44
2	18.165	49.08	.37013	.50703	61.75
3	21.689	56.41	.38450	.50990	69.50
4	15.987	43.43	.36809	.49488	56.40
5	20.721	54.49	.38026	.50313	69.36
6	19.322	49.13	.39327	.49828	62.64
7	20.518	52.13	.39361	.49586	66.58
8	18.612	48.46	.38410	.49050	62.05
9	19.763	51.41	.38443	.48968	66.30
10	19.545	51.45	.37991	.48452	67.03
11	18.844	50.81	.37090	.47735	63.07
12	18.515	49.89	.37115	.47264	63.51
13	18.250	49.50	.36869	.46705	63.35
14	17.837	48.79	.36556	.46460	63.47
15	17.710	48.94	.36184	.46254	61.80
16	17.466	48.41	.36078	.45977	62.22
17	16.999	47.38	.35880	.45686	60.57
18	16.792	47.50	.35351	-	-
19	16.987	48.58	.34967	.45166	63.62
20	16.347	46.84	.34895	-	-
21	16.368	46.97	.34846	.44702	61.18
22	16.044	46.16	.34760	.44557	61.06

Composite S1 Consisting of: C- 16 -8, C- 17 -8

RUN NO.	PMAX MW	IMAX MA	VMAX VOLTS	VOC VOLTS (Combined Averages for Both S1 and S2)	ISC MA (Combined Averages for Both S1 and S2)
1	19.276	64.19	.30028	.42266	68.83
2	19.090	63.17	.30220	.42224	68.31
3	19.110	61.91	.30868	.42009	68.09
4	19.548	63.16	.30949	.41971	66.95
5	19.520	63.36	.30809	.41853	67.25
6	19.227	62.98	.30527	.41781	66.87
7	19.185	62.89	.30504	.41582	65.49
8	18.877	62.46	.30221	.41418	65.77
9	18.745	62.59	.29950	.41212	66.34
10	18.288	62.10	.29449	.40901	65.74
11	17.779	61.13	.29082	.40348	64.74
12	17.064	60.11	.28387	.39692	63.79
13	17.180	59.98	.28645	.39287	63.20
14	16.642	59.65	.27901	.39161	63.71
15	16.073	55.63	.28893	.38833	62.20
16	16.071	58.14	.27642	.38624	62.37
17	15.608	55.97	.27886	.38405	61.13
18	15.654	55.92	.27996	-	-
19	15.355	56.12	.27359	.37968	60.94
20	15.134	56.27	.26896	-	-
21	15.362	57.39	.26769	.37737	59.54
22	14.836	54.64	.27152	.37360	59.03

CHARACTERISTICS FOR COMPOSITES
UNCORRECTED FOR LIGHT LEVEL

Composite S2 Consisting of: C- 18 -8, C- 19 -8

RUN NO.	PMAX MW	IMAX MA	VMAX VOLTS	VOC VOLTS	ISC MA
1	14.655	47.61	.30783		
2	14.624	47.68	.30669		
3	14.370	45.55	.31549		
4	14.546	46.60	.31212		
5	14.620	47.00	.31103		
6	14.619	45.14	.32383		
7	14.613	44.81	.32614		
8	14.281	46.75	.30545		
9	14.143	46.56	.30376		
10	13.923	46.45	.29976		
11	13.486	45.66	.29534		
12	12.934	44.99	.28749		
13	12.748	44.22	.28830		
14	12.466	42.03	.39658		
15	12.271	43.82	.28006		
16	12.117	43.19	.28055		
17	11.838	42.44	.27895		
18	11.650	42.12	.27657		
19	11.616	42.75	.27189		
20	11.441	41.64	.27474		
21	11.273	41.21	.27353		
22	11.131	40.77	.27302		

Composite T Consisting of: C12- 40 -8, C12- 41 -8, C12- 42 -8, C12- 43 -8, C12- 44 -8, C12- 46 -8

RUN NO.	PMAX MW	IMAX MA	VMAX VOLTS	VOC VOLTS	ISC MA
1	23.678	65.92	.35918	.49760	76.91
2	22.324	65.05	.35857	.49221	75.92
3	23.328	64.92	.35931	.48651	75.12
4	22.301	62.14	.35887	.48395	74.12
5	22.015	61.10	.36030	.47839	72.75
6	21.789	61.30	.35544	.47394	72.31
7	21.472	61.21	.35077	.46885	71.06
8	21.133	58.30	.36251	.46337	70.86
9	20.761	58.72	.35354	.45994	71.59
10	20.127	59.88	.33614	.45314	69.57
11	19.608	59.56	.32922	.45569	67.36
12	19.481	59.60	.32686	.44551	68.24
13	19.116	59.20	.32290	.43862	68.30
14	18.570	57.03	.32563	.43300	67.84
15	18.483	58.04	.31848	.43169	66.33
16	18.115	57.37	.31574	.42872	65.81
17	17.591	56.45	.31155	.42399	64.59
18	17.281	55.26	.31273	. -	-
19	17.655	55.61	.31186	.41906	69.42
20	17.001	55.17	.30817	. -	-
21	16.830	53.15	.31664	.41517	67.23
22	16.561	55.02	.30103	.41248	66.15

CHARACTERISTICS FOR COMPOSITES
UNCORRECTED FOR LIGHT LEVEL

Composite U Consisting of: H8A-8494-8, H8A-8496-8, H8A-8502-8, H8A-8504-8, H8A-8507-8, H8A-8509-8

RUN NO.	PMAX MW	IMAX MA	VMAX VOLTS	VOC VOLTS	ISC MA
1	20.442	59.12	.34576	.47505	69.23
2	20.044	58.55	.34236	.47166	68.20
3	20.475	59.27	.34543	.46749	67.37
4	19.940	57.69	.34562	.46553	66.82
5	19.869	58.22	.34127	.46171	66.28
6	19.499	56.25	.34664	.45851	64.75
7	19.321	56.94	.33932	.45442	65.12
8	18.870	55.24	.34162	.45151	65.05
9	18.645	54.53	.34190	.44705	65.00
10	18.109	54.87	.33003	.44195	63.67
11	17.490	53.98	.32404	.43472	62.61
12	17.197	53.41	.32196	.43220	62.34
13	16.858	52.39	.32180	.42766	62.58
14	16.495	52.02	.31706	.42312	62.24
15	16.223	52.38	.30973	.42027	61.04
16	15.918	50.34	.31623	.41868	61.11
17	15.602	51.18	.30485	.41456	59.49
18	15.341	50.84	.30175	. -	-
19	15.525	51.30	.30237	.40996	65.77
20	15.062	50.31	.29939	. -	-
21	14.886	50.48	.29486	.40682	62.57
22	14.426	49.17	.29341	.40435	62.97

Composite W Consisting of: C3- 18 -8, C3- 19 -8, C3- 20 -8, C3- 21 -8, C3- 22 -8, C3- 23 -8

RUN NO.	PMAX MW	IMAX MA	VMAX VOLTS	VOC VOLTS	ISC MA
1	17.069	48.90	.34908	.46898	69.21
2	16.887	49.14	.34366	.46332	68.32
3	16.836	48.72	.34559	.45879	67.95
4	16.522	47.73	.34619	.45622	66.85
5	16.187	47.10	.34370	.45151	66.18
6	15.847	46.82	.33848	.44570	65.20
7	15.760	47.10	.33463	.44258	64.77
8	15.530	46.71	.33245	.43887	64.72
9	15.094	46.28	.32615	.43342	64.97
10	14.692	45.83	.32054	.42554	63.56
11	14.276	45.43	.31424	.41848	62.67
12	14.340	45.12	.31780	.42241	63.15
13	14.287	45.68	.31277	.41508	63.40
14	13.655	44.42	.30737	.40865	62.26
15	13.653	44.44	.30726	.40814	61.33
16	13.430	43.79	.30673	.40636	61.95
17	13.160	43.43	.30304	.40208	60.50
18	12.835	42.97	.29870	. -	-
19	13.181	43.11	.30536	.39708	52.68
20	12.673	42.81	.29605	-	-
21	12.510	42.15	.29609	.393217	51.17
22	12.043	41.67	.28898	.38951	50.19

CHARACTERISTICS FOR COMPOSITES

UNCORRECTED FOR LIGHT LEVEL

Composite X Consisting of: C1- 16 -8, C1- 17 -8, C1- 18 -8, C1- 19 -8, C1- 20 -8, C1- 21 -8

RUN NO.	PMAX MW	IMAX MA	VMAX VOLTS	VOC VOLTS	ISC MA
1	15.082	47.07	.32042	.43122	65.05
2	14.844	46.45	.31954	.43135	64.26
3	15.208	47.02	.32347	.42908	64.16
4	14.897	45.80	.32526	.42902	63.16
5	14.942	45.58	.32780	.42863	62.88
6	14.724	45.44	.32403	.42824	62.00
7	14.661	45.12	.32494	.42735	61.95
8	14.580	45.19	.32260	.42670	61.87
9	14.417	44.27	.32564	.42531	62.32
10	14.271	44.92	.31768	.42364	61.42
11	14.148	44.70	.31651	.42002	60.71
12	13.737	44.18	.31094	.41507	60.53
13	13.705	44.56	.30755	.41185	61.03
14	13.436	43.86	.30632	.40951	60.92
15	13.351	42.77	.31215	.40602	59.95
16	13.110	41.90	.31286	.40312	59.87
17	12.485	42.52	.29364	.39792	58.72
18	12.178	41.48	.29360	-	-
19	12.333	43.01	.28632	.39219	51.46
20	11.975	40.98	.29219	-	-
21	11.828	41.40	.28566	.38771	50.16
22	11.609	40.20	.28875	.38435	49.66

Composite , Consisting of:

RUN NO.	PMAX MW	IMAX MA	VMAX VOLTS	VOC VOLTS	ISC MA

CHARACTERISTICS FOR COMPOSITES
UNCORRECTED FOR LIGHT LEVEL